FLEET TECHNOLOGY LIMITED

91-04720/

EVALUATION OF TOUGHNESS OF CONVENTIONAL SHIP STEELS AT INTERMEDIATE LOADING RATE, AND ITS IMPLICATIONS UNSOLICITED PROPOSAL A7-025

Final Report

By

L. Malik and M. Tomin*

Work on the project was conducted under the auspices of the Canada Centre for Mineral and Metallurgical Technology, and the Canadian Coast Guard (Northern)

DSS Contract Serial No. : 23440-7-9227/01-SQ

DSS File No. : 06SQ.23440-7-9227

CANMET Project No. :

Scientific Authority : Dr. W.R. Tyson

MICROMEDIA

Date: January 1991

*L. Malik and M. Tomin are with Fleet Technology Limited and Reltec Advisory Services Inc. respectively.

131 pp

CONTRACT SERIAL NO. 79227-01-SQ
CONTRACT REQUISITION NO. 23440-7-9227
CONTRACTOR: FLEET TECHNOLOGY

TABLE OF CONTENTS

		Page
Executive Summary		(iii)
Acknowledgments		(v)
1.0	INTRODUCTION	1
1.1	The Rolfe Approach	1
1.2	The NKK Approach	2
1.3	Fracture Control Plan for Arctic Ships	4
2.0	OBJECTIVES OF THE PRESENT INVESTIGATION	7
3.0	INVESTIGATION AND RESULTS	8
3.1	Steel Procurement	8
3.2	Steel Characterization	8
3.2.1	Chemical Composition of Steels	8
3.2.2	Metallography	8
3.2.3	Room Temperature Tensile Tests	9
3.2.4	Charpy Vee Notch Testing	9
3.2.5	Comparison of Steels Investigated With Ship Steel Specifications	10
3.3	Nil-Ductility Transition (NDT) Temperature	10
3.4	Crack Tip Opening Displacement Tests	11
3.4.1	Selection of Strain Rate for Intermediate Loading Rate Tests	11
3.4.2	Calculation of Cross-Head Rate for Intermediate Loading Rate CTOD Tests	11
3.4.3	CTOD Tests	13
3.5	Compact Crack Arrest Toughness Testing	14
4.0	DISCUSSION	16
4.1	Brittle Fracture Initiation Resistance Required	16
4.2	Fracture Toughness of the Steels in Relation to the 0.1mm CTOD (Int.) Criterion	18
4.3	Specification for Structural Steelss for Arctic Ship Hulls (Brittle Fracture Initiation Resistance)	19
4.4	Statistical Significance of the Results	21
4.5	Significance of the Results With Respect to CASPRR	22
4.6	Compact Crack Arrest Behaviour	22
5.0	SUMMARY	25
6.0	REFERENCES	26

TABLE OF CONTENTS (Cont'd)

TABLES AND FIGURES

APPENDIX A Steel Selection Requirements Specified in CASPRR

APPENDIX B Statistical Significance of the Results (by M. Tomin, Reltec Advisory Services Inc.)

APPENDIX C Significance of CTOD Results With Respect to CASPRR (By M. Tomin, Reltec Advisory Services Inc.)

EXECUTIVE SUMMARY

The CTOD fracture toughness of several grades of steels, having Charpy Vee Notch absorbed energy values near the minimums specified for ship steels, has been determined at two loading rates, viz. quasi-static, and an intermediate loading rate (corresponding to a strain rate of $\sim 5 \times 10^{-2} s^{-1}$) believed to be the highest that can be anticipated in the midship region of icebreakers.

A conservative criterion suggested is that if a steel exhibits 0.1mm CTOD at the applicable intermediate stress intensity rate and the design temperature, then it should possess sufficient resistance against unstable fracture initiation from cracks, up to 250mm long, present in the midship region. Based on the CTOD, and NDT and CVN results for the series of steels investigated, it is concluded that the CASPPR requirements for steel toughness are adequate in this regard, and some suggestions are offered for their improvement.

The crack arrest behaviour of the steels was also examined using the compact crack arrest test, however, results from an accompanying program on short crack arrest toughness need to be available before definitive conclusions can be reached.

Correlations between the CTOD toughness of the steels, and their NDT temperature and CVN toughness were also sought. The correlation between the intermediate loading rate CTOD toughness and the NDT temperature was quite good. However, that between the CTOD toughness and CVN toughness was relatively poor, most likely due to the differences in the behaviour between the conventional and thermomechanically treated steels included in the program. The shift in the 0.1mm CTOD transition temperature between the quasistatic and intermediate loading rates was also examined, and it corresponded quite well with the data of Barsom and Rolfe.

SOMMAIRE

La ténacité à la rupture CTOD de plusieurs nuances d'acier, ayant des valeurs d'énergie absorbée lors des essais de résilience proche aux minimums prescrit pour des navires d'acier, a été déterminé à deux vitesses de sollicitation, viz. quasi-statique, et un taux de sollicitation intermédiaire (correspondant à une vitesse de déformation de $\simeq 5 \times 10^{-2}s^{-1}$) étant pensé a être la valeur maximale prévue dans la région centrale de la coque de brise-glaces.

Un critère conservatif indique que si l'acier démontre 0.1mm CTOD à un taux de sollicitation intermédiaire et à la température de conception, le matériel devrait donc posséder suffisamment de résistance contre l'initiation de rupture instable aux fissures, jusqu'à 250mm de longueur, présente dans la région centrale de la coque.

Le comportement de l'arrêt de fissure de l'acier fut aussi étudié en utilisant 'l'essai d'arrêt de fissuration avec eprouvette compacte', par conséquence les résultats d'un autre programme de CANMET/CCG sur 'la ténacité d'arrêt de fissure courte' doit être disponible avant que des conclusions définitive peuvent être prises.

Des corrélations entre les ténacités CTOD des aciers, leurs températures NDT et ténacités CVN furent aussi voulues. La corrélation entre le taux de sollicitation intermédiaire de ténacité CTOD et la température NDT était bonne. Par contre, celle entre la ténacité CTOD et CVN était relativement mauvaise, probablement dû aux différences dans le comportement de l'acier suite à des traitements différents un conventionnel et l'autre thermo-statique, utilisés lors du programme d'essai. Le déplacement dans la température de transition dans la courbe CTOD à 0.1mm entre un taux de sollicitation quasi-statique et un taux intermédiaire fut aussi étudié, et les données obtenues correspondes très bien aux résultats de Barsom et Rolfe.

ACKNOWLEDGEMENTS

The authors is grateful to Dr. W. Tyson (MTL-CANMET) and Mr. J. McCallum (Canadian Coast Guard Northern) for guidance and many helpful discussions during the course of the investigation. The cooperation and assistance of Mr. R. Bouchard (MTL-CANMET) is also greatly appreciated.

1.0 INTRODUCTION

As a result of the notch toughness evaluation of various steel plates in the failed Liberty Ships during the 1940's, the requirement for 21J (15 ft.lbs.) minimum Charpy Vee Notch (CVN) absorbed energy at the minimum design temperature was established for steel plates to be used in ship construction. This criterion represented an acceptably low probability of fracture initiation in service. All the same, crack arrestors were recommended to be incorporated to prevent catastrophic failure, should a brittle fracture initiate and propagate. Though initially developed for ships, by the early 1950's, the 21J criterion was also being used for other structures, as well as for assessing steel toughness in general.

Over the next two decades or so, the size of the ships increased, and associated with this was an increase in the strength and thickness of structural steels used in ships. As well, there were changes, mostly positive, in design of details, fabrication techniques and weld quality (soundness) so that with time, the 21J (15 ft.lbs.) criterion lost its significance.

During the 1960's and 70's with tremendous strides being made in the field of fracture mechanics, it was inevitable that fracture mechanics principles were applied to establish toughness requirements for steels to be used in ship structures. The two major efforts in this regard have been due to Rolfe et al[1,2] and by Nippon Kaiji Kyokai[3,4]. These two approaches are briefly discussed below.

1.1 The Rolfe Approach

The basic premise of the scheme presented by Rolfe et al[1] is that the ship hull can be subjected to dynamic loads of yield point magnitude when the effects of residual stresses and strain concentration are included, and that there is a significant probability of large undetected through thickness flaws existing in the ship at some time during the life of the ship. Therefore, to prevent catastrophic failures, they recommended a two pronged approach - design against unstable fracture initiation, and design for long crack arrest.

For the former, they suggested that the steel exhibit a reasonable level of elastic-plastic behaviour at the minimum design temperature, and that is ensured when

Steel NDT Temperature (°C) = Minimum Design Temperature (°) - 18°C

Since the NDT (nil ductility transition) temperature is the upper limit of dynamic plane strain behaviour, and at this temperature[1,5]:

$$\frac{K_{Id}}{\sigma_{yd}} \simeq 3\sqrt{mm}$$

it is anticipated that based on typical transition curve behaviour, $K_{Id}/\sigma_{yd} \simeq 4.5\ \sqrt{mm}$ at the design temperature (NDT + 18°C), so that through thickness yielding would occur prior to fracture under impact loading conditions. For stress in the range 100 to 175 MPa, the criterion implies critical defect size of 225mm to 75mm (approximately).

For 50mm plates, the upper limit for plane strain behaviour occurs when

$$\frac{K_{Id}}{\sigma_{yd}} \simeq 4.5\sqrt{mm}$$

and therefore the correction factor of "18°C" would need to be increased, although Rolfe et al[1] recommend that the criteria proposed above need not be changed for steel plates up to 50mm thick on account of probabilistic aspects of incidence of fracture in practice.

Secondly, to maintain a fail-safe philosophy, these authors also require incorporation of properly designed crack arrestors fabricated from steels with a very high level of notch toughness. Since actual measurement of dynamic toughness above the limits of plane strain behaviour is expensive, and difficult if not impossible, the steel toughness requirements have been presented (based on experimental results) in terms of absorbed energy at the minimum design temperature in 16mm thick dynamic tear specimens.

1.2 The NKK Approach

This approach was formulated by the Japanese Classification Society NKK (Nippon Kaiji Kyokai) in 1979 and is based on wide plate test (centre-notched tension tests) results for ships steels[3,4].

The suitability of a steel for any particular location or structural member of the ship structure is judged in two stages. First, its minimum fracture toughness, K_c, is estimated from the CVN specification (a certain minimum number of Joules at a specified temperature). Next, it is compared to the fracture toughness requirement for that location based on design conditions (service and residual stresses, service temperature and assumed allowable crack lengths). The steps involved in calculating the minimum anticipated fracture toughness can be summarized as follows:

Step 1: Estimate an absorbed energy transition temperature (T_E °C) corresponding to 50% fibrous fracture, from minimum specified CVN absorbed energy (E_T in kg.m) at the test temperature T_t using the equation

$$E_T = \frac{1}{\sqrt{2\Pi}} \int_{-\infty}^{T_t - T_E} \exp\left\{-\frac{1}{2}\left(\frac{T_t - T_E}{20}\right)^2\right\} dT_t$$

Step 2: Estimate the brittle fracture initiation temperature T_i (°C) as a function of the energy transition temperature (T_E), the steel thickness (t, mm) and yield strength (σ_y, kg mm^{-2}) as follows:

$$T_i = (0.00321\sigma_y + 0.391).T_E + 2.74\sqrt{t} - 278.59$$

This equation had been established based on wide plate tests (see Figure 1) with a centre machined notch 80mm in length, and an applied stress of $0.5\sigma_y$.

Step 3: Estimate the fracture toughness (K_c - blunt notch in kg $mm^{-3/2}$) of the steel using the expressions:

$$K_c = K_o \exp\{-k_o/(T + 273)\}$$

where $k_o = 562°K$ (experimentally obtained material constant)

and $K_o = 5.6\sigma_y \exp\{562/(273 + T_i)\}$

The agreement between the estimated and actual values is shown in Figures 2(a) and (b).

Step 4: Estimate the fracture toughness (K_{cf} - fatigue sharpened notch) based on the experimentally established relationship:

$$K_{cf} = 0.68\ K_c$$

The procedures outlined above thus can be used to generate a table giving the minimum anticipated value for fracture toughness of steel plates for hull use as a function of its strength, thickness, CVN specification and temperature, and this is shown in Table 1 as reproduced from Reference 4.

For steel selection, these values need to be compared with the minimum fracture toughness needed based on the design parameters, and can be represented by the equation:

$$K_{c(required)} = (\alpha + ß)\ \sigma_y\sqrt{\pi a}$$

where 2a, the maximum allowable through thickness crack length, is assumed to be 250mm (for base material); α is the design stress as a fraction of the yield strength σ_y (also called the coefficient of utilization) and ß is the magnitude of the residual (and reaction) stresses as a function of σ_y. The crack configuration assumed is as shown in Figure 3(a), i.e. the high tensile weld longitudinal residual stresses are assumed to be perpendicular to the plane of the flaw; and for this situation, ß is assumed to be 0.6.

Once the thickness and coefficient of utilization are established for a structural member, it is then straight forward to calculate $K_{c(required)}$ and then select a steel grade using the data in Table I.

It should be added that a similar semi-empirical approach has also been formulated on the basis of CTOD toughness (δ) of the steels instead of the K based values[4]. However, the allowable flaw size based on the CTOD approach is found to be smaller by a factor of four compared to that based on the K approach. The relationship used between the CTOD toughness (δ), the applied stress (σ) and the allowable flaw size is given below and seems empirical in nature:

$$\delta = \frac{3.5a \cdot \sigma_y(\alpha+\beta)}{E}$$

However, if the CTOD and K_c values for the steels are deemed to represent the same fracture toughness, then using the relationship

$$K^2 = m \bullet \delta \bullet \sigma_y \bullet E$$

the value of m can be computed. These values, shown below, range from 2.2 to about 5.0. In contrast, m is usually taken to be 1 and 2 for plane stress and plane strain conditions, respectively.

Yield Strength, MPa	K_c, MPa $\sqrt{m}$	δ, mm	m
240	145.4	.152	2.80
240	157.2	.149	2.22
240	165.5	.140	3.94
240	228.8	.161	6.54
320	184.5	.204	2.51
320	215.1	.191	3.66
320	261.6	.197	5.20

The K based NKK approach described above is compatible with steel grade/toughness selection in various classification society rules such as those from Det Norske Veritas, Lloyds and ABS. The rules have been applied successfully to ships operating in open sea waters, and the usual design temperature for such ship construction is 0°C.

1.3 Fracture Control Plan for Arctic Ships

The minimum design temperature for structural members in arctic ships that are exposed to the environment (i.e. above the waterline), is understood to be -40°C, compared to 0°C for the ships navigating in open waters.

Application of the Rolfe approach as presented above would require, for a 25mm thick plate, an NDT temperature of $\simeq$ -58°C for the structural steels, and implicitly, a similar requirement for heat affected zone and weld metal. With conventionally processed structural steel (IACS Grades A to E category steels), it is virtually impossible to obtain such low NDT temperatures. Even accelerated cooled steels, available only from a few offshore mills, could have difficulty in reliably meeting such a requirement. For example, Kawasaki's MACS EH36 steel, 50mm thick and produced about four years ago, has an NDT temperature of -55°C[6].

Notwithstanding the above, one must note the undue conservatism in this approach since IACS or ABS Grades A, B and C have a long history of successful application in ships, yet they would not pass the Rolfe criterion. One possible explanation for this apparent anomaly is that steels frequently have much better toughness than the minimum specified. Secondly, a major source of conservatism in this approach as pointed out by Pense et al[2], arises from the assumption of dynamic loading rates (strain rates of the order of $10s^{-1}$) when in fact the strain rate due to service loads in the critical midship region is expected to be much lower, and the steels can be expected to exhibit correspondingly higher toughness.

In this context, it is worth pointing out that in 1978, under the auspices of the Ship Structures Committee in the USA, the toughness of several grades of ship steels was evaluated at three different loading rates, using dynamic tear specimens[7]. The three cross head rates used were: 0.1 (quasistatic); 25.4 (intermediate); and 8000 mm/s (dynamic). While the fracture toughness at the dynamic loading rate was distinctly lower than that at the other two rates, the difference between the values at the quasistatic and intermediate loading rates was relatively small, as is clearly seen from the data in Table II.

Whether the direct application of the NKK approach is adequate for a design temperature of -40°C is difficult to say. While the empirical correlations seem reasonable, the fracture toughness values measured or required are based on quasistatic loading rate. To the extent that actual strain rates in the critical mid-ship region are higher, the prevailing toughness of the steel could be lower than that envisaged by the empirical correlations leading to a degree of unconservatism. Countering this is the assumption that there are residual and reaction stresses present whose magnitude is 60% of the base material yield strength. This seems unrealistically high since for a flaw, ~250mm long and perpendicular to the weld, the flaw tips are at a sufficient distance away from the weld so as to be outside the influence of weld longitudinal tensile residual stresses, and the magnitude of the reaction (or fabrication/assembly) stresses is expected to be much lower. As a matter of fact, Sommerville et al[8] indicate that for thicknesses relevant to warship hulls, the welding of the longitudinals on to the hull plating introduced compressive stresses into the latter (~50 MPa magnitude).

All the same, the NKK approach with one modification, is the basis of the structural steel toughness requirements in the Proposed Revisions to the Canadian Arctic Shipping Pollution Prevention Regulations[9] and these are reproduced in Appendix A. The modification relates to the assumption regarding the magnitude of the residual/reaction stresses present, viz., they are assumed to be 20% of the yield strength instead of 60% (i.e. ß = 0.2 instead of 0.6).

The steel grade selected on the above basis for any structural member was also checked to ensure that near the weld itself, where residual stresses could be yield magnitude (ß = 1.0), brittle fracture could not initiate from small flaws (15% of plate thickness for thickness less than 50mm and 7.5mm for thickness greater than 50mm). This of course assumed that the weld metal and HAZ have the same fracture toughness as the base material, and that the empirical relationships are valid for these microstructurally different regions as well.

While the toughness requirements for structural steel in the proposed CASPR Regulations may be perfectly adequate, it was felt desirable to place these in the context of a broader fracture control plan, and to verify these taking into account service strain rates in the mid-ship regions.

However, in reassessing the fracture control plan for arctic ships, it must be remembered that:

(i) icebreakers have been navigating the arctic waters for several years, and except for Grade A steel, other steels conforming to IACS or ABS or DnV specifications have not posed any significant unstable fracture problems;

(ii) sole reliance on control of unstable fracture initiation places unduly stringent toughness and inspection/quality assurance demands on the weld zone, whereas sole reliance on arrest of long cracks (at -40°C) warrants special steels.

A judicious approach that has evolved with industry-government consensus for toughness requirements in the draft CSA S473 Standard "Code for the Design, Construction, and Installation of Fixed Offshore Structures, Part III - Steel", follows a philosophy of fracture prevention based on a combination of resistance to crack initiation, and resistance to crack propagation[10]. A similar approach for steel selection for arctic ships would require consideration of:

(i) **Prevention of initiation of unstable fractures from long fatigue cracks (with tips in base material) at strain rates encountered in midship regions (Figure 3(a)).**

(ii) **Prevention of initiation of unstable fracture from flaw tips located in the heat affected zone (Figures 3(b) and 3(c)).**

(iii) **Short crack arrest capability of structural steel and its heat affected zone**

There is a significant research effort being devoted globally to the subject of brittle fracture initiation resistance of weld metals and heat affected zones[11-14]. Some of these areas are quite complex and therefore instead of specifying toughness for complete prevention of brittle fracture initiation in the weld zone, this approach would focus on quality assurance to minimize flaw incidence, and a certain minimum level of toughness. As a result, there would be a finite but acceptably small probability of brittle fracture initiation in the weld zone.

Once the possibility of brittle fracture initiation from small flaws in the heat affected zone (or for that matter, weld metal) is accepted, then for flaws oriented perpendicular to the weld axis, these will need to be arrested in the base material. The steel toughness requirement for arresting relatively small cracks would of course be less than that for arresting long cracks.

However, flaws such as lack of sidewall fusion, hydrogen induced cold cracking, etc. can be in the heat affected zone, and oriented parallel to the weld axis. Once initiated, these cracks could propagate along the heat affected zone, or deviate into weld metal or base material. Whether they could be arrested in the heat affected zone or not is difficult to say, though it is conceivable that local brittle zones may not have that significant an effect on short crack arrest capability, as on brittle fracture initiation.

2.0 OBJECTIVES OF THE PRESENT INVESTIGATION

With the perspective described in the previous section, the focus of the present program has been to:

(i) assess, at an appropriate strain rate, the CTOD toughness of several grades/heats of steel that are typical of those used in the recent past for icebreaker fabrication, and that have their Charpy Vee Notch toughness close to the usual minimums specified for ship grade steels. These, and certain other requirements are listed in Table III(a), (b) and (c).

(ii) assess the plain strain crack arrest toughness of the selected steels using the recently established ASTM procedure E1221-1989.

(iii) assess the implications of the above for the draft regulations (CASPPR).

3.0 INVESTIGATION AND RESULTS

3.1 Steel Procurement

It was envisaged that four steels would be investigated in the project, the main objective being that their CVN toughness should be close to 25 to 40J in the temperature range 0° to -40°C. The objective was to assess the fracture toughness of steels when the CVN properties are near to the minimum specified.

These four steels, identified in the program as A, B, C (each 25mm thick), and D (50mm thick) were procured from one North American steel mill. A small amount of 50mm thick, Kawasaki MACS EH36 (Mod.) steel was also available and included in the investigation, its identification in the program being E. Finally, the relevant data for a steel, identified as WP and being investigated in another program[15], are also included to have an enlarged data base.

Steels A, B and D were evaluated in the transverse direction only, i.e. all specimens (tensile, CTOD, Compact Crack Arrest) had their longitudinal axis perpendicular to the rolling direction so that the fracture plane was parallel to the rolling direction. Steels E* and WP were tested in the longitudinal direction only, and steel C in both the longitudinal and the transverse directions.

3.2 Steel Characterization

All the steels were first characterized in terms of their chemical analyses, microstructure, hardness, and Charpy Vee Notch toughness. These findings are summarized below.

3.2.1 Chemical Composition of Steels

A small portion of material from each steel was removed and sent to an independent laboratory for chemical analysis. In addition to the usual elements specified in various regulations and specifications, oxygen and nitrogen analyses were also obtained. The results, along with the rolling practices for the steels, as indicated on mill test reports, are summarized in Table IV.

Two samples were analyzed for steel C to confirm that both the plates from this heat were indeed identical.

3.2.2 Metallography

One full thickness, ~40mm X 20mm specimen was removed from each steel to confirm the rolling direction, and to examine the microstructure. The rolling direction was confirmed to be as marked on the steel plates for plates A, B, C, D, and WP. Steel E did not have any rolling direction marked.

(*Only a limited amount of steel E was available, and in order to maximize the number of specimens that could be extracted, only one direction could be tested, which was initially assumed to be transverse but based on the CVN results and metallography, was found to be the longitudinal one).

The steel microstructures are shown in Figures 4 to 9. All the steels have a ferrite-pearlite microstructure. The main differences amongst them are in their ferritic grain sizes on account of the differing rolling practices, and in the amount of pearlite, which reflects the carbon content of the steels.

Steels A and B have the coarsest grain size ($\simeq$25μm) as they were hot rolled. Steels C and D had been normalized leading to ferritic grain size of $\simeq$15μm. Steel E has the finest grain size though the ferrite grain is slightly elongated on the longitudinal section.

3.2.3 Room Temperature Tensile Tests

Two round tensile specimens, 12.5mm diameter and 50mm gauge length were machined from the quarter thickness location of each steel, and tested at room temperature. The cross-head rate was .053 mm/s giving a strain rate of $\simeq 10^{-3}s^{-1}$. The results obtained are summarized in Table V.

Vickers hardness traverses (10kg load) were also performed on the sections mounted for metallography. The hardness was uniform through the thickness and did not differ between the longitudinal and the transverse sections. The average hardness for each steel is also shown in Table V.

3.2.4 Charpy Vee Notch Testing

Approximately twenty specimens were removed from each of the steels in both the transverse and longitudinal directions to establish the CVN transition curves for both directions. All specimens were extracted such that their axis lay at the steel plate's quarter thickness location. The specimens were standard size (10mm X 10mm X 55mm) and machined and tested as per ASTM E23.

The absorbed energies along with lateral expansion and percent shear values are reported in Tables VI to XI. The same data are also plotted in Figures 10 to 15. The smooth curves were visually drawn, and correspond approximately to the lower bound for the average CVN toughness value at each temperature. From the curves so drawn, transition temperature corresponding to any particular absorbed energy value can be determined, and Table XII in fact presents this summary for the various steels investigated.

3.2.5 Comparison of Steels Investigated With Ship Steel Specifications

Based on the results presented in the previous sections, and ship steel specifications as presented in Table III(a), (b) and (c), the nearest equivalent ABS grades for the steels investigated in the program are included in Table IV. The non-conformances for each steel are as follows:

Steel A : None

Steel B : Acceptable toughness in the longitudinal direction, but poor in the transverse direction. Would be acceptable if testing carried out in longitudinal direction only; steel should have been control rolled or normalized, but was not.

Steel C : Carbon content at the high end of the allowable product analysis.

Steel D : None

Steel E : None

Steel WP : None

3.3 Nil-Ductility Transition (NDT) Temperature

Following the procedures outlined in ASTM E208, up to eight specimens were tested to establish the NDT temperature for each steel. Their orientations were the same as selected for the CTOD tests reported later on. The specimens were size P2 (~130mm X 50mm X 19mm) and were machined such that they retained one of the original plate surfaces. Lincoln Wearweld electrodes were used to deposit the brittle beads, their hardness being typically HRC 45. The drop weight energies were 350J consistent with the yield strength of the steels.

The detailed results as well as the NDT temperature established for each steel is shown in Table XIII.

Steels A, B and WP are as rolled or control rolled, and have their NDT temperature in the range of -5° to -15°C; steels C and D are normalized and their NDT temperatures are in the -35° to -40°C range. Steel E, on the other hand, is an accelerated cooled one with excellent CVN toughness, and though it does have the lowest NDT temperature of all the steels (-55°C), it is still reasonably close to the NDT temperatures for the normalized steels.

3.4 Crack Tip Opening Displacement Tests

3.4.1 Selection of Strain Rate for Intermediate Loading Rate Tests

Since the primary objective of this program has been to assess the fracture toughness of ship structural steels at an intermediate loading rate that represents a maximum value that can be anticipated in the midship regions of icebreakers, literature was searched to review the experimental or theoretical findings in this regard. The available data is summarized in Table XIV.

It is clear that in the midship region of icebreakers, the strain rates are unlikely to exceed $5 \times 10^{-2} s^{-1}$. At the same time, it should be pointed out that local strain rates at the point of collision can be much higher. According to Nibbering[16], the shock energy is dissipated within a short distance from the point of impact or collision, and consequently, the strain rate experienced in midship region is much lower.

Since the time of the above literature review, Sumpter[17] and Machida et al[18] have also summarized the strain rates experienced in ship hull structures, and their findings, summarised in Tables XV(a) and (b), are consistent with the findings presented earlier in Table XIV.

3.4.2 Calculation of Cross-Head Rate for Intermediate Loading Rate CTOD Tests

The strain rate ($\dot{\varepsilon}$) data collected from various ships essentially signify the rate at which the stress (σ) increases. In the presence of flaws, this translates into a stress intensity factor rate, K, whose magnitude depends on the flaw size itself. Therefore, in order to simulate a certain strain rate or loading rate in the CTOD test procedure, a flaw of a certain size needs to be assumed to be present in the ship structure.

For the purposes of this calculation, the flaw size assumed is the same as in References 3 and 4, viz., a through thickness flaw of length (2a) equal to 250mm in an infinite plate.

For such a situation,

$$K = \sigma \sqrt{\pi a} \qquad \text{where } \sigma = \text{applied stress}, \; a = 125 \text{ mm}$$

$$\text{therefore, } \dot{K} = \dot{\sigma} \sqrt{\pi a}$$

$$= E \dot{\varepsilon} \sqrt{\pi a}$$

$$= 6537.6 \text{ MPa} \sqrt{\text{m}} \cdot s^{-1} \qquad \text{for } \dot{\varepsilon} = 5 \times 10^{-2} \qquad [1]$$

In a three point bend CTOD test, using B x 2B specimens where

B = specimen thickness,

Specimen width, $W = 2B$

Span, $S = 4W$

and crack depth, $a = 0.5W$,

$$\dot{K} = \frac{\dot{P} \cdot S}{B \cdot W^{1.5}} f(a/W) = 2.66$$

For $a/W = 0.5$, $f(a/W) = 2.66$

$$\dot{K} = \frac{8\dot{P}}{W^{1.5}} (2.66) \qquad [2]$$

The non-dimensional compliance C for B x 2B specimens has been shown by Faucher and Tyson(19) to be given by:

$$C = \frac{E \cdot B \cdot \dot{\Delta}}{\dot{P}} = 13 (1 - a/W)^{-2}$$

where $\dot{\Delta}$ = cross-head rate

$\dot{P}$ = loading rate

E = Young's modulus

and a/W is in the range 0.45 to 0.55.

Therefore, $$\dot{P} = \frac{E \cdot B \cdot \dot{\Delta}}{13} (1 - a/W)^2 \qquad [3]$$

Substituting the value $\dot{P}$ from Equation [3] into Equation [2],

$$\dot{K} = 42.36 \times 10^3 \, \dot{\Delta} \, W^{-0.5}$$

or, $$\dot{\Delta} = 2.36 \times 10^{-5} \cdot \dot{K} \, W^{0.5} \qquad [4]$$

Inputting the value of $\dot{K}$ from Equation 1,

$$\dot{\Delta} = 0.154 \, W^{0.5}$$

Therefore, in order to simulate in a CTOD test as defined above, a strain rate of 5×10^{-2} S^{-1} applied to an infinite plate containing a 250mm long through thickness flaw, the cross-heat rates need to be as follows:

Plate thickness:

25.4mm, $\dot{\Delta}$ = 34.8 mm/s

50.8mm, $\dot{\Delta}$ = 49.2 mm/s

It can be added at this stage that for the CTOD tests conducted at a quasistatic loading rate, the cross-head rates were 0.0127 and 0.0169 mm/s for 25.4 and 50.8mm thick plates, and following the calculations above, these correspond to strain rates of 1.83×10^{-5} and $1.72 \times 10^{-5} s^{-1}$, respectively.

3.4.3 CTOD Tests

Full thickness, BX2B CTOD specimens were machined from each of the steels investigated. The dimensions, fatigue precacking and subsequent test procedures corresponded to the British Standard BS5762.

Essentially, the fatigue precracking of the machine notched specimens was continued until the crack at the surface reached a limit of one half of the specimen width, i.e. a/W = 0.5. The final stage of the precracking ($\sim$1.5mm) was carried at a peak stress intensity factor of no more than 22 MPa$\sqrt{m}$. The specimens, enclosed in a chamber cooled with liquid nitrogen, were allowed to soak for at least ten minutes before commencement of the test.

All tests at the quasistatic loading rate were carried out at Fleet Technology laboratories whereas those at the intermediate loading rate were carried out at the Metals Technology Laboratories (CANMET). In order to take into account the increase in the steel's yield strength with strain rate, tensile tests were carried out at the intermediate 'strain rate' at MTL, and the results are summarized in Table XVI. The temperature dependence of yield strength was measured for the WP steel only and these data are tabulated in Table XVII. For the remaining steels, Irwin's formula given below was used to correct the yield strength (in MPa) for the effect of temperature.

Corrected Yield Strength = Room Temperature Yield Strength + $(10^5/(491 + 1.8T) - 189$

where T is the test temperature in °C.

The CTOD results at the quasistatic loading rate are summarized in Tables XVIII to XXIV. For specimens that exhibited some stable crack growth before unstable fracture, i.e. for specimens exhibiting δ_u behaviour, the extent of the crack growth is also tabulated. The three readings correspond to quarter, half and three-quarter thickness locations, respectively. Although several CTOD results are noted as invalid, in most cases, this was due to the crack length being marginally outside the allowable range, and the results are quite valid in the context of the objectives of the program.

The CTOD values at the intermediate loading rate as computed at MTL (CANMET) are shown in Table XXV, and a typical load versus crack mouth opening displacement trace is shown in Figure 16.

The results summarized in Tables XVIII to XXV are also shown plotted in Figures 17 to 23. In these figures, two curves have been drawn for each set of data (quasistatic and intermediate loading rates). The solid line plots represent the lower bound of all the data points, and the broken line plots are drawn as the approximate lower bound of the average of CTOD value at each test temperature. The transition temperature for a specific CTOD value can be read from these plots, and these are tabulated in Tables XXVI and XXVII.

3.5 Compact Crack Arrest Toughness Testing

It is only about two years ago that the procedure for determining compact crack arrest toughness of steels has been formalized in an ASTM Standard (E1221 "Standard Test Method for Determining Plane-Strain Crack Arrest Fracture Toughness, K_{Ia}, of Ferritic Steels"). The test procedure has been finalized only after a significant amount of round robin testing which apparently demonstrated that consistency and reproducibility of results was quite acceptable. Some of the results obtained by Ripling and Crossley[21] are shown in Figure 24.

In the present program, the dimensions of the specimen and test procedures conformed to ASTM E1221. The dimensions of the specimens tested are shown in Figure 25. All specimens were extracted such that the intended fracture plane in the specimens was the same as for the CTOD specimens, i.e. parallel to the rolling direction for steels A, B and D; perpendicular to rolling direction for steel WP; and both directions for steel C. Due to the limited material availability, this test was not carried out for steel E.

Specimen preparation involved squaring of the blank specimen, machining of the deep through thickness groove and the circular hole for seating the split pin and wedge for loading during the test. A brittle weld bead was deposited at the root of the deep grooves using Lincoln wearweld electrodes. A 3mm deep, ~0.4mm wide notch was electro-discharged machined into the weld bead, leaving nominally 4mm of the brittle weld bead. The brittle fracture of this ligament when the specimen is loaded in steps by the split pin-wedge arrangement, endeavours to inject a fast running crack into the test material. The energy required to initiate the crack in the brittle weld bead and the test material, and the distance it propagates into the test material due to energy dissipation are then used to calculate the plain strain compact toughness of the material. (The specimen is side-grooved before conducting the test in order to facilitate crack propagation in the plane, and to provide plain strain conditions.) The crack propagation distance into the test material was measured after heat tinting the specimen at 250°C for 1 hour. For all steels but one, the tests were conducted at -5° or -40°C, the design temperatures for below and above waterline regions respectively in icebreaking ships.

The results of the various tests conducted and the results obtained are shown in Table XXVIII(a) and (b), as well as in Figures 26 and 27.

In the case of steel WP, where several specimens could be tested, the effect of higher temperatures in increasing the crack arrest toughness is quite evident, especially above the NDT temperature, and the trend is similar to that obtained by Ripling and Crossley. For the remaining steels, however, there is significant scatter in data, and no trends are apparent.

Thus, steel B has the poorest CVN toughness of all the steels tested in the transverse orientation, yet at -5°C, its crack arrest toughness is apparently higher than that for steel A. Steel C did not give any valid values at -5°C, and perhaps it could be argued that the steel had too good an arrest toughness at this temperature (35°C above the NDTT) to be measured by this procedure. Steel D, on the other hand, gave acceptable results, presumably due to its larger thickness.

At -40°C, all steels gave valid results; however, their respective crack arrest toughnesses are broadly within the same range, average values being from 53.6 to 61 MPa$\sqrt{m}$. Surprisingly, steel A seems to have higher crack arrest toughness at -40°C than at -5°C, and this is comparable to that of steel C in the longitudinal direction.

4.0 DISCUSSION

4.1 Brittle Fracture Initiation Resistance Required

It has been recently argued by Sumpter[17] that to prevent brittle fracture initiation in ships, the base material should possess a fracture toughness of 125MPa$\sqrt{m}$ minimum determined at the appropriate minimum service temperature, material thickness and strain rate. This level of fracture toughness is sufficient to prevent brittle fracture initiation from ~1m long through thickness cracks in large plates subject to an applied stress of 100MPa maximum, and from 50mm long crack transverse to the weld axis and therefore subject to the 100MPa applied stress as well as up to 300MPa weld longitudinal stresses. In both cases, the crack tips are obviously located in the base material; and the residual/reaction stresses are assumed to be negligible for 1m long cracks, as crack tips are sufficiently far from the weld zone.

In the NKK approach, on the other hand, the allowable flaw size is only 250mm, but the sum of applied and residual stresses is assumed to be equal to the yield strength (α = 0.4 and β = 0.6) leading to a fracture toughness requirement of 147 to 220 MPa$\sqrt{m}$ for yield strength in the range 235 to 350 MPa. However, this fracture toughness is needed at a quasistatic rate only.

The fracture toughness requirement estimated in the NKK approach has several arbitrary assumptions and an objective approach would be to follow Sumpter though depending upon design and fabrication, the applied stress and residual/reaction stress values could be different.

In icebreakers, service stresses are unlikely to exceed 0.4 times the steel's nominal yield strength[23]. However, due to the greater opportunities to inspect icebreakers and repair, if necessary, during the off season, assumption of 1m long crack seems to be overly conservative and the authors feel that maximum allowable crack size of 250mm is quite reasonable. In contrast, the assumption of negligible reaction or residual stresses for 250mm long cracks may be non-conservative. The basis for this assumption by Sumpter et al is Sommerville's measurements reported earlier, wherein compressive residual stresses were introduced in the hull plate due to the welding of the longitudinal stiffeners. In reality of course, there are numerous other attachments and transverse stiffeners as well, and it is believed that reaction and residual stresses equal to 20% of the yield strength should be included in estimating the fracture toughness requirements. Based on these assumptions, the fracture toughness requirements and corresponding CTOD toughness requirements can be computed as follows:

Yield Strength (MPa)	2a (mm)	Applied Stress (MPa)	Reaction/Residual Stress (MPa)	Fracture Toughness Required (MPa$\sqrt{m}$)	CTOD Required (mm)
235	250	100	$.2\sigma_y$	92	.086
350	250	140	$.2\sigma_y$	125	.118
415	250	160	$.2\sigma_y$	149	.140

The CTOD values above have been computed using the equation

$$\delta = \frac{K^2}{m \bullet E \bullet \sigma_y}$$

where m = 2 for plain strain condition. The value of m is once again believed to be conservative since as mentioned earlier in Section 1.2, based on Japanese data comprising K_c and δ values on the same steels, the values of m were found to range from 2.2 to 5.0

From the above discussion, it is inferred that if steels with nominal yield strength of 350 MPa or less have a CTOD fracture toughness of 0.1mm at the minimum service temperature and the applicable strain or stress intensity rate, then the likelihood of brittle fracture initiation in the base plate from 250mm long cracks should be negligibly small. The 0.1mm CTOD criterion also seems reasonable as this point is usually at the lower knee of the transition curves and above this temperature, the CTOD toughness rises rapidly.

It should be noted that the fracture toughness represented by 0.1mm CTOD also affords protection against unstable fracture initiation for 50mm long crack subject to a total stress (applied and residual) equal to typical weld metal yield strength, as shown below:

Steel CTOD (mm)	Yield Strength (MPa)	Fracture Toughness (MPa$\sqrt{m}$)	2a (mm)	Total Allowable Stress (MPa)
0.1	235	99.5	50	354
0.1	350	121.2	50	432
0.1	415	132.0	50	471

The total allowable stress represents both the applied and residual stress components. Since a certain amount of mechanical stress relief of the longitudinal residual stresses can be expected after a few load cycles in service, these can be expected to reduce in magnitude to:

≈ Initial Residual Stress - Peak Service Stress
(≈ yield level)

so that during subsequent service, the total stresses will be approximately equal to the weld metal yield strength, which in turn is not expected to exceed the values given in the 'total allowable stress' column above for each of the three yield strength levels.

4.2 Fracture Toughness of the Steels in Relation to the 0.1mm CTOD (Int.) Criterion

Before assessing the steels investigated in this program with respect to the above criterion, it needs to be resolved if the 0.1mm CTOD transition temperature should be based on the lower bound curves (Table XXVI) or the lower bound curves through the averages at each temperature (Table XXVII). It is the author's opinion that the latter values should be used since there is already a considerable degree of conservatism due to the following:

(i) the intermediate loading rate CTOD toughness values have been determined at the upper limit for strain rate and stress intensity rate that is anticipated in the icebreaker midship region;

(ii) the CTOD specimens are highly constrained, and the CTOD values in wide plate tests have been shown to be larger than those determined from three point bend specimens by a factor of at least 3 (see Figure 28, also Ref. 15);

In light of the above, Table XXIX compares 0.1mm CTOD transition temperatures of the steels with their respective CVN transition temperatures for absorbed energies usually specified depending on the steel's yield strength and test orientation.

It is clear that the CVN transition temperature is not a good indicator for the 0.1mm CTOD transition temperature (intermediate loading rate) since the former usually under-estimates the latter. The largest unconservative differences are observed for steels E and WP; both of these have been tested in the longitudinal direction.

For steel E, this may be expected since it is known that accelerated cooled steels, though always having excellent CVN toughness, may not always show a corresponding improvement in other parameters to measure the fracture resistance, such as the NDT temperature. Similarly, steel WP may suggest that treatments such as controlled rolling increase CVN toughness far more than the fracture toughness measured by CTOD or similar tests. It could be further inferred that for the same CVN transition temperature, hot rolled steels have better fracture toughness than control rolled ones (steel WP versus steels A and B).

In the normalized steel C, the two transition temperatures are similar for both the orientations and one is tempted to attribute it to the normalizing heat treatment. However, this equality does not hold for the normalized steel D, partly due to the larger thickness of steel D.

Based on the 0.1mm intermediate loading rate CTOD criterion, it is noted that all steels meet the requirement at -5°C; however, at -40°, only steels C and E meet this requirement. Steel D fails to meet the criterion by 8°C in terms of the transition temperature or by $\simeq$.02mm CTOD at -40°C.

For the purposes of comparison only, the actual fracture toughness of the steels (quasistatic loading rate CTOD) is compared to the minimum value expected based on the NKK approach (see Table XXX). The latter gives fracture toughness as K_c and, these have been converted to CTOD, δ using

$$\delta = \frac{K^2}{m \bullet \sigma_y \bullet E} \qquad \text{where } m = 2$$

It is seen that these requirements are met (within 10%) for all steels except steels B and WP. For steel B, it could be argued that its CVN transition temperature is 30° higher than required by specification and therefore the minimum expected toughness at -40°C (0.21mm) should be met only at -10°C. The actual CTOD values of 0.2 and 0.17mm at -5° and -40°C are not that far from this requirement. For steel WP, however, the CTOD toughness is less than the minimum anticipated, and perhaps 'controlled rolling' is the only factor to which this might be attributed, as discussed before.

4.3 Specification for Structural Steels for Arctic Ship Hulls (Brittle Fracture Initiation Resistance)

Due to the costs involved, it may not always be practical to specify steel based on its fracture toughness at intermediate loading rates. It is therefore preferable to seek correlation with more simply measured toughness parameters that can be used for specification purposes. The three candidates in this regard are the CVN toughness, the NDT temperature and the quasistatic CTOD toughness.

To this end, Figure 29 shows CVN energy absorbed at the 0.1 and 0.2mm CTOD transition temperatures plotted against the corresponding CTOD transition temperatures, and based on this, it is difficult to specify a reasonable absorbed energy value at the design temperature that would also ensure that 0.1mm intermediate loading rate CTOD criterion, is also met.

A value of 40J could be considered, however, it would be nonconservative for steels E and WP. Further, the value would have to be equally applicable to the longitudinal and the transverse orientation.

The relationship between the intermediate loading rate CTOD transition temperature and the NDT temperature of the steels is shown in Figure 30. It is seen that there is a reasonable one to one correlation between the NDT temperature and the 0.1mm CTOD transition temperature. Thus, if the steel NDT temperature is specified to be equal to the design temperature, then five of the seven steels would meet the 0.1mm criterion, and two will be unconservative by only $\sim$3°C. Further, if the definition of the NDT temperature were to be changed from the highest break temperature (as in ASTM E208) to the lowest no-break temperature as in CSA S473 "Fixed Offshore Steel Structure" (a difference of 5°C), then all steels would meet the 0.1mm CTOD (intermediate loading rate) at the NDT/design temperature specification.

At this stage, it is also worthwhile to plot the fracture toughness of the steels against (T-NDTT) where T is the test temperature and NDTT is the nil ductility transition temperature, and compare the data to the design reference curves proposed by Pellini[26]. Since these are plotted in terms of 'K', the CTOD data obtained in this investigation were converted to K using the relationship

$$K^2 = m \bullet \sigma_y \bullet E \bullet \delta \qquad (m = 2)$$

The resulting plots are shown in Figures 31(a) and (b), and it is clear that the design reference curves do provide a lower bound for the data obtained in this investigation.

Finally, one could endeavour to draft toughness specifications in terms of CTOD, albeit at the quasistatic loading rate since that is how a vast majority of laboratories conduct the test. This requires an assessment of the shift in the 0.1mm CTOD transition temperature due to difference in the strain or stress intensity rate only. For the steels investigated in this program, the data are included in Table XXVII, and this shift is seen to range from 34° to 65°C at the 0.1mm CTOD level. It should be reiterated that this shift is due to a change in the stress intensity rate from $\sim$2.4 MPa$\sqrt{m}$ s^{-1} to 6538 MPa$\sqrt{m}$ s^{-1}, i.e. $\sim$3.5 orders of magnitude.

In literature, the effect of loading rate on fracture toughness has been reported in some detail by Barsom and Rolfe[25]. They evaluated the toughness of various steels at three strain rates, viz. quasistatic ($\dot{\varepsilon} = 10^{-5}s^{-1}$), intermediate ($\dot{\varepsilon} = 10^{-3}s^{-1}$) and dynamic $10s^{-1}$). Over this range of six orders of magnitude in strain rate, they found that shift in transition temperature range is given by

$$T_{shift}(°C) = 119.4 - 0.121\ \sigma_y$$

where σ_y is the yield strength in MPa. Moreover, based on the fracture toughness results at the intermediate loading rate, it seems that the shift is linearly related to the logarithm of the strain rate. Based on this assumption, the shift in transition temperature as a function of yield strength can be calculated to be as follows:

Yield Strength (MPa)	Shift between quasistatic and dynamic loading rate (°C)	Calculated shift between quasistatic and intermediate loading rate in this program (°C)
280	85.5	49
350	77.1	44
410	69.9	40

The observed shifts are in reasonable agreement with the calculated ones for steels B, C, D and WP. However, for steels A and E, they are significantly larger (more than 10°C).

All the same, the above calculations demonstrate that a 50°C shift in 0.1mm CTOD transition temperature could be assumed so that quasistatic CTOD tests would need to meet 0.1mm criterion at (design temperature -50°C).

In discussing the effect of loading rate on fracture toughness, it is pertinent to review other findings reported in the literature. As mentioned earlier, one of the earliest studies was due to Francis et al[7] and their results were presented in Table II. Though the stress intensity rate corresponding to the intermediate loading rate is quite close to the intermediate loading rate employed in this study, with respect to the quasistatic rate, it is higher by a factor of 250 only (2.4 orders of magnitude compared to the ~3.5 in this study). All the same, in Francis' study, the fracture toughnesses for the three ship steels at temperatures down to -40°C are quite good, the lowest value being 352 MPa$\sqrt{m}$ at the intermediate loading rate. Noticeable differences in fracture toughness at quasistatic and intermediate loading rates are observed only at -62°C. Unfortunately, the CVN properties and the NDT temperature of the steels are not available, and it is difficult to place this data in the context of the present program except perhaps to speculate the steels had very good toughness so that test temperature range is primarily in the upper shelf region.

The effect of loading rate on CTOD has also been examined in Japan[18], though the data is available for one steel only. For a 75mm thick, 380 MPa yield steel, the cross head rate was varied by two orders of magnitude (.015 and 1.5 mm/s), the corresponding stress intensity rates being ~2.8 and 280 MPa$\sqrt{m}s^{-1}$; the shift in 0.1mm CTOD transitions temperature was only about 10°C which is much lower than that calculated on the basis of the Barsom-Rolfe relationship.

A possible explanation may lie in the fracture toughness versus stress intensity rate results obtained by Sumpter et al[23] and reproduced in Figure 32. These authors concluded that fracture toughness exhibits a sudden transiion at around 10^3MPa$\sqrt{m}s^{-1}$; below this value, and over the range 5 X 10^3 to 5 X 10^4 MPa$\sqrt{m}s^{-1}$, the toughness is reasonably constant. However, the validity of such an argument may depend on the limited strain rate dependence of the yield strength at the test temperature.

Another obvious implication of this in regard to the present study is that the intermediate stress intensity rate used, 6537 MPa$\sqrt{m}s^{-1}$, is a conservatively high estimate of the stress intensity rate that could be encountered in the midship region, and it is believed that only in rare instances would the stress intensity rate exceed 1000 MPa$\sqrt{m}$ when its effect on fracture toughness may be more pronounced.

4.4 Statistical Significance of the Results

The discussion in the preceding sections has followed a deterministic approach wherein conservative values are assumed for the stresses, flaw size and the fracture toughness of the steel. In reality, each of these parameters has its own statistical distribution, and these can be subjected to statistical/reliability analysis to compute the probability of failure.

Such an exercise was indeed carried out as part of this program and it is summarized in Appendix B.

4.5 Significance of the Results With Respect to CASPPR

The steel selection requirements in CASPPR are included in Appendix A. It was considered worthwhile to assess the fracture toughness of the steels investigated in relation to the underlying assumptions of the CASPPR requirements regarding applied and residual stresses, flaw size, etc., assuming the steels were required to meet the grades indicated as closest equivalents in Table IV. This evaluation is included in Appendix C, and concludes that the current requirements are adequate from the point of view of resistance to brittle fracture initiation.

4.6 Compact Crack Arrest Behaviour

The results of the compact crack arrest tests for individual steels were presented earlier in Section 3.5. Because of the limited data, it is useful to examine the data base together and this can be done[21,26] by using the steel NDT temperature as the reference. Accordingly, Figure 33 shows the crack arrest toughness of various steels as a function of (test temperature - NDTT)°C. There is a fair amount of scatter in results and this could not be reduced by taking into account the dynamic yield strength of steels, i.e. by plotting log (K_a/σ_{yd}) vs. (T-NDTT), as proposed by Graville[27]. All the same, the data do show that below the NDTT temperature, there is relatively little change in the crack arrest toughness, whereas above the NDTT temperature, there can be a sharp increase. Steels A and D however, do not appear to conform to this trend. For steel D, this is partly attributable to its higher thickness, but for steel A, it must be treated as an anomaly since its crack arrest toughness values are higher at -40°C than at -5°C.

Looking at the data at the NDT temperature or below, it is noted that at -40°C, the average crack arrest toughness for all steels is $\simeq$59 MPa$\sqrt{m}$; and at the NDT temperature, the average crack toughness value, considering only the valid data points, is also $\simeq$59 MPa$\sqrt{m}$. In contrast, Ripling and Crossley[21] observed (see Figure 24) that at the NDTT temperature, the lower bound crack arrest toughness is $\simeq$70 MPa$\sqrt{m}$, the average value being closer to 80MPa$\sqrt{m}$. Considering that crack arrest toughness is expected to be similar to the dynamic fracture toughness of the steels and that at the NDT temperatures, the dynamic fracture toughness is proportional to the dynamic yield strength ($\simeq$525 MPa for 350 MPa static yield strength), then the crack arrest toughness should be of the order of 50 MPa$\sqrt{m}$ only. The values obtained in this investigation are much closer to this expected value than are those of Ripling and Crossley, for an even lower strength steel.

In contrast, Nagamoto[28] and Sumpter[17] have suggested that crack arrest toughness of the order of 150 to 200 MPa$\sqrt{m}$ is needed for long crack arrest. However, the focus of the fracture control methodology being proposed here in this context is the arrest of short cracks that might emanate from the weld zone.

In order to estimate the flaw size that may be arrested, let us assume a through thickness flaw of length 2a in an infinite plate; then

$$K_{ca} = \sigma\sqrt{\pi a}$$

$$\text{or } 2a = \frac{2K_{ca}^2}{\pi\sigma^2}$$

where K_{ca} = crack arrest toughness
= 59 MPa$\sqrt{m}$ at NDTT

and σ = stress including both the applied and residual stress components

In order to see the relationship between the flaw size that could be arrested at a given stress, the above equation has been plotted in Figure 34.

If one assumes yield level tensile residual stresses present in the weld, and peak applied stress level of approximately 130 MPa, then for a 350 MPa yield strength steel, $\sigma \simeq$ 480 MPa which means that a through thickness pop-in of a size of 10mm or less only could be arrested in the base material.

One could question the assumption of through thickness cracks, transverse to the weld, being present in the weld metal or heat affected zone, as such cracks, to begin with, are most likely to be semi-elliptical surface cracks. However, in the event of inadequate HAZ or weld metal initiation toughness, the crack is likely to pop, and propagate through the weld zone thickness so that the base material would be required to arrest a through thickness crack of length which is approximately equal to the weld width.

Clearly, if the crack arrest toughness of the steel is 59 MPa$\sqrt{m}$ or even 80 MPa$\sqrt{m}$ at the NDT temperature, it would not be sufficient to arrest such a crack, since for K_{ca} = 80 MPa$\sqrt{m}$ and σ = 480 MPa, the arrestable crack size, 2a, will be $\simeq$17mm. In a 25mm thick weld, full penetration butt welds would easily exceed this dimension.

At the same time, it should be recognized that a crack in such an orientation would be propagating out of the weld tensile residual stress field, thereby increasing the probability of crack arrest. Assuming residual stresses to be zero, the half length of the arrestable through thickness crack would be $\simeq$65mm, and it is quite conceivable that the residual stresses indeed would be zero or compressive at such a distance from the weld centreline.

Further, it should be noted that the compact crack arrest test determines a lower bound plain strain crack arrest toughness, and the actual crack arrest toughness may be somewhat higher. It is hoped that the investigation sponsored by CANMET/ CCG[15] wherein short crack arrest tests are being conducted on the 500mm wide panels, will shed more light on this.

It would therefore seem that a specification implying 0.1mm CTOD at an intermediate loading rate affords adequate protection against brittle fracture initiation and most likely against short crack arrest also, although the latter needs to be confirmed.

5.0 SUMMARY

The CTOD fracture toughness of several steels suitable for ship fabrication has been determined at the highest stress intensity rate anticipated in mid-ship region of icebreakers. These data are correlated with the steel's CVN toughness, NDT temperature and quasistatic loading rate CTOD toughness, and also compared with the fracture toughness values expected based on the NKK approach to specify ship steel toughness. The crack arrest toughness of the steels, using compact crack arrest specimens, has also been determined.

It is concluded, as a result of this investigation, that:

(i) steels demonstrating 0.1mm CTOD at the applicable intermediate stress-intensity rate and design temperature should possess adequate resistance to unstable fracture initiation;

(ii) the 0.1mm CTOD transition temperature (lower bound of averages) at the intermediate stress intensity rate of 6.3×10^3 MPa$\sqrt{m}s^{-1}$ correlates quite well with the steel's NDT temperature;

(iii) correlation with CVN properties is relatively poor. This lack of correlation with CVN properties seems to be related to the steel rolling practice, i.e. on line accelerated cooling and controlled rolling apparently enhance the CVN toughness far more than the improvement in the NDT temperature or the CTOD value. The CVN specifications therefore seem adequate for hot rolled and normalized steel (up to about 25mm thickness) but are not indicative of fracture toughness of thermomechanically treated steels;

(iv) although it is recommended in CASPRR that steel plates should have their rolling direction parallel to the principal stress direction, it cannot always be guaranteed in practice. It is therefore suggested that CVN quality control testing should always be performed in the transverse orientation, and the absorbed energy requirements should be the same as in the longitudinal direction;

(v) the shift in transition temperature with respect to the quasistatic loading rate is consistent with data of Barsom and Rolfe;

(vi) analysis of the results indicates that the steel toughness requirements in the proposed CASPR Regulations are adequate from the point of view of resistance to brittle fracture initiation;

(vii) the plain strain crack arrest toughness of the steels at their respective NDT temperatures is consistent with predictions, and approximately 60 MPa$\sqrt{m}$. The calculated maximum length of arrestable short running cracks (through thickness), based on plain strain crack arrest toughness, is relatively small ($\sim$9mm). The significance of these results for CASPPR is yet to be established.

6.0 REFERENCES

[1] Rolfe, S.T. et al, "Fracture Control Guidelines for Welded Steel Ship Hulls". U.S. Coast Guard, SSC Report 244 (1974).

[2] Pense, A.W., "Evaluation of Fracture Criteria for Ship Steels and Weldments". U.S. Coast Guard, SSC Report 307.

[3] Nippon Kaiji Kyokai Document submitted to IACS, "Minimum Service Temperature of Hull Structural Steels", July 1979.

[4] Yajima, H. and Tada, M., "Materials Selection for Hull Steel Plates Based on Fracture Toughness". Technical Review published by Nagasaki Technical Institute, Mitsubishi Heavy Industries, Ltd., Feb. 1981, p. 52.

[5] Tyson, W. et al, "Dynamic Toughness-Fracture Mechanics Interpretation of the Drop Weight (NDT) Test". International Journal of Fracture 25(1984), p.133-141.

[6] Bala, S.R. et al, "HAZ Toughness of Two Candidate Steels for Offshore Structures". Report submitted by AMCA International to CANMET/SSC; SSC File 23SQ.23440-4-9056.

[7] Francis, P.H. et al, "The Effect of Strain Rate on the Toughness of Ship Steels". U.S. Coast Guard, SSC Report 275 (1978).

[8] Sommerville, W.L. et al, "Measurement of Residual Stresses in Stiffened Panels". Journal of Strain Analysis, Vol. 12, No. 2, (1977).

[9] "Report of the Subcommittee on the Proposed Revisions to the Arctic Shipping Pollution Prevention Regulations", Coast Guard Northern Report TP 9981.

[10] Contract Report, "Toughness Requirements for Offshore Steel Structures Used in an Arctic Environment" (DSS File 233046-5012/01-GS, Aug. 1987); submitted by Sandwell, Swan, Wooster.

[11] "Statistical Significance of Local Brittle Zones in Heat Affected Zones of Welded Structures", Joint DSS/CANMET-Private Industry Sponsored Contract No. 23440-8-9207/01-SQ with Fleet Technology Limited (in progress).

[12] Proc. of the OMAE Conference, February 1988 - 4 Sessions on Local Brittle Zones in Heat Affected Zones.

[13] Fleet Technology Limited Final Report E62522C on "Effect of Welding Procedural Variables on Weld Metal Toughness" (DSS Contract OSQ85-00137 (1989)).

[14] Braid, J.E.M. et al, "Toughness of Weld Metals for Fabrication of Cold Marine Structures and Vessels". CANMET Report MTL88-25, April 1988.

[15] "Study of Wide Plate Tests of Structural Steels for Arctic Ships", CANMET/CCG/SSC Sponsored Project, SSC File No. 003SQ.23440-9-9014/A.

[16] Nibbering, J.J.W., "Brittle Fracture in Fatigue Loaded Structures: Influence of Shock Loads". Proc. of Study Session on Fracture Toughness Evaluation of Steels for Arctic Marine Use, Ottawa, October 1983.

[17] Sumpter, J.D.G. et al, "Fracture Toughness of Ship Steels". Paper No. 2, Spring Meeting, Royal Institute of Naval Architects (1988).

[18] Machida, S. et al, "Japanese Research Activities in Offshore Fracture Mechanics Applications", App. Mech. Rev., Vol. 41, No. 2, Feb. 1988, p. 96.

[19] Faucher, B. and Tyson, W.R., "A Comparison of Crack Mouth Opening and Load Line Displacement for J Integral Evaluation Using Bend Specimens". ASTM STP 856, pp.279-293, 1985.

[20] Jones, R.L. et al, "The Effect of Strain Rate on the Tensile and Fracture Properties of BS4360 'A' Grade Ship Steel". Fatigue Fracture Engineering Materials Structures, Vol. 14, No. 1, p.131-141 (1991).

[21] Ripling, E.J. and Crossley, "Crack Arrest Fracture Toughness of a Structural Steel (A36)". Welding Journal, March 1982, Vol. 61, No. 3, p. 65s.

[22] Remzi, E.M., "Crack Arrest Test Methods and Properties for Structural Steels". TWI Members Report 282/1985, August 1985.

[23] Sumpter. J.D.G., et al, "Rate and Size Effects on Fracture Toughness of Mild Steel". Presented at Canadian Fracture Conference 21, held at DREA, Halifax, April 1990.

[24] Pisarski, H.G. et al, "Comparison of HAZ Fracture Toughness Generated From CTOD and Wide Plate Tests". Proc. 8th International OMAE Conf., The Hague, March 1989.

[25] Barsom, S.T. and Rolfe, J.M, "Fracture and Fatigue Control in Structures - Application of Fracture Mechanics". Book published by Prentice Hall (1977).

[26] Pellini, W.S., "Guidelines for Fracture-Safe and Fatigue-Reliable Design of Steel Structures". Book published by TWI 1983.

[27] Graville, B.A., "Crack Arrest Requirements for Arctic Structures", Contract Report (DSS File 23440-8-9190/01-SQ).

[28] Nagamoto, R. et al, "Fracture Toughness of 50kg/mm^2 Class New CR Process Steel Plates". Bull. Soc. Naval Arch. of Japan, 152, p. 405-416.

TABLES

TABLE I: Minimum K_c Values of Steel Plates for Hull Use, Specified in IACS Rules (base metal)

(unit : kg, $\overline{mm}/mm^2$)

Steel	Grade	Temp. (°C)	Thickness (mm)								
			10	15	20	25	30	35	40	45	50
Mild steel	A	0	518	534	507	482	471	459	448	438	428
		−10	507	493	469	446	435	425	415	405	396
		−20	466	453	431	410	400	390	381	372	364
		−30	425	414	393	374	365	356	348	340	332
		−40	385	375	356	339	330	323	315	308	301
		−50	345	336	320	304	297	290	283	276	270
	B	0	628	594	578	548	534	520	507	482	471
		−10	581	549	534	507	493	481	469	446	435
		−20	534	505	491	466	453	442	431	410	400
		−30	487	461	448	425	414	403	393	374	365
		−40	441	417	406	385	375	365	356	339	330
		−50	396	374	364	345	336	328	320	304	297
	D	0	727	685	646	628	611	578	563	548	534
		−10	672	633	597	581	565	534	520	507	493
		−20	618	582	549	534	519	491	478	466	453
		−30	564	531	501	487	473	448	436	425	414
		−40	511	481	454	441	429	406	395	385	375
		−50	458	432	407	396	385	364	355	345	336
	E	0	1 168	1 084	1 009	974	941	880	851	824	798
		−10	1 080	1 003	933	901	870	814	787	762	738
		−20	993	922	858	828	800	748	723	700	678
		−30	906	841	783	756	730	682	660	639	619
		−40	820	762	709	684	661	618	598	579	560
		−50	736	684	636	614	593	554	536	519	503
50kg mm² class high-tensile steel ($\sigma_y \leq 32$kg mm²)	AH	0	711	676	643	627	598	584	571	553	545
		−10	658	625	595	580	553	540	528	516	504
		−20	605	574	546	533	508	496	485	474	463
		−30	552	524	499	487	464	453	443	433	423
		−40	500	475	452	441	420	410	401	392	383
		−50	448	426	405	395	377	368	360	352	344
	DH	0	913	867	837	792	770	750	730	711	693
		−10	844	820	774	732	712	694	675	658	641
		−20	776	753	711	673	655	637	621	605	589
		−30	708	688	649	614	598	582	566	552	538
		−40	641	623	588	556	541	527	513	500	487
		−50	575	559	528	499	486	473	460	448	437
	EH	0	1 255	1 173	1 135	1 064	1 031	999	969	941	913
		−10	1 160	1 085	1 049	984	953	924	896	870	844
		−20	1 066	997	964	904	876	849	824	799	776
		−30	973	910	880	825	800	775	752	729	708
		−40	881	824	797	747	724	702	681	661	641
		−50	791	739	715	671	650	630	611	593	575

TABLE II: Francis et al [7] Data on Effect of Strain Rate on Average Fracture Toughness (MPa√m) at Various Test Temperatures (Instrumented Dynamic Tear Specimens)

Steel	ABS-DS			ABS EH32			ABS-CS			ASTM A517-D		
Stress Intensity Rate MPa√m s^{-1}	23	5.7×10^3	1.8×10^6	23	5.7×10^3	1.8×10^6	23	5.7×10^3	1.8×10^6	23	5.7×10^3	1.8×10^6
-62°C	318	97		387	362		402	289				
-51°C							403	393				
-40°C	458	352		367	394		416	425		121	130	
-29°C	469	409		374	387		398	393	48	162	174	
-18°C	467	440		380	427		417	424	43	151	185	
0°C	473	513							144	185	162	
20°C				351	386		367	468	133	243	293	194

TABLE IIIA: Heat Treatment Requirements for Ship Steels

Grade	ABS	DnV	Lloyds
A	—	—	—
B	—	—	—
D	Normalize >35mm; control rolling permitted	Normalize >25.5mm Normalize >12.5mm***	Normalize or control roll >25mm
E	Normalize	Normalize	Normalize
AH32	Normalize >50mm	Normalize >19mm Normalize >12.5mm*** (control rolling allowed as a substitute)	Similar to DnV with minor differences
DH32	Normalize >25mm* Normalize >13mm**		
EH32	Normalize	Normalize	Normalize
AH36	Normalize >50mm	Normalize >19mm Normalize >12.5mm*** (control rolling allowed as a substitute)	Similar to DnV with minor differences
DH36	Normalize >25mm* Normalize >13mm**		
EH36	Normalize	Normalize	Normalize

* Al treated
** Nb or V treated
***Nb treated

TABLE IIIB: Minimum Yield Strength (MPa) Requirements for Ship Steels

Rules	Grade									
	A	B	D	E	AH32	DH32	EH32	AH36	DH36	EH36
ABS	235	235	235	235	315	315	315	360	360	360
DnV	265	—	265	265	315	315	315	355	355	355
Lloyds	235	235	235	235	315	315	315	355	355	355

TABLE IIIC: Minimum CVN Toughness (J @ °C) Requirements for Ship Steels (50.8mm or less)

Rules	Orientation	Grade									
		A	B (@ 0°C)	D (@ -10°C)	E (@ -40°C)	AH32 (@ 0°C)	DH32 (@ -20°C)	EH32 (@ -40°C)	AH36 (@ 0°C)	DH36 (@ -20°C)	EH36 (@ -40°C)
ABS	L	–	27J	27J	27J	34J	34J	34J	34J	34J	34J
	T	–	19J	19J	19J	23J	23J	23J	23J	23J	23J
DnV	L	–	–	27J*	27J	31J	31J	31J	34J	34J	34J
	T	–	–	20J*	20J	22J	22J	22J	24J	24J	24J
Lloyd	L	–	27J	27J	27J	31J	31J	31J	34J	34J	34J
	T	NOT SPECIFIED									

*For DnV, Grade D requirements are at -20°C.

TABLE IV: Chemical Analysis of Various Steels (wt %)

Steel Identity (Thickness, mm)	Nearest Eqvt. ABS Steel Grade	Rolling Practice*	C	Mn	Si	P	S	Cr	Ni	Cu	Al	V	Nb	N_2
A (25)	B	HR	0.18	0.96	0.23	0.013	0.013	N.A.	0.013	0.016	0.039	<0.002	<0.01	0.0052
B (25)	DH32	HR	0.17	1.2	0.23	0.016	0.015	N.A.	0.014	0.016	0.047	0.057	N.A.	0.0065
C-1 (25) C-2	EH36	N	0.23 0.23	1.22 1.25	0.22 0.24	0.012 0.012	0.018 0.020	N.A.	N.A.	0.02 0.02	0.04 0.04	0.03 0.04	N.A.	0.0058
D (50)	EH36	N	0.20	1.21	0.18	0.013	0.010	0.1	0.02	0.02	0.03	0.04	<0.01	0.0059
E (50)	EH Mod.	TMCP	0.07	1.3	0.27	0.008	0.005	N.A.	0.017	<0.01	0.039	<0.002	0.015	0.003
WP (25)	DH36	CR	0.17	1.07	0.23	0.018	0.012	0.13	0.10	0.20	0.043	0.055	<0.01	0.0066

*HR = Hot rolled; CR = Control rolled; N = Normalized; TMCP = Thermomechanical controlled processing; N.A. = Not Analyzed

TABLE V: Room Temperature Tensile Properties and Hardness of the Steels

Steel I.D.	Orientation	Upper Yield Strength (MPa)	Lower Yield Strength (MPa)	Ultimate Tensile Strength (MPa)	% Elongation	Avg. Hardness (HV_{10})
A	Transverse	—	280*	481	36.0	141
	Transverse	—	281*	481	37.0	(137 to 143)
B	Transverse	—	352*	547	31.0	175
	Transverse	—	354*	547	32.0	(163 to 186)
C	Transverse	363	353	539	34.5	
	Transverse	368	355	539	30.5	159
						(156 to 165)
	Longitudinal	344	332	544	33.5	
	Longitudinal	387	350	533	35.0	
D	Transverse	362	340	515	36.0	155
	Transverse	340	333	520	36.0	(136 to 169)
E	Longitudinal	431	404	490	33.0	165
	Longitudinal	436	417	507	29.0	(160 to 173)
WP	Longitudinal	401	373	543	31.0	172
	Transverse	386	376	544	29.0	(166-175)

(* 0.2% offset values)

TABLE VI: CHARPY V-NOTCH TEST RESULTS FOR STEEL A

TRANSVERSE				LONGITUDINAL			
Test Temp. °C	Absorbed Energy, J	Lat. Expan. (mm)	% Shear	Test Temp. °C	Absorbed Energy, J	Lat. Expan. (mm)	% Shear
+20	66	1.14	70	+20	121	1.80	70
+20	65	1.35	60	0	79	1.32	50
0	57	1.12	60	0	117	1.80	70
0	52	1.09	50	0	132	1.83	70
0	45	0.94	50	0	133	1.96	70
0	43	1.02	60	-10	113	2.06	80
-10	39	0.81	40	-20	54	1.02	30
-10	39	0.84	40	-20	33	0.61	20
-20	34	0.58	10	-30	58	1.17	40
-20	37	0.79	30	-30	61	1.14	30
-30	27	0.64	10	-40	60	1.12	30
-30	27	0.53	20	-40	15	0.43	10
-30	19	0.36	10	-40	56	1.09	50
-40	26	0.53	10	-50	11	0.51	10
-40	28	0.58	10	-50	19	0.36	30
-50	15	0.38	10	-50	45	0.51	20
-50	18	0.48	10	-60	15	0.25	10
				-60	11	0.30	10
				-70	12	0.86	20
				-70	5	0.23	10

TABLE VII: CHARPY V-NOTCH TEST RESULTS FOR STEEL B

TRANSVERSE				LONGITUDINAL			
Test Temp. °C	Absorbed Energy, J	Lat. Expan. (mm)	% Shear	Test Temp. °C	Absorbed Energy, J	Lat. Expan. (mm)	% Shear
+20	26	0.56	30	+20	141	1.85	70
+20	27	0.81	30	+20	138	1.78	70
+20	23	0.48	10	-10	92	1.50	50
0	18	0.46	10	-10	50	1.04	30
0	23	0.71	20	-20	98	1.50	60
-10	16	0.41	10	-20	77	1.32	40
-10	14	0.30	10	-20	77	1.27	50
-20	16	0.43	10	-20	72	1.19	30
-20	15	0.46	10	-30	58	0.94	40
-20	14	0.43	10	-30	56	1.07	30
-20	10	0.23	10	-40	45	0.79	20
-20	20	0.51	10	-40	39	0.71	20
-30	11	0.41	10	-50	28	0.74	30
-30	14	0.38	10	-50	33	0.74	20
-30	14	0.43	10	-50	8	0.28	10
-40	8	0.28	10	-50	27	0.64	10
-40	8	0.20	10	-60	10	0.30	10
-50	14	0.28	10	-60	5	0.25	20
-50	7	0.18	10	-70	12	0.28	10
				-70	10	0.28	10

TABLE VIII: CHARPY V-NOTCH TEST RESULTS FOR STEEL C

TRANSVERSE (PLATE C1)			
Test Temp. °C	Absorbed Energy, J	Lat. Expan. (mm)	% Shear
+20	60	1.30	50
+20	57	1.24	50
0	45	1.04	50
0	49	1.12	50
-10	39	0.91	40
-10	42	0.97	40
-20	34	0.86	40
-20	33	0.76	40
-40	25	0.56	10
-40	22	0.58	10
-40	22	0.64	20
-40	23	0.61	20
-60	20	0.46	10
-60	15	0.30	10
-70	18	0.38	10
-70	18	0.41	10

TRANSVERSE (PLATE C2)			
-40	24	0.66	20
-40	27	0.66	20
-40	24	0.56	20

TRANSVERSE (PLATE C3)			
-40	24	0.58	20
-40	20	0.53	20
-40	24	0.61	20

LONGITUDINAL (PLATE C1)			
Test Temp. °C	Absorbed Energy, J	Lat. Expan. (mm)	% Shear
0	129	1.93	80
0	133	1.98	100
-10	114	1.73	70
-10	76	1.35	40
-20	79	1.35	60
-20	90	1.47	60
-40	57	1.02	20
-40	60	1.07	20
-50	56	1.07	30
-60	33	0.79	10
-60	35	0.76	10
-70	25	0.51	10
-70	16	0.36	10
-80	8	0.33	10
-80	26	0.53	10
-80	28	0.71	20

LONGITUDINAL (PLATE C2)			
-40	66	1.24	50
-40	76	1.27	40
-40	60	1.09	40

LONGITUDINAL (PLATE C3)			
-40	50	1.04	40
-40	58	0.81	40
-40	71	1.32	50

TABLE IX: CHARPY V-NOTCH TEST RESULTS FOR STEEL D

TRANSVERSE				LONGITUDINAL			
Test Temp. °C	Absorbed Energy, J	Lat. Expan. (mm)	% Shear	Test Temp. °C	Absorbed Energy, J	Lat. Expan. (mm)	% Shear
+20	93	1.70	90	+20	142	2.03	100
+20	93	1.63	90	+20	139	2.08	100
0	43	1.22	50	-20	75	1.32	50
0	39	1.22	50	-20	84	1.37	50
-20	39	1.07	30	-20	103	1.73	50
-20	38	0.81	30	-40	66	1.19	40
-40	26	0.58	20	-40	65	1.19	40
-40	30	0.61	20	-50	50	1.02	20
-50	23	0.53	20	-50	43	0.81	20
-50	22	0.56	20	-60	16	0.38	10
-60	10	0.28	10	-60	25	0.53	10
-60	9	0.20	0	-70	18	0.43	10
				-70	9	0.25	5
				-70	9	0.20	5

TABLE X: CHARPY V-NOTCH TEST RESULTS FOR STEEL E

TRANSVERSE				LONGITUDINAL			
Test Temp. °C	Absorbed Energy, J	Lat. Expan. (mm)	% Shear	Test Temp. °C	Absorbed Energy, J	Lat. Expan. (mm)	% Shear
-40	136	2.59	NB	-30	144	2.34	100
-40	137	2.31	NB	-30	133	2.64	100
-60	122	2.44	NB	-80	137	2.36	100
-70	137	2.62	NB	-80	95	2.44	100
-70	144	2.44	NB	-90	94	2.62	100
-80	137	2.46	NB	-90	138	2.64	100
-80	130	2.59	NB	-90	18	0.30	10
-85	24	0.53	10	-100	119	2.34	100
-85	16	0.51	20	-100	12	0.33	10
-90	19	0.36	20	-100	14	2.62	100
-90	19	0.43	20	-100	7	0.18	10
-100	8	0.25	10	-100	140	2.69	100
-115	7	0.15	10	-100	12	0.36	30
				-110	11	0.36	30
				-110	134	2.72	100

TABLE XI: CHARPY V-NOTCH TEST RESULTS FOR STEEL WP

TRANSVERSE				LONGITUDINAL			
Test Temp. °C	Absorbed Energy, J	Lat. Expan. (mm)	% Shear	Test Temp. °C	Absorbed Energy, J	Lat. Expan. (mm)	% Shear
20	65	1.2	60	20	136	2.00	80
20	80	1.5	80	20	129	2.20	NB
10	60	1.18	40	0	122	1.68	60
10	61	1.25	50	0	123	1.78	60
0	49	1.05	40	0	129	1.70	70
0	57	1.25	50	0	126	1.68	60
-10	41	0.93	30	-20	85	1.50	30
-20	38	0.80	30	-20	58	1.00	20
-20	34	0.75	30	-20	84	1.33	40
-20	23	0.58	20	-20	56	0.88	30
-30	34	0.65	20	-20	73	1.25	30
-40	9	0.20	10	-40	70	1.25	30
-40	26	0.53	20	-40	66	1.15	30
-40	20	0.55	10	-40	78	1.38	20
-40	26	0.55	10	-40	68	1.08	20
-50	22	0.43	10	-50	14	0.33	0
-60	8	0.20	10	-50	35	0.30	10
-60	18	0.38	10	-50	16	0.30	0
-60	14	0.33	5	-60	30	0.63	10
-70	12	0.30	0	-60	14	0.30	0
-80	3	0.18	0	-60	18	0.40	0
-80	7	0.23	0	-60	24	0.53	0
				-60	19	0.33	0
				-60	9	0.25	0
				-70	9	0.28	0
				-70	11	0.23	0
				-70	9	0.25	0
				-70	14	0.40	0
				-80	8	0.23	0
				-80	9	0.25	0

TABLE XII: Summary of CVN Energy Absorbed Transition Temperatures (°C)

Steel	NDT Temp. (°C)	Transverse				Longitudinal		
		40J	34J	27J	23J*	40J	34J	27J
A	-15	-9	-14	-23	-40	-25	-29	-33
B	-5	>22	>22	22	10	-40	-44	-48
C	-40	-10	-19	-33	-38	-51	-58	-64
D	-35	0	-28	-40	-49	-45	-49	-54
E	-55	-78	-80	-82	-85	-105	-79	<-108
WP	-10 to -15	-10	-18	-26	-32	-34	-40	-44

*19J for Steel A

TABLE XIII: Results of NDT Drop Weight Tests (ASTM E208, P2 Size Specimen)

Steel I.D.	Temperature (°C)												NDT Temperature (°C)
	-55	-50	-45	-40	-35	-30	-25	-20	-15	-10	-5	0	
A			B	B		B		B	B	NB NB	NB		-15
B			B	B		B		B	B		B	NB NB	-5
C				B	NB NB								-40
D				B	B B	NB NB	NB						-35
E	NB B	NB NB											-55
WP (Plate 1) (Plate 2)								B	B	NB NB			-15
										B	NB,NB		-10

(B = Break; NB = No Break)

TABLE XV(a): Estimates for Strain Rates and Stress Intensity Rates Relevant to Various Ship Loading Conditions

Loading Condition	Strain Rate sec^{-1}	Time to Reach 100 MPa sec	Stress Intensity Rate, K $MPa\sqrt{m}/sec$
Hull girder bending under wave action	10^{-4}	5	5
Slamming (midships deck)	2.10^{-3}	250.10^{-3}	10^{2}
Slamming (forward deck)	2.10^{-2}	25.10^{-3}	10^{3}
Slamming (local hull plate)	6.10^{-1}	10^{-3}	3.10^{4}
Collision (local hull plate)	2	250.10^{-6}	10^{5}
Shock (whipping)	20	25.10^{-6}	10^{6}

TABLE XV(b): Examples of Strain Rate Acting on Various Steel Structures

Item		An order of strain rate (S^{-1})
Specimen	Static fracture toughness test	10^{-6} - 10^{-5}
	Dynamic fracture toughness test (K_{ID} test)	10^{+1}
Steel Structure	Deck or bottom of ship hull due to wave induced loading	10^{-4}
	Inner hull of ship due to sloshing or slamming	10^{-3}
	Offshore structure at the collision of a drift ice	10^{-2}
	Offshore structure at the collision of a supply vessel	10^{-2}
	Icebreaking vessel at the collision of an iceberg	10^{-1}
	Bridge	10^{-3}

TABLE XIV: Summary of Strain Rates Measured in Ships

Ship	Location	Strain Rate sec^{-1}	Comments	Reference
Sealand McLean SL-7 Containership	Midship (50' seas; whipping)	1.1×10^{-3}	3.2×10^{-3} if yield strain reached in 1/4 cycle of whipping (1.25 cycles/sec.)	(1) SSC-317 "Determination of Strain Rates in Ship Hull Structure: A Feasibility Study
Universe Ireland (Tanker)	Midship (Wave Induced)	5×10^{-6}		
Fotini L Ocean Bulk Carrier	Midship (Whipping)	9×10^{-4}		
Stevart Cost Gr Lake Ore Carrier	Midship (Springing)	5.1×10^{-4}		
Model Tests	---	3.2×10^{-2}	Model testing of collisions	(2) Chang, P.Y.; HARAD Report PS-284 506 Referred to in (1)above
Containership	---	6×10^{-3}	Analytical estimates based on collapse time of 0.18 sec in a collision	(3) Reckling, K.A.; "Overall Structural Response of a Ship Struck in a Collision" SSC-SNAME, ST-14, 1981
---	Midship	10^{-1}	Smallest load rise time estimated: 10ms. Assume corresponding increase in stress: 30 ksi	(4) SSC-307, Pense,A.W. "Evaluation of Fracture Criteria for Ship Steels in Weldments"
I.B. Sisu, Baltic Icebreaker	Bow	6×10^{-2} 10^{-1} to 1.4×10^{-1} 10^{-1}	- max. measured during ice impact - based on extreme strain rate distribution estimates - suggested to be used for analysis	(5) Kujala & Riska "Evaluation of Some Factors Influencing Materials Selection for Arctic Vessels", Ottava 1983
Kigoriak	---	3×10^{-2}	Icebreaking operation	Ghoneim and Johansson "Fracture Toughness Requirements for Arctic Steels in Static and Dynamic Applications" Ottava, 1983
MV Arctic	Hull	7.3×10^{-4}	Ice ramming	Hakala and Kivimaa "MV Arctic Ramming Tests Trials Report" Tech. Res. Centre of Finland Rpt.LAI-539B-84
Kigoriak Robert LeMeur	---	5×10^{-4} to 2×10^{-3}	Ice ramming	Letter Tue-Fee to John McCallum (1983)
Kigoriak MV Arctic Kigoriak MV Arctic Kigoriak MV Arctic	Deck Deck Bow Plate Bow Plate Bow Frame Bow Frame	2×10^{-3} max. 7×10^{-4} max. 3.2×10^{-2} max. 5×10^{-3} max. 1.3×10^{-2} max. 2.5×10^{-3} max.	Ice ramming	Letter to A. Murray of Fleet Technology (author unknown)
M.S. Attis	Bow	8.8×10^{-3} 6×10^{-4}	Sea slamming 2.5m aft across the bulkhead	Nibbering (1983) Ottava Conf.
---	---	5×10^{-3}	Slamming	Francis (1978)

TABLE XVI: Tensile Data - Intermediate ε

Specimen #	Temp. (°C)	Yield Strength (Lower) (MPa)	Yield Strength (Upper) (MPa)	UTS (MPa)	% Elongation (in 50mm)	Reduction in Area (%)
AT-52	20	353.5	353.5	536.9	25.6	59.6
AT-58	5	357.8	369.9	535.9	36.4	59.0
AT-56	-5	371.8	383.6	---	---	59.1
AT-57	-20	372.9	444.9	551.8	38.7	59.2
AT-54	-30	382.6	468.5	558.1	34.0	59.1
BT-45	20	393.8	408.3	578.4	25.8	57.8
BT-44	-5	428.3	441.2	603.3	29.2	54.6
BT-45	-40	475.9	514.7	628.2	29.0	52.7
BT-46	-50	486.3	522.9	633.2	27.2	56.0
CL-6	-40	461.2	580.5	626.9	33.4	65.8
CL-7	-50	477.8	609.9	635.9	28.2	63.9
CL-8	-60	496.4	607.3	645.7	37.9	63.9
CT-4	-20	442.1	540.5	616.0	34.8	57.1
CT-6	-30	458.1	527.0	625.4	28.4	56.8
CT-7	-40	468.3	576.8	632.4	28.7	56.5
CT-8	-50	484.6	593.5	641.4	30.7	56.6
CT-10	-60	504.4	606.8	649.8	28.7	54.9
DT-1	-5	421.1	540.2	588.6	31.3	59.8
DT-2	-10	426.3	517.3	589.5	29.3	61.1
DT-3	-20	434.0	550.2	590.5	32.5	59.9
DT-4	-40	469.7	553.2	611.1	33.0	60.1
DT-5	-60	495.2	609.2	625.4	31.2	60.1
ET-5	-40	521.3	585.4	608.2	29.1	80.1
ET-7	-60	550.7	666.0	660.4	27.3	76.8
ET-6	-80	579.6	638.7	635.0	26.6	76.8

TABLE XVII: Tensile Properties of Steel WP - Below Ambient Temperatures

Temp. (°C)	Specimen Orientation	Lower Yield Strength (MPa)	Upper Yield Strength (MPa)	Ultimate Tensile Strength	% Elongation
20	Longitudinal Transverse	373 376	401 386	543 544	31.0 29.0
-20	Longitudinal Transverse	388 390	391 413	576 576	33.5 35.0
-40	Longitudinal Transverse	400 391	455 433	586 572	31.5 32.0
-75	Longitudinal Transverse	432 443	482 460	623 622	33.5 35.0

TABLE XVIII: CTOD Results for Steel A (Quasistatic Loading Rate)

Specimen I.D.	Temp (°C)	a/W	B (mm)	W (mm)	RT Yield (MPa)	CTOD (mm)	Mode of Failure	Validity Check*	Stable Crack Growth (mm)
AT89	-30	0.518	25.37	50.80	280	0.592	U	Valid	2.06, 4.47, 3.33
AT90	-30	0.516	25.22	50.71	280	0.504	U	Valid	1.00, 1.54, 0.90
AT91	-50	0.529	25.32	50.72	280	0.629	U	Valid	1.58, 2.53, 1.25
AT92	-50	0.535	25.37	50.68	280	0.337	U	Valid	0.65, 0.87, 0.77
AT93	-70	0.525	25.28	50.79	280	0.131	C	Valid	
AT94	-70	0.521	25.37	50.76	280	0.319	U	Valid	0.57, 0.26, 0.45
AT95	-90	0.522	25.37	50.71	280	0.113	C	Valid	
AT96	-90	0.522	25.43	50.66	280	0.103	C	Valid	
AT97	-110	0.516	25.43	50.72	280	0.079	C	Valid	
AT98	-100	0.525	25.32	50.61	280	0.116	C	Valid	
AT99	-100	0.530	25.45	50.71	280	0.147	C	Valid	
AT110	10	0.536	25.02	50.39	280	0.666	M	Valid	
AT111	10	0.536	25.12	50.38	280	0.660	M	Valid	
AT112	-40	0.525	25.06	50.32	280	0.210	C	Valid	
AT113	-40	0.528	25.11	50.44	280	0.713	M	Valid	
AT114	-40	0.528	25.16	50.36	280	0.660	M	Valid	

*Valid for all eight requirements.

Invalid Codes:
1. K_f exceeds max. limit
2. Max. diff. between a_o1 and a_o3 > 5%W
3. $a_{max} - a_{min}$ > 10%W
4. Minimum fatigue crack length < 1.25mm or 2.5%W
5. a_o/W ratio not between 0.45 and 0.55
6. Slope of crack plane > 10°
7. Multinucleation effects present
8. a/W ratio not between 0.15 and 0.7

TABLE XIX: CTOD Results for Steel B (Quasistatic Loading Rate)

Specimen I.D.	Temp (°C)	a/W	B (mm)	W (mm)	RT Yield (MPa)	CTOD (mm)	Mode of Failure	Validity Check*	Stable Crack Growth (mm)
BT85	-10	0.451	25.41	50.75	352	0.176	C	Valid	
BT86	-10	0.520	25.45	50.78	352	0.243	M	Valid	
BT87	20	0.523	25.40	50.80	352	0.222	C	Valid	
BT88	20	0.533	25.41	50.85	352	0.257	M	Valid	
BT89	-30	0.527	25.49	50.83	352	0.262	M	Valid	
BT90	-30	0.529	25.49	50.81	352	0.192	C	Valid	
BT100	-50	0.514	25.38	50.75	352	0.072	C	Valid	
BT101	-50	0.522	25.44	50.74	352	0.228	U	Valid	0.67, 0.99, 0.78
BT103	-70	0.538	25.45	50.75	352	0.105	C	Valid	
BT104	-60	0.532	25.42	50.78	352	0.112	C	Valid	
BT105	-60	0.515	25.46	50.74	352	0.132	C	Valid	
BT106	-70	0.519	25.39	50.49	352	0.115	C	Valid	
BT108	-100	0.513	25.38	50.82	352	0.035	C	Valid	
BT107	-90	0.532	25.51	50.75	352	0.100	C	Valid	
BT110	-90	0.520	25.57	50.86	352	0.067	C	Valid	
BT109	-40	0.520	25.49	50.69	352	0.184	U	Valid	0.21, 0.73, 0.50

* Valid for all eight requirements

Invalid Codes:

1. K_f exceeds max. limit
2. Max. diff. between a_o1 and a_o3 > 5%W
3. $a_{max} - a_{min}$ > 10%W
4. Minimum fatigue crack length < 1.25mm or 2.5%W
5. a_o/W ratio not between 0.45 and 0.55
6. Slope of crack plane > 10°
7. Multinucleation effects present
8. a/W ratio not between 0.15 and 0.7

TABLE XX: CTOD Results for Steel C (Quasistatic Loading Rate, Longitudinal to the Rolling Direction)

Specimen I.D.	Temp (°C)	a/W	B (mm)	W (mm)	RT Yield (MPa)	CTOD (mm)	Mode of Failure	Validity Check	Invalidity Code	Stable Crack Growth (mm)
CL5	-20	0.590	24.32	48.92	387	0.823	M	Invalid	5	
CL15	-30	0.590	24.28	48.95	387	0.458	M	Invalid	5	
CL29	-40	0.571	24.32	49.02	387	0.900	M	Invalid	5	
CL30	-40	0.556	24.32	48.93	387	0.792	M	Invalid	5	
CL31	-60	0.572	24.33	49.01	387	0.348	U	Invalid	5	0.26, 0.47, 0.31
CL32	-60	0.557	24.33	48.98	387	0.842	M	Invalid	5	
CL33	-80	0.557	24.33	48.68	387	0.277	U	Invalid	5	0.27, 0.33, 0.23
CL34	-80	0.552	24.36	49.00	387	0.395	U	Invalid	5	0.70, 1.38, 1.15
CL35	-100	0.545	24.31	48.90	387	0.055	C	Valid		
CL36	-100	0.556	24.32	48.93	387	0.055	C	Invalid	5	
CL37	-90	0.548	24.30	48.87	387	0.317	U	Valid		0.38, 0.37, 0.32
CL38	-90	0.547	24.32	48.93	387	0.059	C	Valid		
CL39	-70	0.547	24.31	48.95	387	0.161	C	Valid		
CL40	-70	0.557	24.31	48.98	387	0.157	C	Invalid	5	
CL41	-70	0.548	24.26	49.01	387	0.166	U	Valid		

Invalid Codes:

1. K_f exceeds max. limit
2. Max. diff. between a_o1 and a_o3 > 5%W
3. $a_{max} - a_{min}$ > 10%W
4. Minimum fatigue crack length < 1.25mm or 2.5%W
5. a_o/W ratio not between 0.45 and 0.55
6. Slope of crack plane > 10°
7. Multinucleation effects present
8. a/W ratio not between 0.15 and 0.7

TABLE XXI: CTOD Results for Steel C (Quasistatic Loading Rate, Transverse to the Rolling Direction)

Specimen I.D.	Temp (°C)	a/W	B (mm)	W (mm)	RT Yield (MPa)	CTOD (mm)	Mode of Failure	Validity Check	Invalidity Code	Stable Crack Growth (mm)
CT33	-30	0.559	24.38	48.70	365	0.368	M	Invalid	5	
CT34	-30	0.548	24.30	48.76	365	0.373	M	Valid		
CT35	-60	0.556	24.24	48.73	365	0.351	M	Invalid	5	
CT36	-60	0.547	24.33	48.81	365	0.340	M	Valid		
CT37	-80	0.564	24.35	48.67	365	0.112	C	Invalid	5	
CT38	-80	0.555	24.17	48.32	365	0.234	C	Invalid	5	
CT39	-100	0.558	24.37	48.69	365	0.067	C	Invalid	5	
CT40	-70	0.551	24.36	48.77	265	0.389	M	Invalid	5	
CT41	-100	0.547	24.24	48.68	365	0.046	C	Valid		
CT42	-90	0.556	24.37	48.68	365	0.064	C	Invalid	5	
CT43	-90	0.540	24.30	48.69	365	0.237	U	Valid		0.41, 0.40, 0.11
CT44	-70	0.547	24.40	48.77	365	0.334	U	Valid		1.30, 1.98, 0.86
CT45	-75	0.548	24.31	48.78	365	0.233	U	Valid		0.45, 0.63, 0.19
CT46	-120	0.559	24.35	48.67	365	0.016	C	Invalid	5	

Invalid Codes:

1. K_f exceeds max. limit
2. Max. diff. between a_o1 and a_o3 > 5%W
3. $a_{max} - a_{min}$ > 10%W
4. Minimum fatigue crack length < 1.25mm or 2.5%W
5. a_o/W ratio not between 0.45 and 0.55
6. Slope of crack plane > 10°
7. Multinucleation effects present
8. a/W ratio not between 0.15 and 0.7

TABLE XXII: CTOD Results for Steel D (Quasistatic Loading Rate)

Specimen I.D.	Temp (°C)	a/W	B (mm)	W (mm)	RT Yield (MPa)	CTOD (mm)	Mode of Failure	Validity Check	Invalidity Code	Stable Crack Growth (mm)
DT26	-40	0.538	49.12	98.18	352	1.065	U	Valid		
DT28	-40	0.563	48.97	98.34	352	1.177	U	Invalid	5	3.57, 3.77, 2.44
DT29	-60	0.589	49.15	98.32	352	0.121	C	Invalid	5	
DT30	-40	0.547	49.06	98.40	352	0.624	U	Valid		1.97, 2.04, 1.45
DT31	-60	0.556	48.78	98.34	352	0.148	C	Invalid	5	
DT33	-60	0.554	48.84	98.53	352	0.292	U	Invalid	5	0.65, 0.49, 0.59
DT34	-60	0.544	49.05	98.30	352	0.095	C	Valid		
DT35	-50	0.553	49.00	98.32	352	0.814	U	Invalid	5	2.17, 2.64, 1.58
DT36	-50	0.550	48.97	98.32	352	0.519	U	Invalid	5	1.47, 1.13, 1.74
DT37	-70	0.557	48.88	98.32	352	0.146	C	Invalid	5	
DT38	-70	0.551	48.90	98.30	352	0.155	C	Invalid	5	
DT39	-60	0.559	47.83	95.71	352	0.288	U	Invalid	5	0.40, 0.55, 0.14
DT40	-70	0.557	47.88	95.86	352	0.088	C	Invalid	5	
DT56	-90	0.508	51.21	101.49	352	0.147	C	Valid		
DT57	-10	0.519	51.46	101.70	352	0.989	M	Valid		
DT54	-80	0.498	51.36	101.73	352	0.042	C	Valid		
DT55	-80	0.519	51.33	101.55	352	0.090	C	Valid		
DT53	-10	0.507	51.46	101.78	352	1.194	M	Valid		
DT58	-20	0.522	51.18	101.60	352	1.194	M	Valid		

Invalid Codes:

1. K_f exceeds max. limit
2. Max. diff. between a_c1 and $a_c3 > 5\%W$
3. $a_{max} - a_{min} > 10\%W$
4. Minimum fatigue crack length < 1.25mm or 2.5%W
5. a_c/W ratio not between 0.45 and 0.55
6. Slope of crack plane > 10°
7. Multinucleation effects present
8. a/W ratio not between 0.15 and 0.7

TABLE XXIII: CTOD Results for Steel E (Quasistatic Loading Rate)

Specimen I.D.	Temp (°C)	a/W	B (mm)	W (mm)	RT Yield (MPa)	CTOD (mm)	Mode of Failure	Validity Check	Invalidity Code
ET1	-60	0.585	45.88	92.02	434	2.621	TS	Invalid	5
ET2	-80	0.605	46.25	91.97	434	1.749	U	Invalid	5
ET3	-80	0.605	45.89	91.93	434	0.346	U	Invalid	2,5
ET6	-60	0.561	46.07	92.15	434	2.917	TS	Invalid	5
ET12	-110	0.557	45.94	91.74	434	0.115	C	Invalid	2,5
ET16	-110	0.552	46.00	91.89	434	0.088	C	Invalid	5

*Stable crack growth could not be measured due to the considerable deviation of the fracture plane from the fatigue plane.

Invalid Codes:

1 K_f exceeds max. limit
2 Max. diff. between a_o1 and $a_o3 > 5\%W$
3 $a_{max} - a_{min} > 10\%W$
4 Minimum fatigue crack length < 1.25mm or 2.5%W
5 a_o/W ratio not between 0.45 and 0.55
6 Slope of crack plane > 10°
7 Multinucleation effects present
8 a/W ratio not between 0.15 and 0.7

TABLE XXIV: CTOD Results for Steel WP (Quasistatic Loading Rate)

Sample	Temp. (°C)	a/W	B (mm)	W (mm)	Yield Strength (MPa)	CTOD (mm)	Mode of Failure	Validity Check	Invalidity Code	Stable Crack Growth (mm)
L8	-5		26.13	50.75	390	.878	u	VALID		1.52, 2.10, .61
L34	-5		26.20	50.66	390	1.009	m	VALID		
L2	-5		26.11	50.76	390	.678	u	VALID		.56, .98, .62
L44	-20	.515	26.05	50.84	395	.091	c	VALID		
L50	-20	.496	26.09	50.86	395	.151	c	VALID		
L39	-20	.548	26.04	50.58	395	.165	c	VALID		
L51	-20	.528	26.21	50.74	395	.956	u	VALID		.96, 1.59, 1.15
L3	-20	.534	26.16	50.74	395	.117	c	VALID		
L5	-40	.509	26.11	50.83	420	.357	u	VALID		.09, .12, .24
L18	-40	.507	26.13	50.77	420	.247	c	VALID		
L20	-40	.507	26.23	50.76	420	.199	c	VALID		
L32	-40	.489	26.22	50.78	420	.275	u	VALID		.11, .17, .13
L23	-40	.526	26.21	50.80	420	.153	c	VALID		
L25	-40	.506	26.06	50.66	420	.344	u	VALID		.23, .21, .16
L26	-55	.564	26.17	50.78	435	.101	c	INVALID	5	
L7	-55	.564	26.11	50.70	435	.129	c	INVALID	5	
L28	-55	.508	26.15	50.63	435	.095	c	VALID		
L16	-55	.499	26.17	50.74	435	.064	c	VALID		
L17	-55	.501	26.07	50.85	435	.247	u	VALID		.07, .19, .20
L9	-55	.519	26.03	50.80	435	.096	c	VALID		
I12	-75	.520	26.17	50.73	454	.071	c	VALID		
I15	-75	.512	26.15	50.82	454	.056	c	VALID		
I14	-75	.517	26.21	50.70	454	.063	c	VALID		

Invalid Codes:
1 K_q exceeds max. limit
2 Max. diff. between a_o1 and a_o3 > 5%W
3 $a_{max} - a_{min}$ > 10%W
4 Minimum fatigue crack length < 1.25mm or 2.5%W
5 a_o/W ratio not between 0.45 and 0.55
6 Slope of crack plane > 10°
7 Multinucleation effects present
8 a/W ratio not between 0.15 and 0.7

TABLE XXV: CTOD Results for All the Steels at Intermediate Loading Rate

Temp. (°C)	CTOD, mm						
	AT	BT	CL	CT	DT	ET	WP
40							1.1942m
20 20 20	1.9821m	0.7008m 0.2490u					0.3359u 0.3803u 1.1587m
15 15					1.3077m 1.2480m		
10 10 10							0.2395u 0.4147u 0.1826u
5 5	0.4822m 0.2582u				1.3874m 1.3074m		
0 0							0.1261c 0.1131c
-5 -5 -5	0.5423u 0.5738u 0.8520m	0.1660u 0.2632u 0.2225u	1.7926m 1.7897m 1.7850m	1.6438m 1.6587m 1.5957m	1.3169m 1.3750m		
-10 -10					0.3693u 0.4346u		
-20 -20 -20	0.1320c 0.1235c 0.0779c	0.0969c 0.0841c 0.0806c	0.7948u 1.7478m 1.7710m	1.1141m 0.3181u 1.6392m	0.1557c 0.1381c	1.8187m	0.0274c 0.0761c
-30 -30 -30	0.1941u 0.2275u 0.0915c		1.8574m 1.7982m 1.7949m	1.2390u 1.1504u 0.9323u		1.7700m	
-40 -40 -40		0.0498c 0.0488c 0.0460c	0.7848u 0.1206c	0.1088c 0.0692c 0.1206c	0.1004c 0.0939c	0.6298u 0.2468u	0.0960c
-50 -50 -50		0.0383c 0.0281c 0.0442c	0.0143c 0.1194c 0.3379u	0.1522c 0.1426c 0.0899c			
-60 -60 -60			0.0336c 0.0836c 0.1181c	0.0966c 0.0683c 0.0715c	0.0676c	0.1122c	
-80						0.0142c	

TABLE XXVI: Transition Temperature (°C) for Various CTOD Toughness Values (Lower Bound Transition Curves)

Steel	0.1mm CTOD			0.15mm CTOD			0.2mm CTOD			NDTT
	Q.S. Rate	Int. Rate	Shift	Q.S. Rate	Int. Rate	Shift	Q.S. Rate	Int. Rate	Shift	°C
A	-56	-4	52	-49	0	49	-43	3	46	-15
B	-38	-14	24	-20	-3	17	6	8	2	-5
C (Long)	-76	-39	37	-66	-36	30	-55	-31	24	-40
C (Trans)	-79	-33	46	-71	-28	43	-63	-26	37	
D	-63	-24	39	-57	-14	43	-53	-8	45	-35
E	-100	-52	48	-91	-46	45	-85	-42	43	-55
WP	-23	-2	21	-17	6	23	-14	12	26	-10 to -15

Q.S. = Quasistatic Strain Rate
Int. Rate = Intermediate Strain Rate

TABLE XXVII: Transition Temperature (°C) for Various CTOD Toughness Values
(Approximate lower bound curve through the average at each temperature)

Steel	0.1mm CTOD			0.15mm CTOD			.2mm CTOD			NDTT
	Q.S. Rate	Int. Rate	Shift	Q.S.	Int. Rate	Shift	Q.S.	Int. Rate	Shift	°C
A	-95	-30	65	-82	-13	69	-73	-8	65	-15
B	-74	-18	56	-55	-10	45	-22	-5	17	-5
C (Long.)	-90	-56	34	-78	-51	27	-70	-47	23	-40
C (Trans.)	-92	-40	50	-83	-37	46	-78	-33	45	
D	-72	-32	40	-67	-20	47	-60	-16	44	-35
E	-110	-58	52	-106	-52	56	-101	-50	51	-55
WP	-53	-7	46	-38	0	38	-30	5	35	-10 to -15

TABLE XXVIII(A): Results of Compact Crack Arrest Tests (ASTM E1221)

Steel	Specimen	Temp. (°C)	Cycles to Failure	Initiation Stress Intensity, MPa √m	Crack Arrest Toughness, MPa √m	Validity	Invalidity Code*	Comments
A (Trans.)	AT101	-5	5	93.9	52.7	INVALID	4	No fracture
	104	-5	2	122.0	56.0	VALID		
	106	-5	2	78.1	59.7	VALID		
	105	-40	1	80.7	59.1	VALID		
	108	-40	1	84.3	65.0	VALID		
	109	-40	2					
B (Trans.)	BT114	-5	1	113.1	62.9	VALID		
	118	-5	2	129.1	96.5	INVALID	3	
	119	-5	5	167.5	94.0	INVALID	3	Crack left fracture notch
	111	-40	1	90.4	52.1	VALID		
	113	-40	1	92.2	57.4	VALID		
	117	-40	1	98.4	51.4	VALID		
C (Trans.)	CT1	-5	5	–	–	INVALID	4	No fracture
	4	-5	5	–	–	INVALID	4	No fracture
	5	-5	5	–	–	INVALID	4	No fracture
	2	-40	1	99.3	57.3	VALID		
	6	-40	1	117.4	49.9	VALID		
	8	-40	1	104.1	59.4	VALID		
C (Long.)	CL1	-5	5	–	–	INVALID	4	No fracture
	4	-5	5	–	–	INVALID	3,4	No fracture
	7	-5	3	184.4	105.9	INVALID		
	3	-40	1	112.4	83.2	VALID		
	4	-40	1	87.2	46.1	VALID		
	8	-40	1	99.9	54.9	VALID		
D (Trans.)	DT3	-5	5	170.0	51.0	INVALID		
	5	-5	1	107.0	78.1	VALID		
	1	-40	1	84.0	62.6	VALID		
	2	-40	1	75.7	50.2	VALID		
	6	-40	1	95.6	56.3	VALID		
	4	-5	3	118.3	59.6	VALID		

*Invalidity Codes

1 $W-A_o>0.15W$
2 $W-A_o>(Ka/YS_d)^2$
3 $B>(K_a/YS_d)^2$
4 $A_o-A_o>2N$
5 $A_o-A_o>(Ka/YS_d)^2$

TABLE XXVIII(B): Results of Compact Crack Arrest Tests for Steel WP (ASTM E1221)

Specimen	Temp (°C)	Cycles to Failure	Initiation Stress Intensity, MPa √m	Crack Arrest Toughness, MPa √m	Validity Check	Invalidity Code*
CCA2	0	6	186.2	165.9	INVALID	
CCA3	-40	2	109.5	58.2	VALID	2
CCA4	-20	2	116.6	69.0	VALID	
CCA5	0	3	148.6	87.7	VALID	
CCA6	-40	1	117.1	66.9	VALID	
CCA7	-20	2	111.7	74.6	VALID	
CCA9	-40	1	117.9	81.4	VALID	
CCA10	-60	1	90.1	46.3	VALID	
CCA11	-60	1	109.2	59.4	VALID	
CCA12	-60	1	94.1	61.8	VALID	
CCA13	0	6	235.7	87.0	INVALID	1, 2
CCA14	18	6	269.4	156.2	INVALID	2
CCA15	18	6	272.2	137.9	INVALID	2
CCA16	-20	2	128.2	59.8	VALID	
CCA17	0	6	182.8	111.5	VALID	
CCA18	-80	1	82.8	52.3	VALID	
CCA19	-80	1	81.7	59.3	VALID	

*Invalidity Codes

1 $W-A_o>0.15W$
2 $W-A_o>(Ka/YS_d)^2$
3 $B>(K_a/YS_d)^2$
4 $A_a-A_o>2N$
5 $A_a-A_o>(K_a/YS_d)^2$

TABLE XXIX: Comparison of CTOD and CVN Transition Temperatures

Steel and Orientation	0.1mm Int. Loading Rate CTOD Transition Temp. °C	CVN* Transition Temp. °C	Difference (Conservatism)
A(T)	-30	-40	-10
B(T)	-18	+10	+28
C(L)	-56	-58	-2
C(T)	-40	-38	+2
D(T)	-32	-49	-17
E(L)	-58	-105	-47
WP(L)	-7	-40	-33

*19J for Transverse orientation for Steel A

*23J for Transverse orientation for Steels B, C, D

*34J for Longitudinal orientation for Steels C and WP

*40J for Longitudinal orientation for Steel E

TABLE XXX: CTOD Toughness of the Steels in Relation to That Expected Based on NKK Formulation

Steel and Orientation	Nearest Eqvt. ABS Grade and CVN Test Temp.	CVN Reqmts. Satisfied at °C	Min. Quasistatic Rate Fracture Toughness for the nearest equivalent BS Grade calculated from NKK Formulation MPa√m (CTOD, mm)		Actual CTOD, mm			
					Quasistatic		Intermediate Rate	
			@ -5°C	@ -40°C	-5°C	-40°C	-5°C	-40°C
A (Trans.)	B (0°C)	-40	164 (0.23)	120 (0.12)	.65	.48	.20	<.10
B (Trans.)	DH32 (-20°C)	+10	242 (0.40)	175 (0.21)	.20	.17	.20	.05
C (Trans.)	EH36 (-40°C)	-38	330 (0.74)	241 (0.40)		.36	1.6	.10
CL (Long.)	EH36 (-40°C)	-58	330 (0.74)	241 (0.40)	.80	.50	.18	.50
D (Trans.)	EH36 (-40°C)	-49	279 (0.58)	204 (0.30)	≃1.0	≃0.9	>.4	.08
E (Long.)	EH36 (Mod.) (-60°C)	-105	279 (0.46)	204 (0.25)		≃3.0	>.15	≃0.40
WP (Long.)	DH36 (-20°C)	-40	248 (0.40)	181 (0.21)	≃0.8	≃.12	≃.10	≃.05

FIGURES

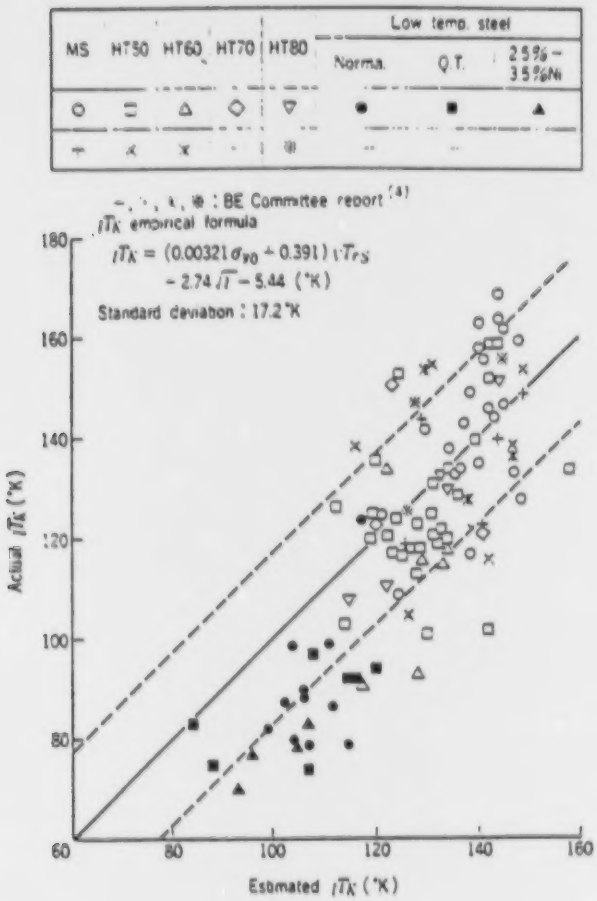

Figure 1: Measured and estimated values of critical temperature for brittle fracture initiation (base material) (Reproduced from Ref. 4)

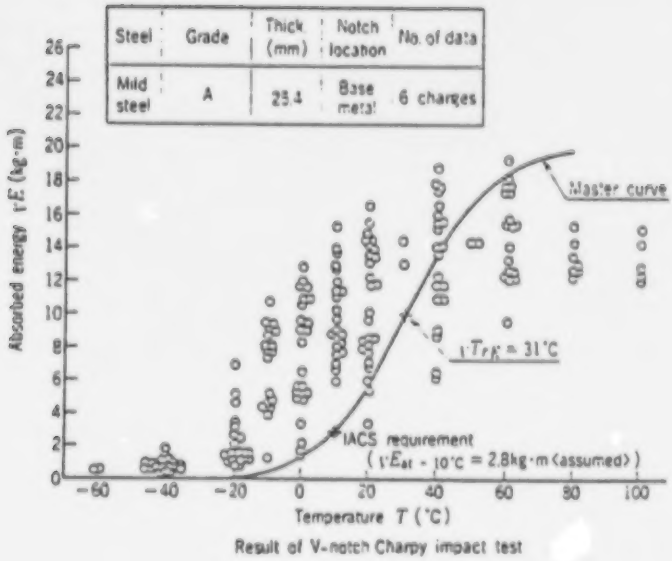
Steel | Grade | Thick. (mm) | Notch location | No. of data
Mild steel | A | 25.4 | Base metal | 6 charges
Absorbed energy vE (kg·m)
Master curve
vTrK = 31°C
IACS requirement
(vEat = 10°C = 2.8kg·m (assumed))
Temperature T (°C)
Result of V-notch Charpy impact test

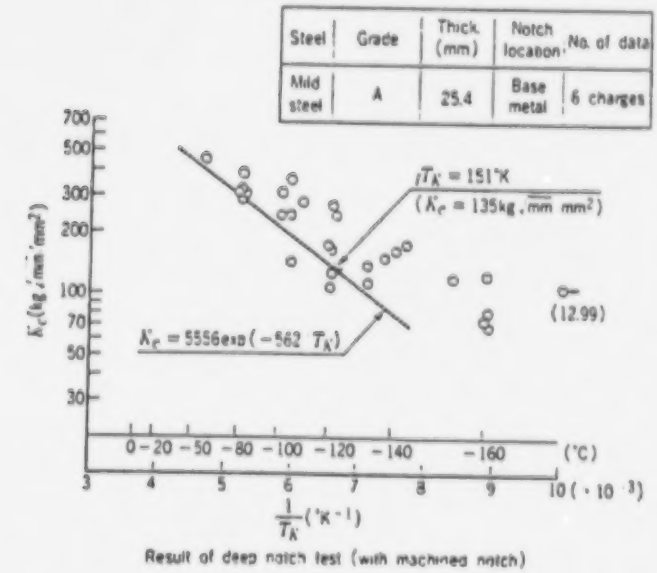
Steel | Grade | Thick. (mm) | Notch location | No. of data
Mild steel | A | 25.4 | Base metal | 6 charges
Kc (kg/mm^-3/2)
TK = 151°K
(Kc = 135kg/mm^-3/2)
(12.99)
Kc = 5556exp(−562 TK)
0 −20 −50 −80 −100 −120 −140 −160 (°C)
3 4 5 6 7 8 9 10 (·10^-3)
1/TK (°K^-1)
Result of deep notch test (with machined notch)

Figure 2(a): Measured and estimated values of fracture toughness of Grade A mild steel plate for hull use (25mm thick) (Reproduced from Ref. 4)

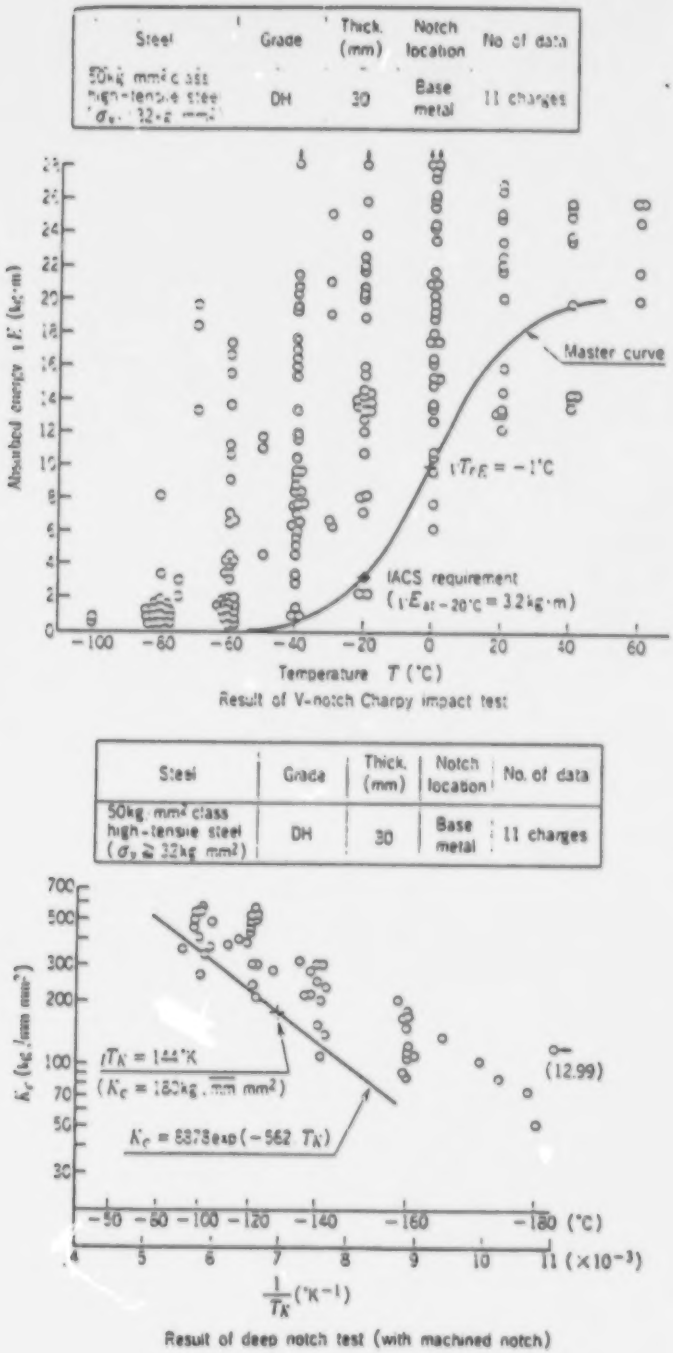

Figure 2(b): Measured and estimated values of fracture toughness of 50 kg/mm² class Grade DH high tensile steel plate for hull use (25.4mm thick) (Reproduced from Ref. 4)

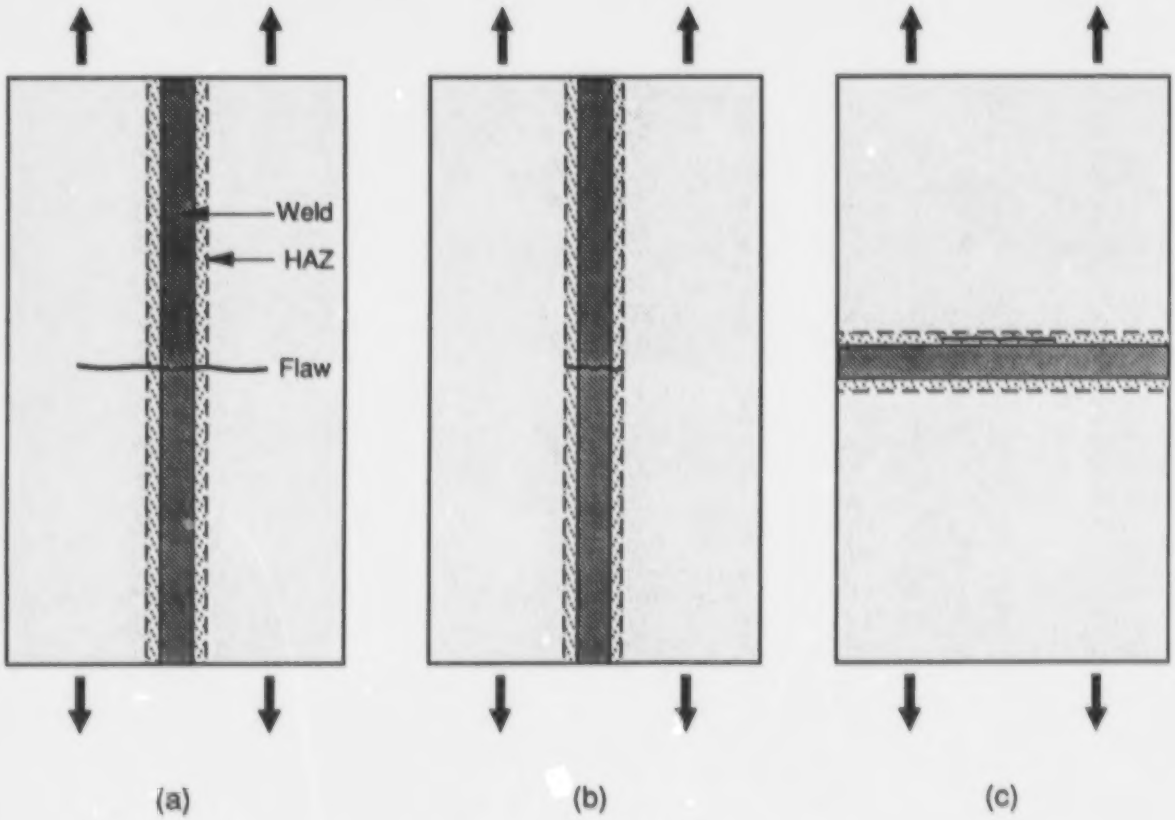

Figure 3: **Various flaw orientations to be considered for assessing base material fracture toughness**

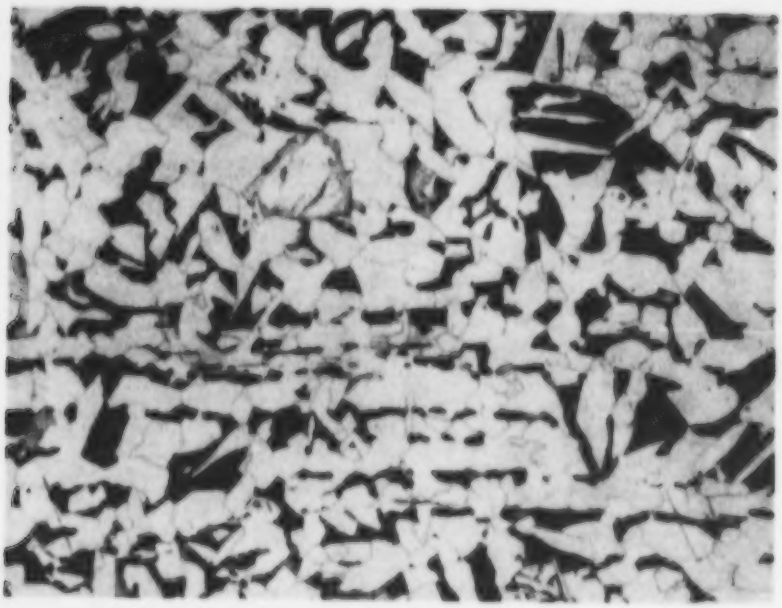

(a) Longitudinal direction (Neg. 11623; X200)

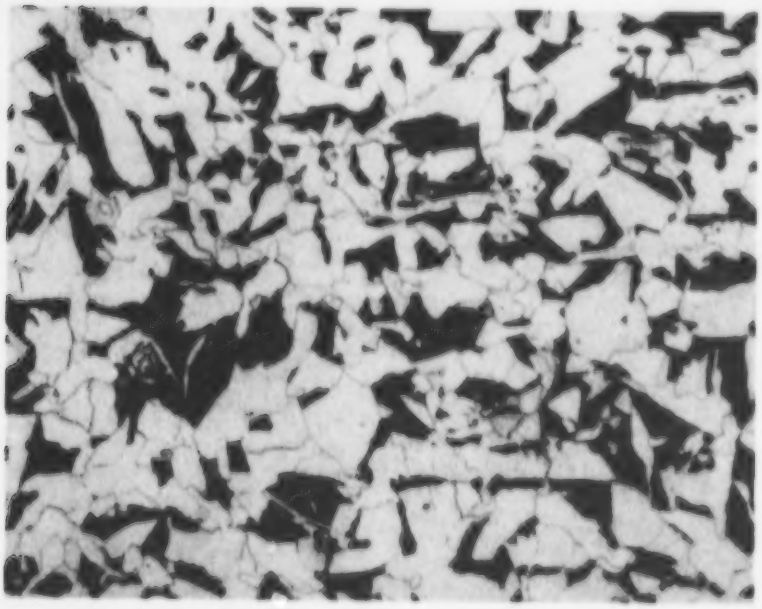

(b) Transverse direction (Neg. 11624; X200)

Figure 4: Microstructure of Steel A

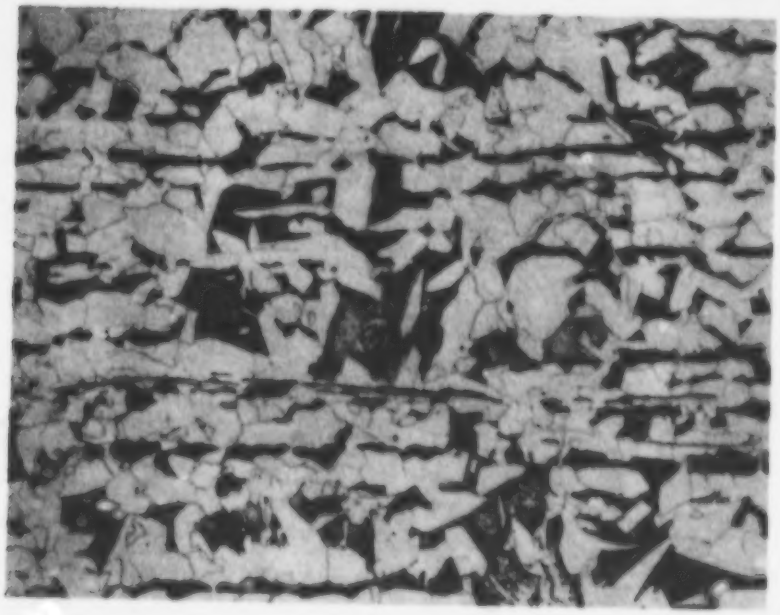

(a) Longitudinal direction (Neg. 11621; X200)

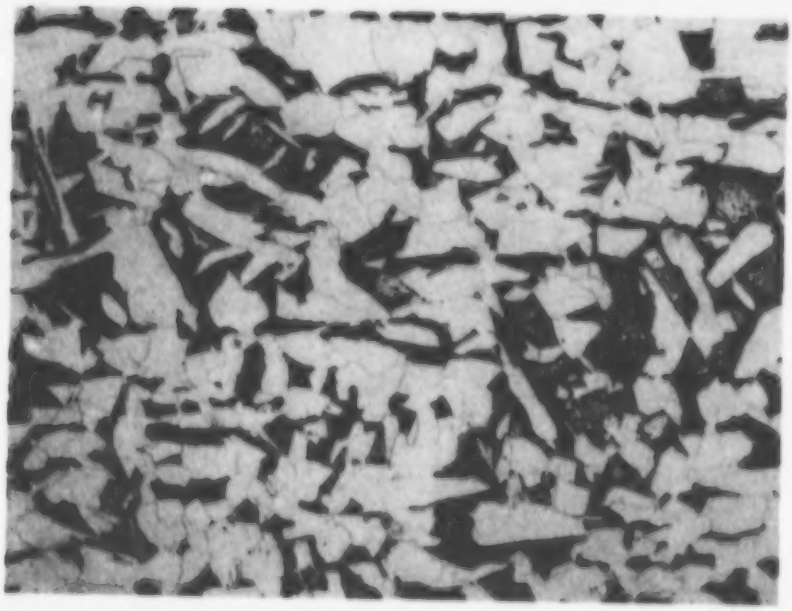

(b) Transverse direction (Neg. 11622; X200)

Figure 5: Microstructure of Steel B

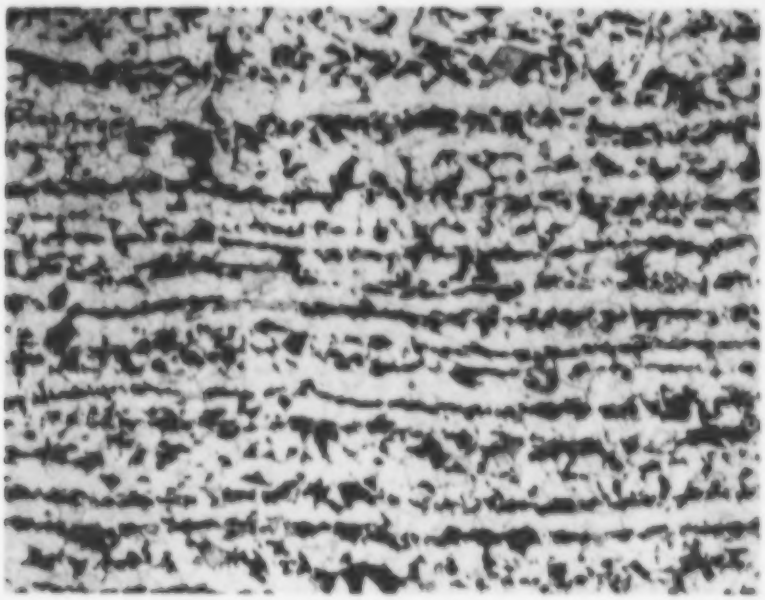

(a) Longitudinal direction (Neg. 11514; X200)

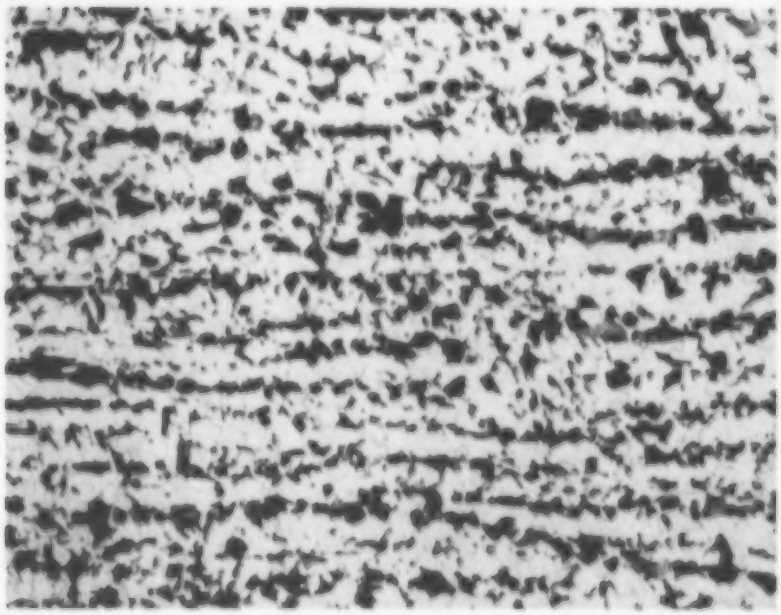

(b) Transverse direction (Neg. 11513; X200)

Figure 6: Microstructure of Steel C

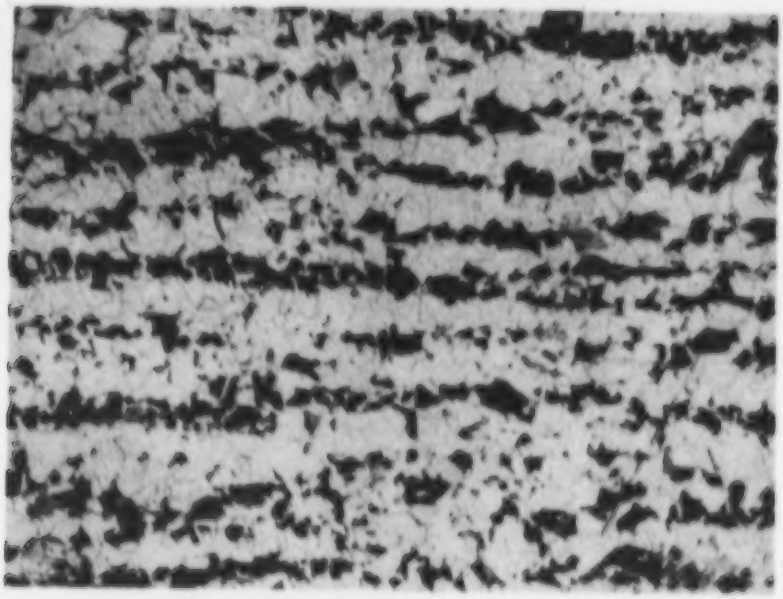

(a) Longitudinal direction (Neg. 11627; X200)

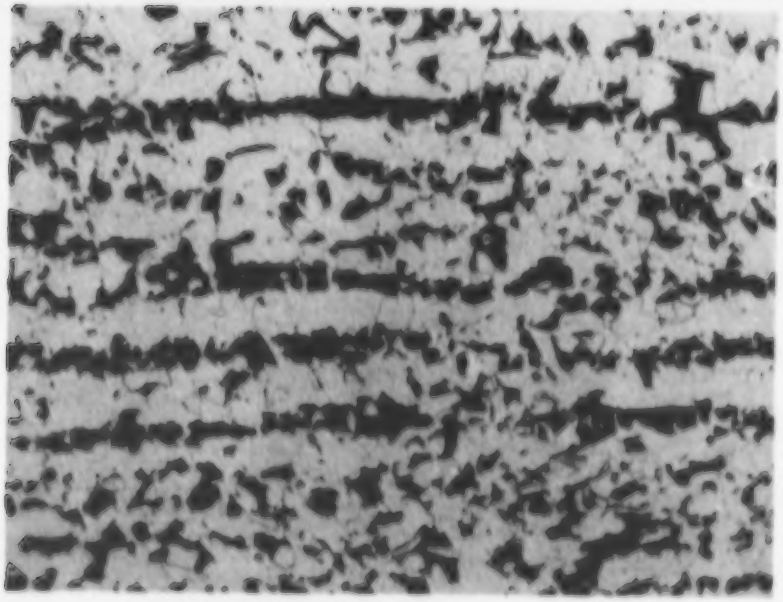

(b) Transverse direction (Neg. 11511; X200)

Figure 7: Microstructure of Steel D

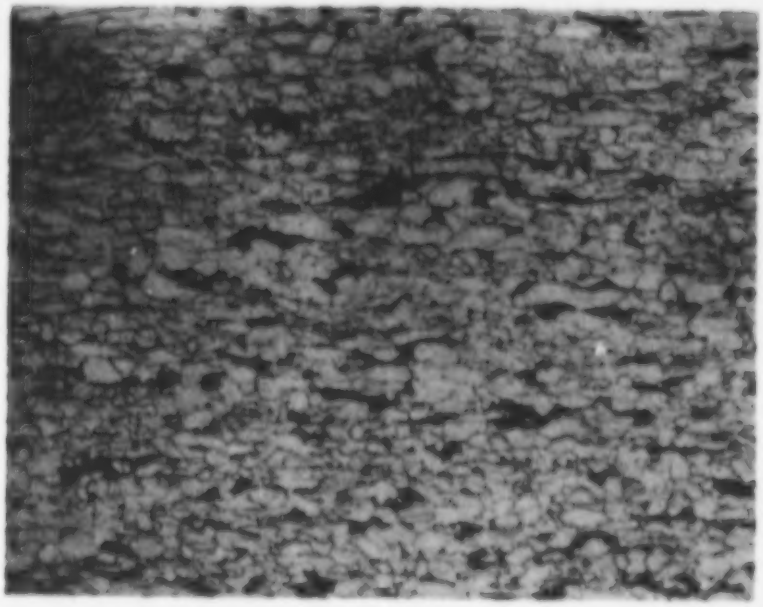

(a) Longitudinal direction (Neg. 11626; X200)

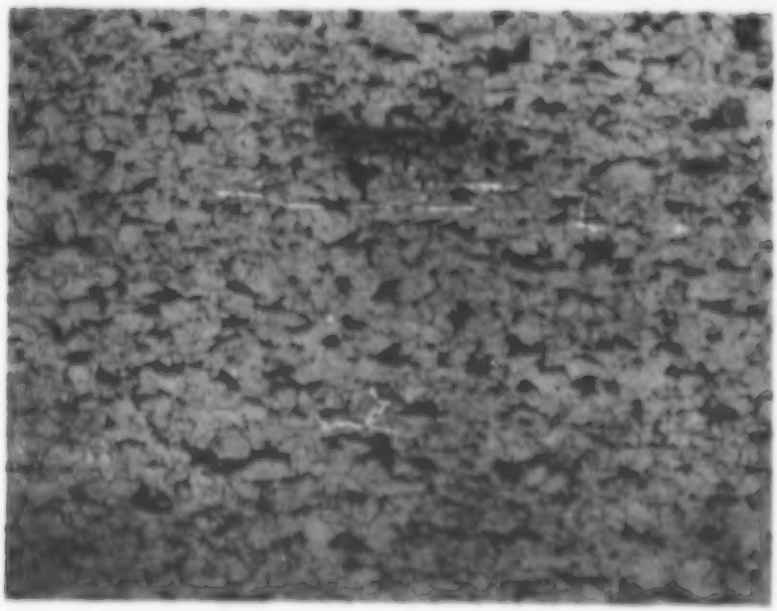

(b) Transverse direction (Neg. 11625; X200)

Figure 8: Microstructure of Steel E

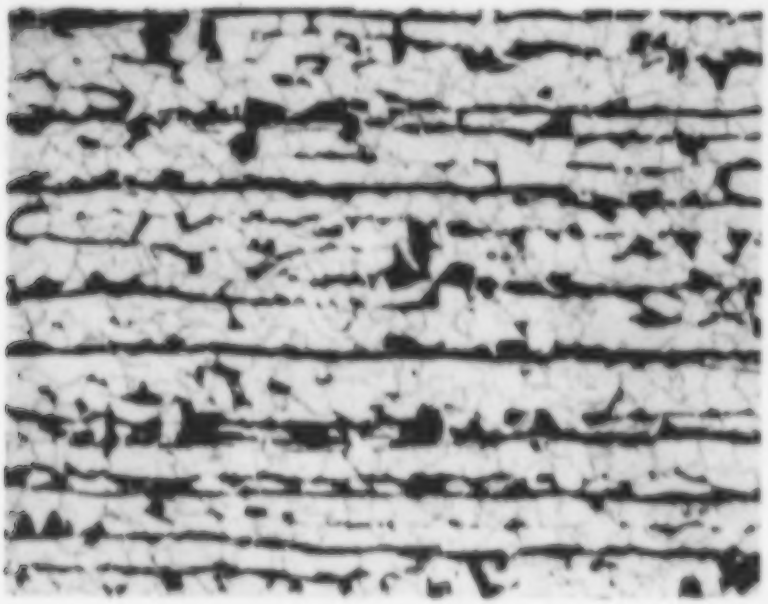

(a) Longitudinal direction (Neg. 12571; X200)

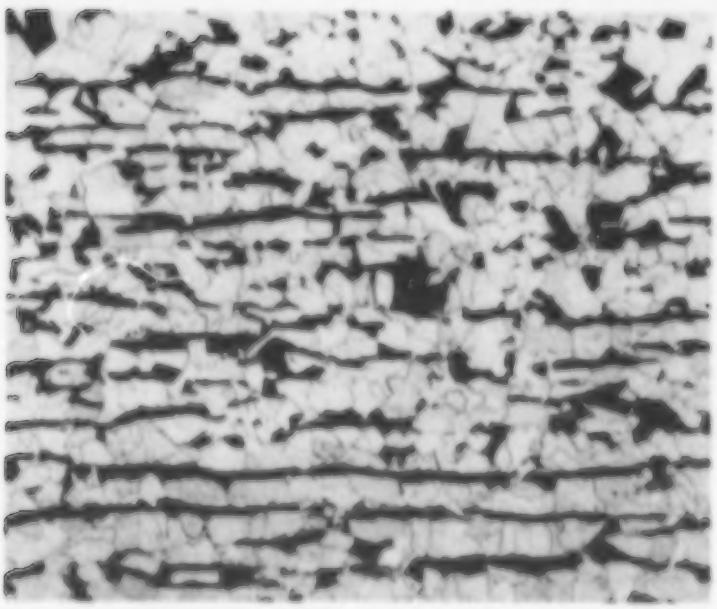

(c) Transverse direction (Neg. 12572; X200)

Figure 9: Microstructure of Steel WP

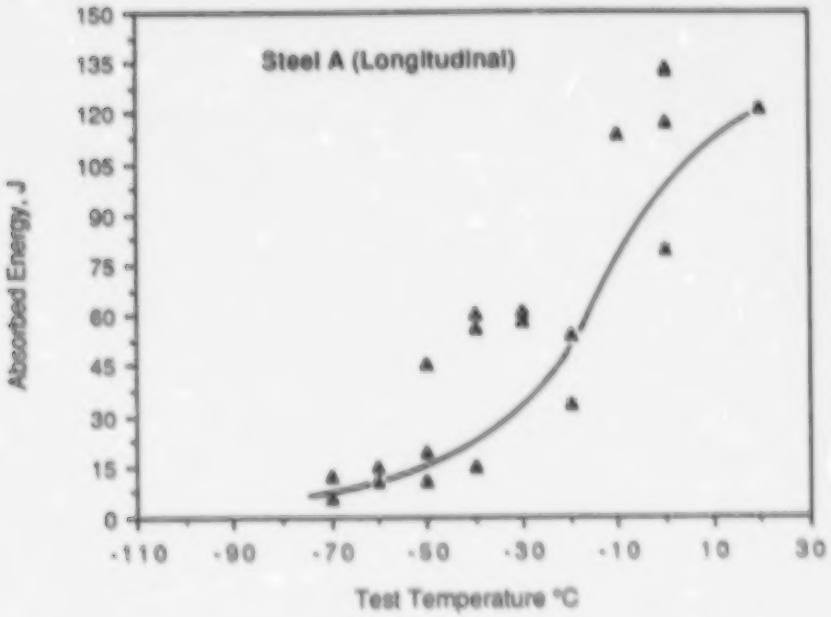

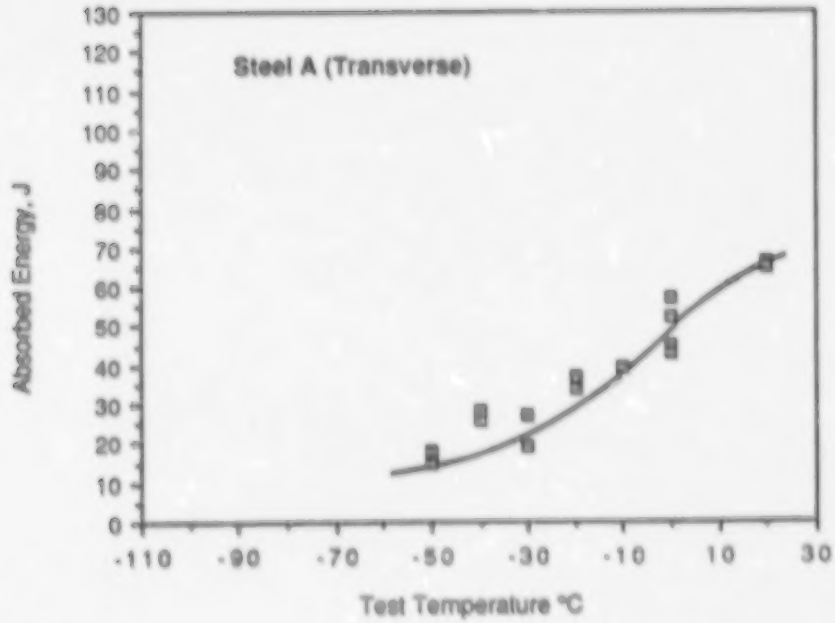

Figure 10: CVN transition curves for Steel A

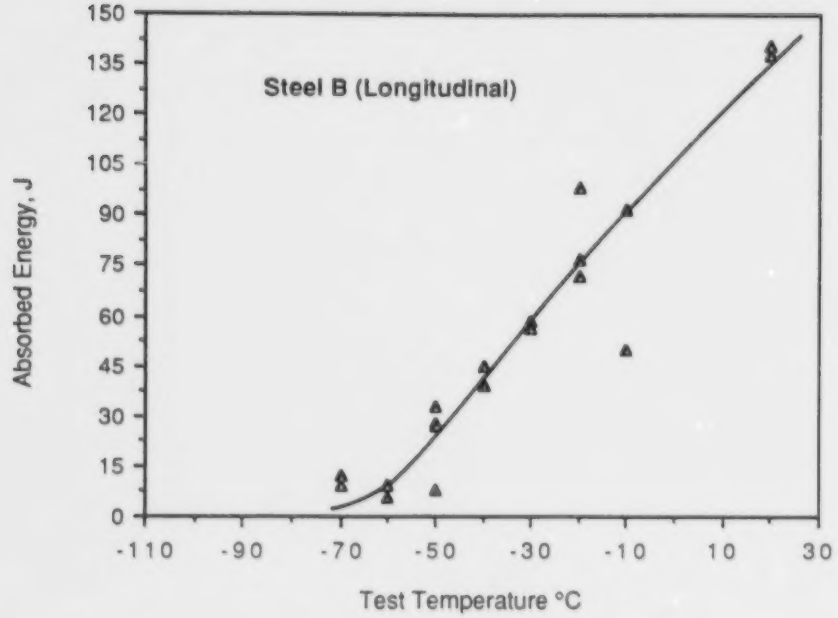

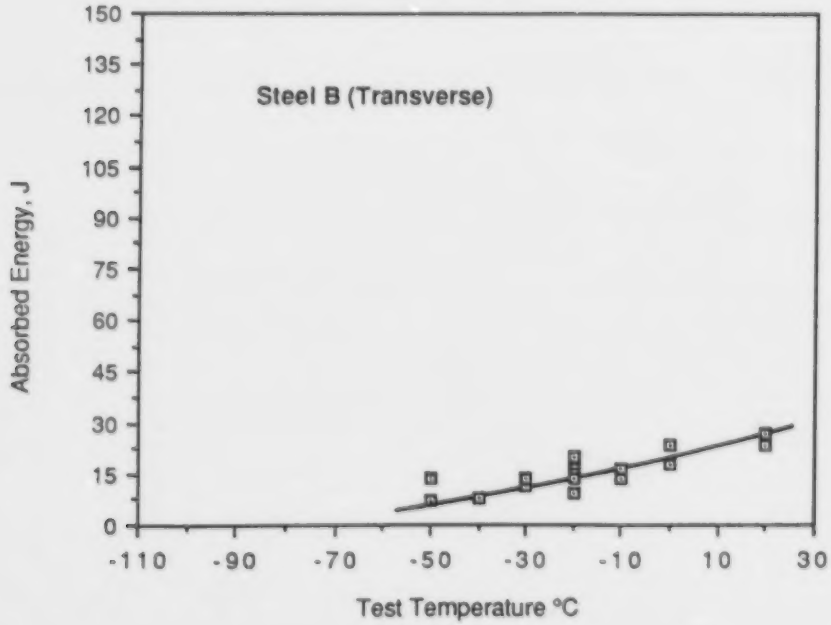

Figure 11: CVN transition curves for Steel B

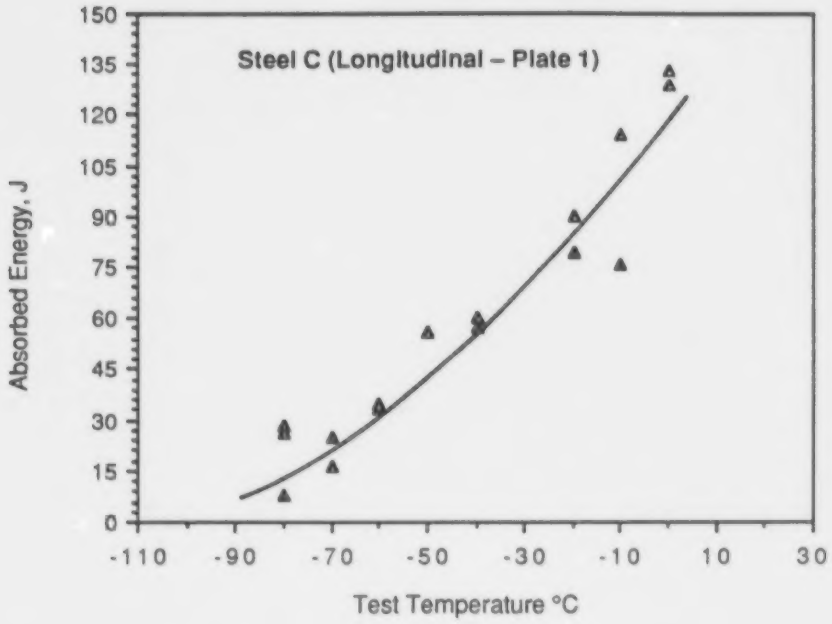

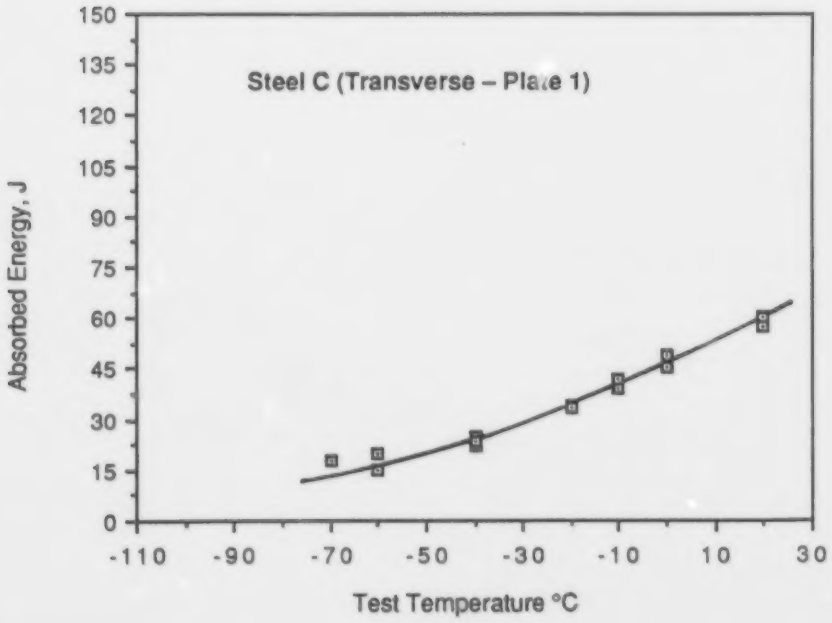

Figure 12: CVN transition curves for Steel C

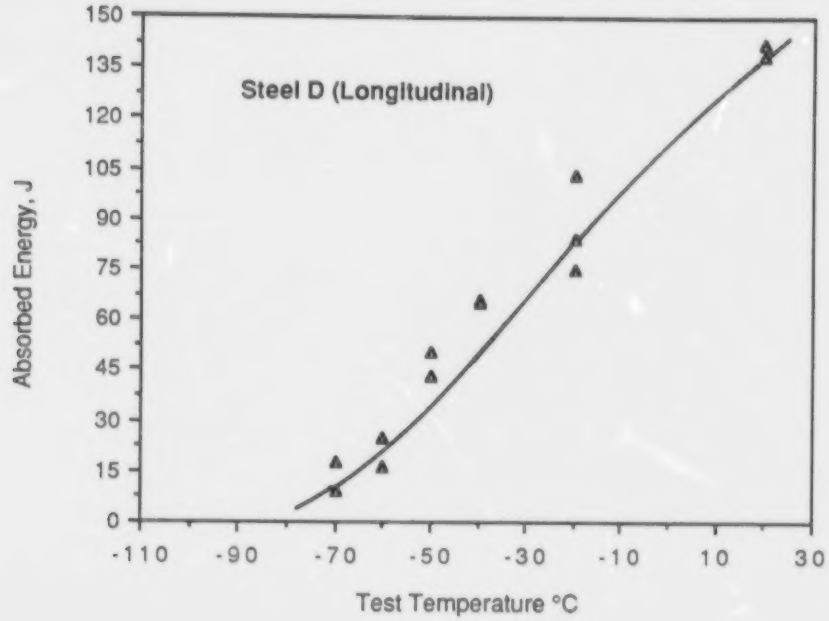

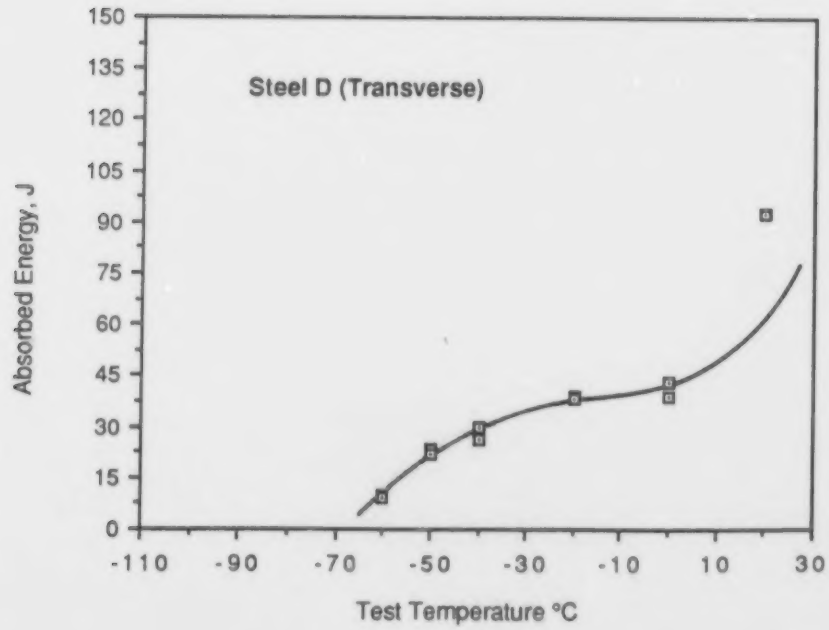

Figure 13: CVN transition curves for Steel D

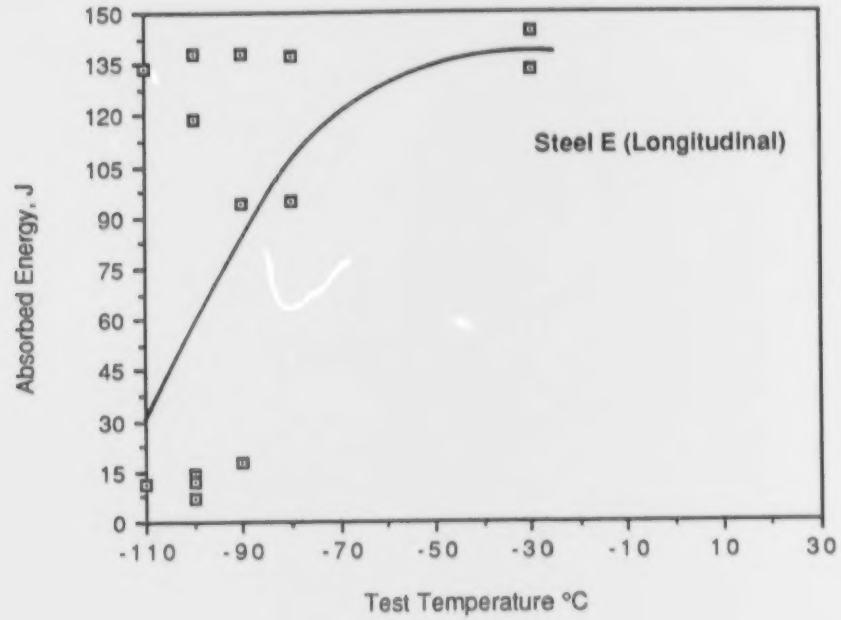

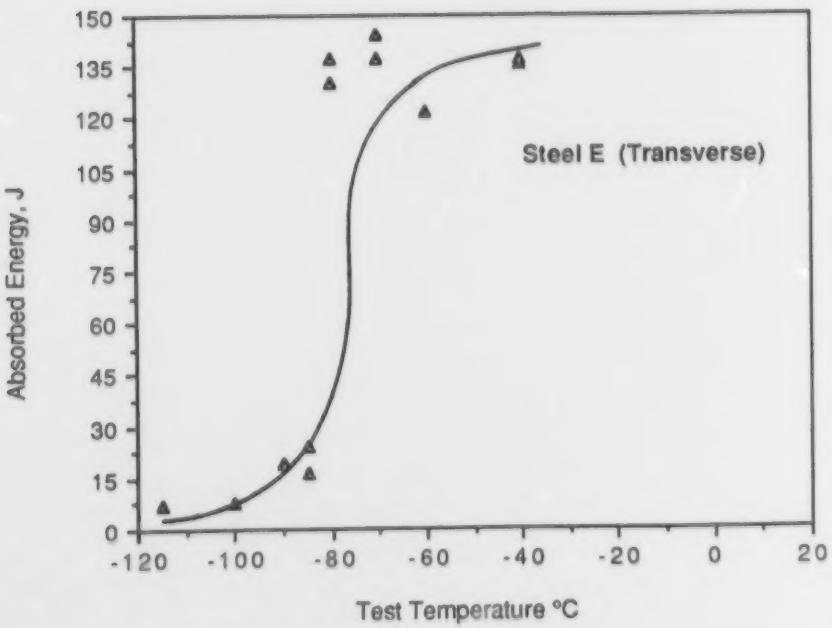

Figure 14: CVN transition curves for Steel E

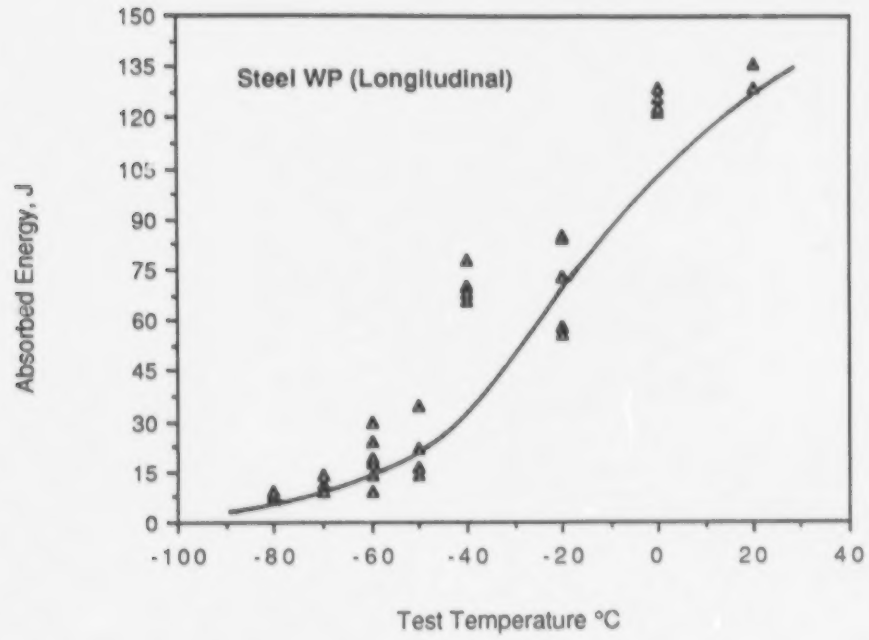

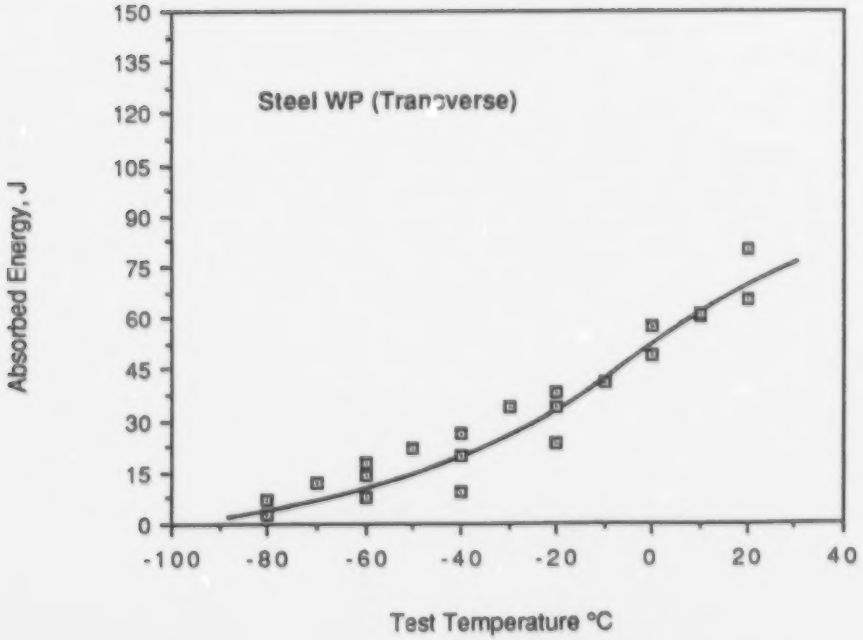

Figure 15: CVN transition curves for Steel WP

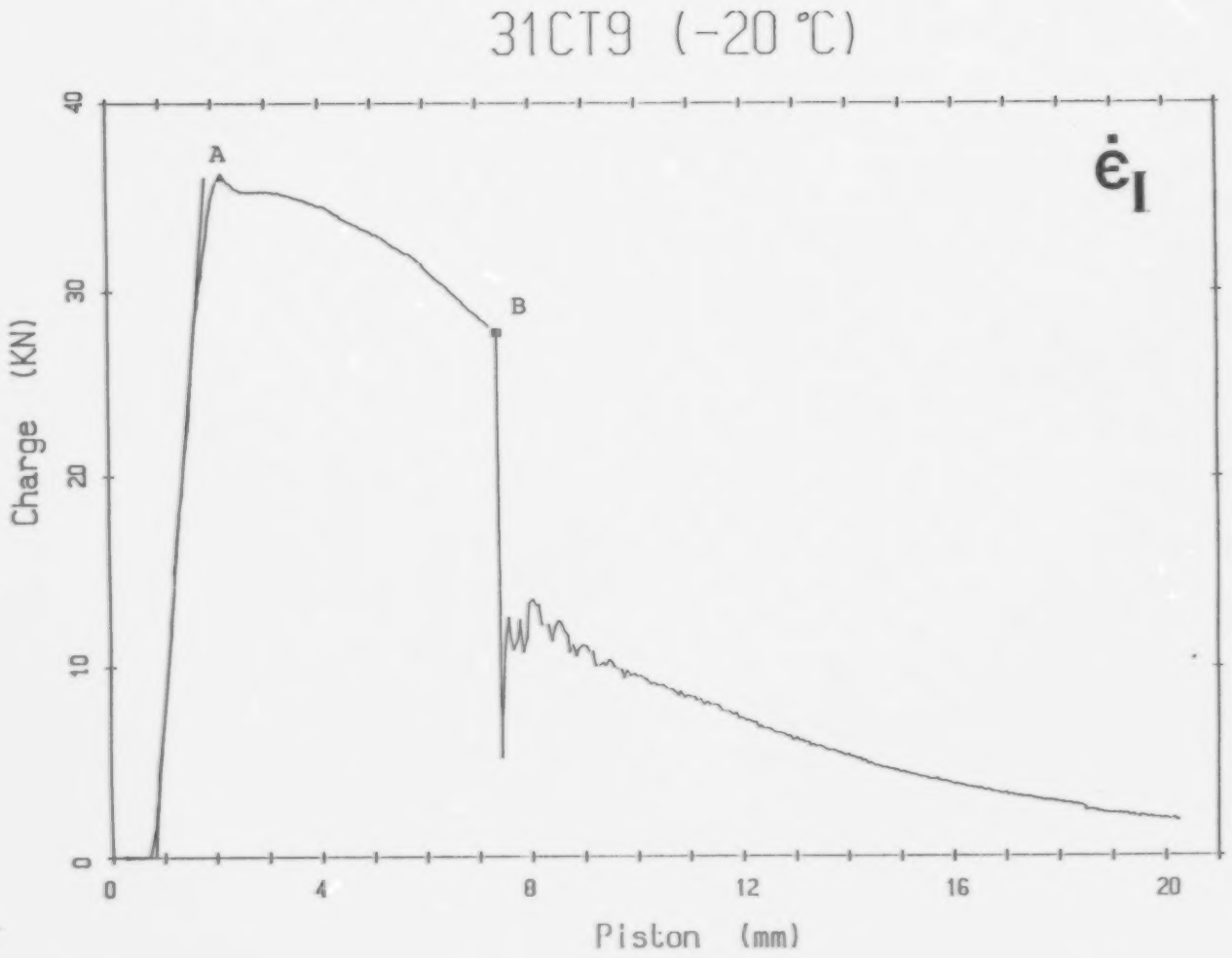

Figure 16: A typical load-crack mouth opening displacement trace for CTOD tests conducted at the intermediate loading rate

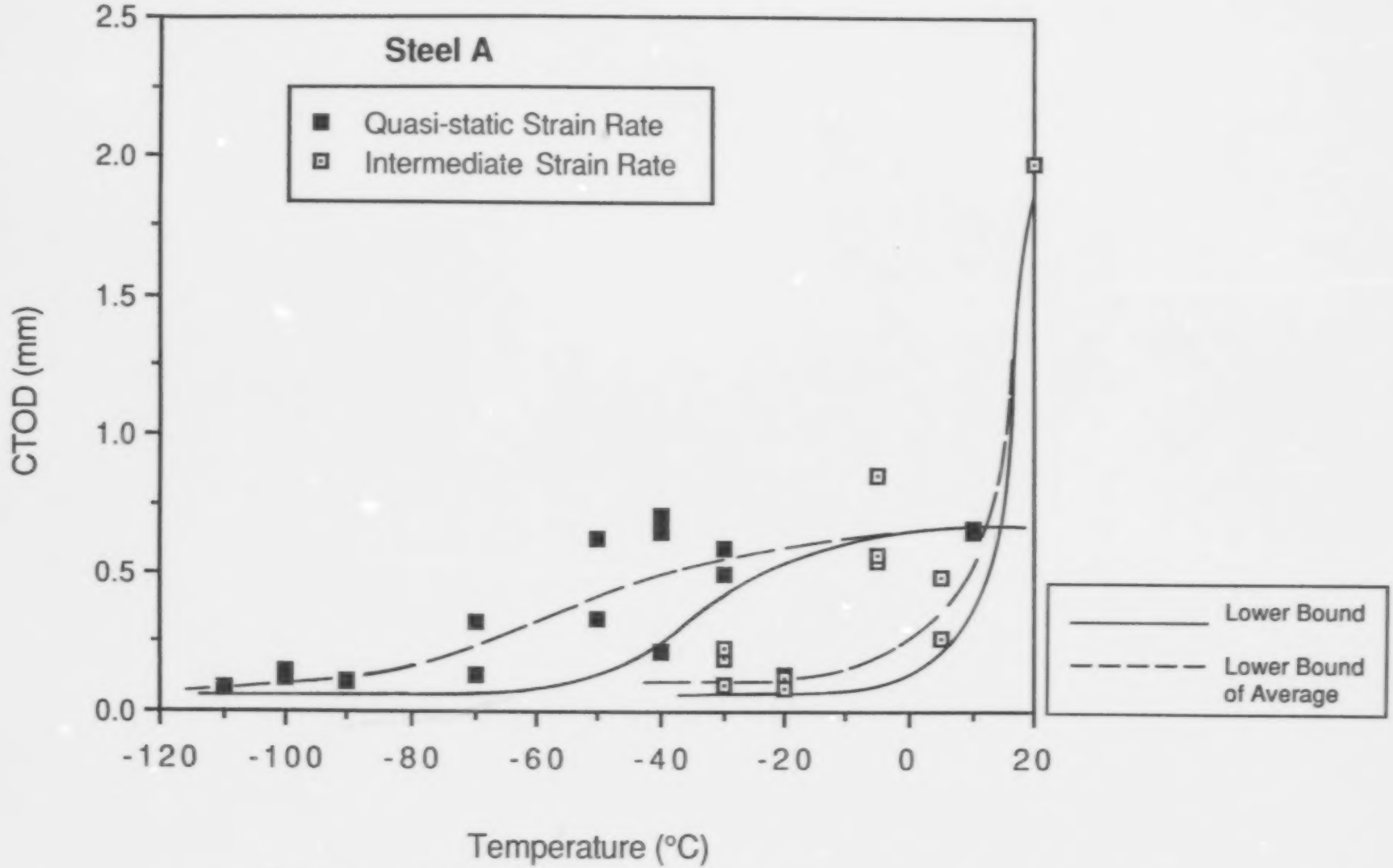

Figure 17: CTOD toughness of Steel A in the transverse orientation

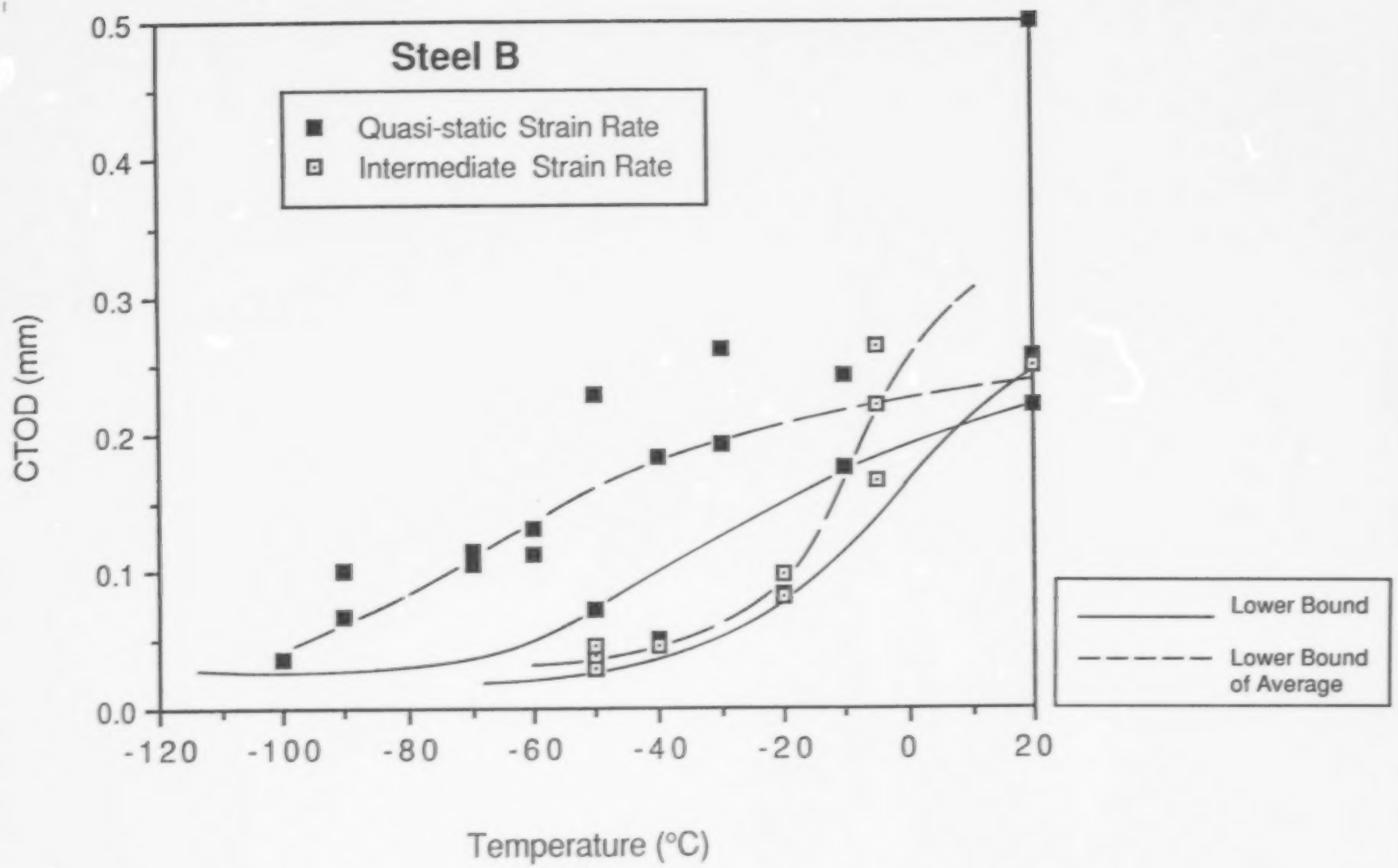

Figure 18 CTOD toughness of Steel B in the transverse orientation

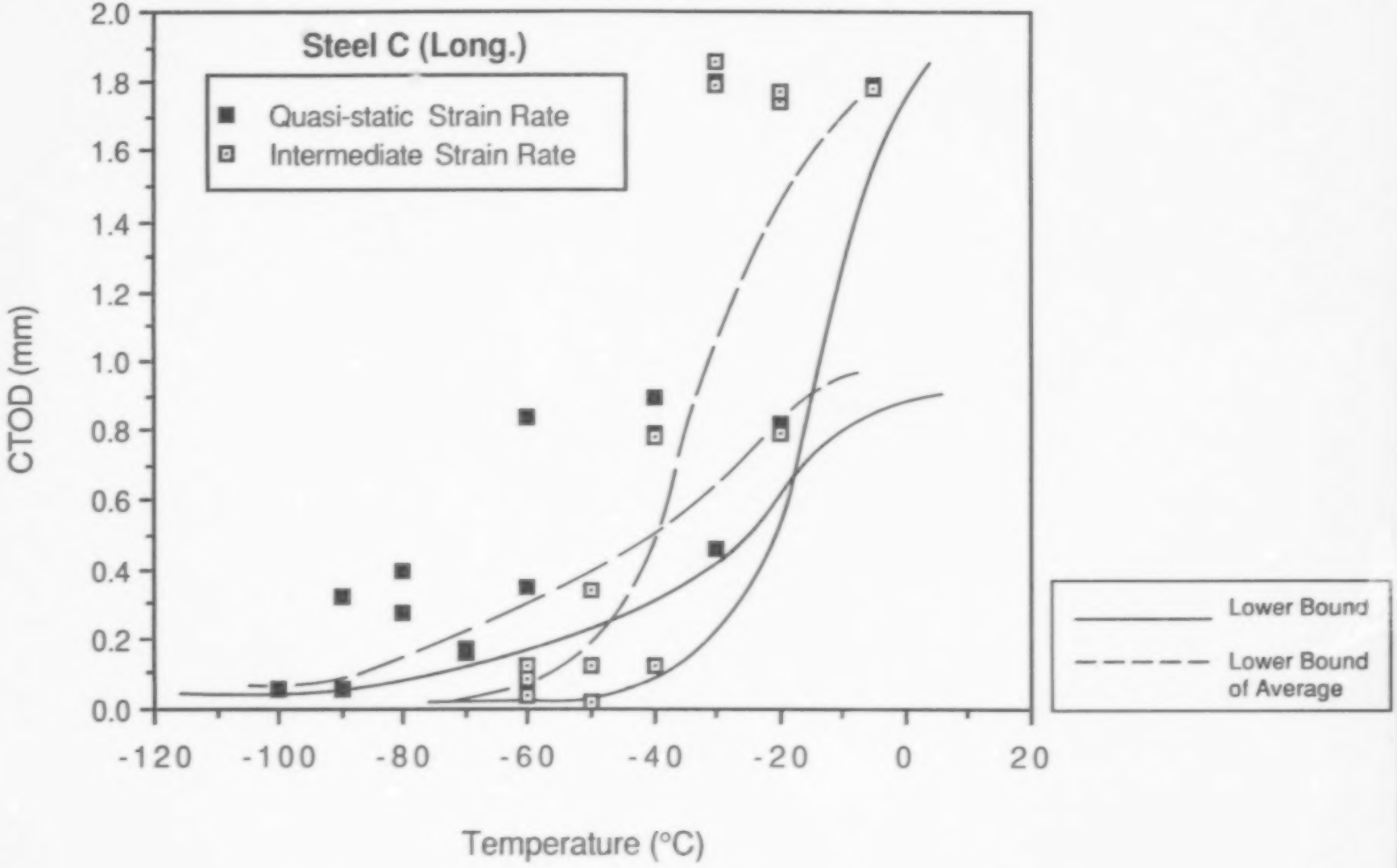

Figure 19: CTOD toughness of Steel C in the longitudinal orientation

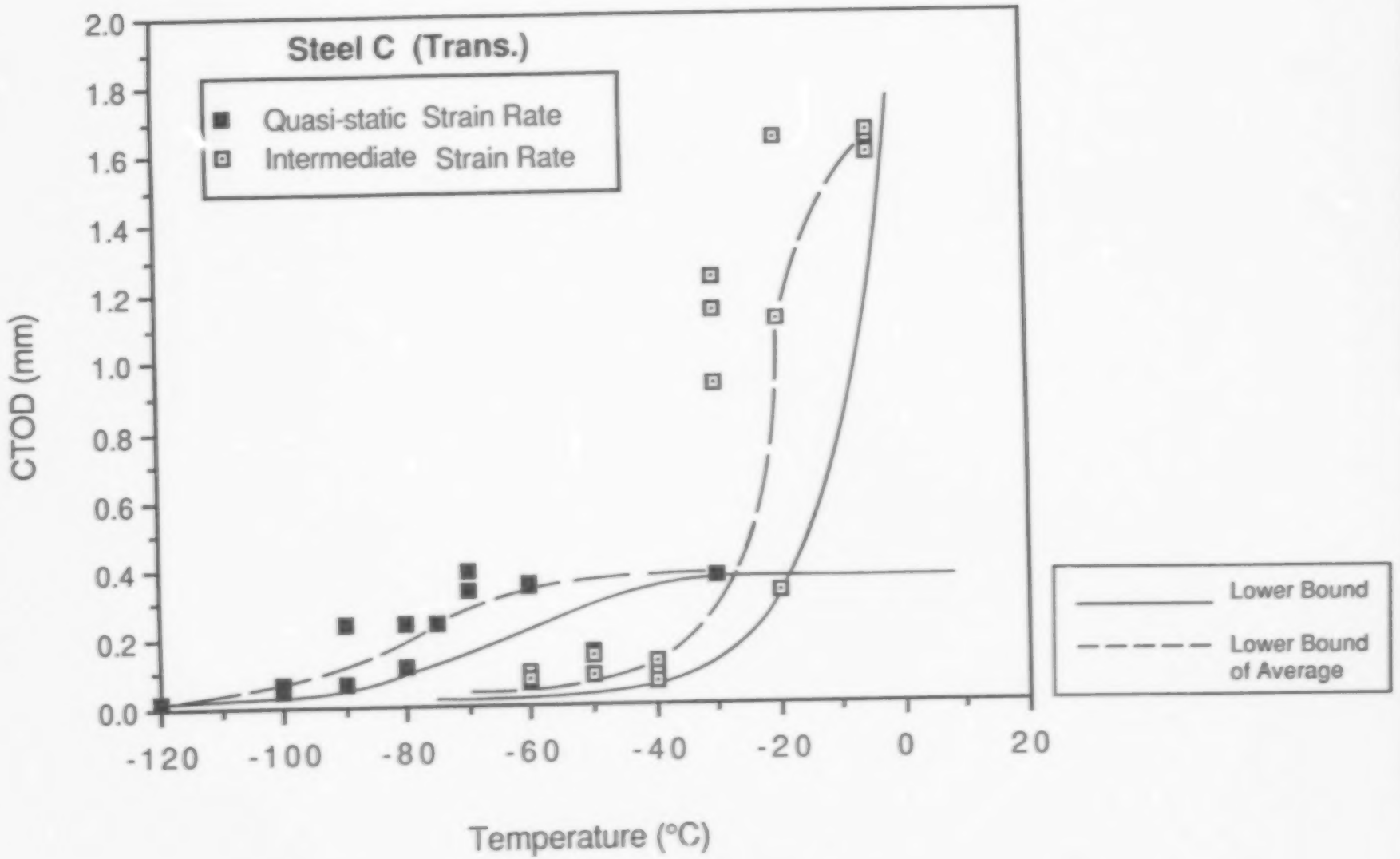

Figure 20: CTOD toughness of Steel C in the transverse orientation

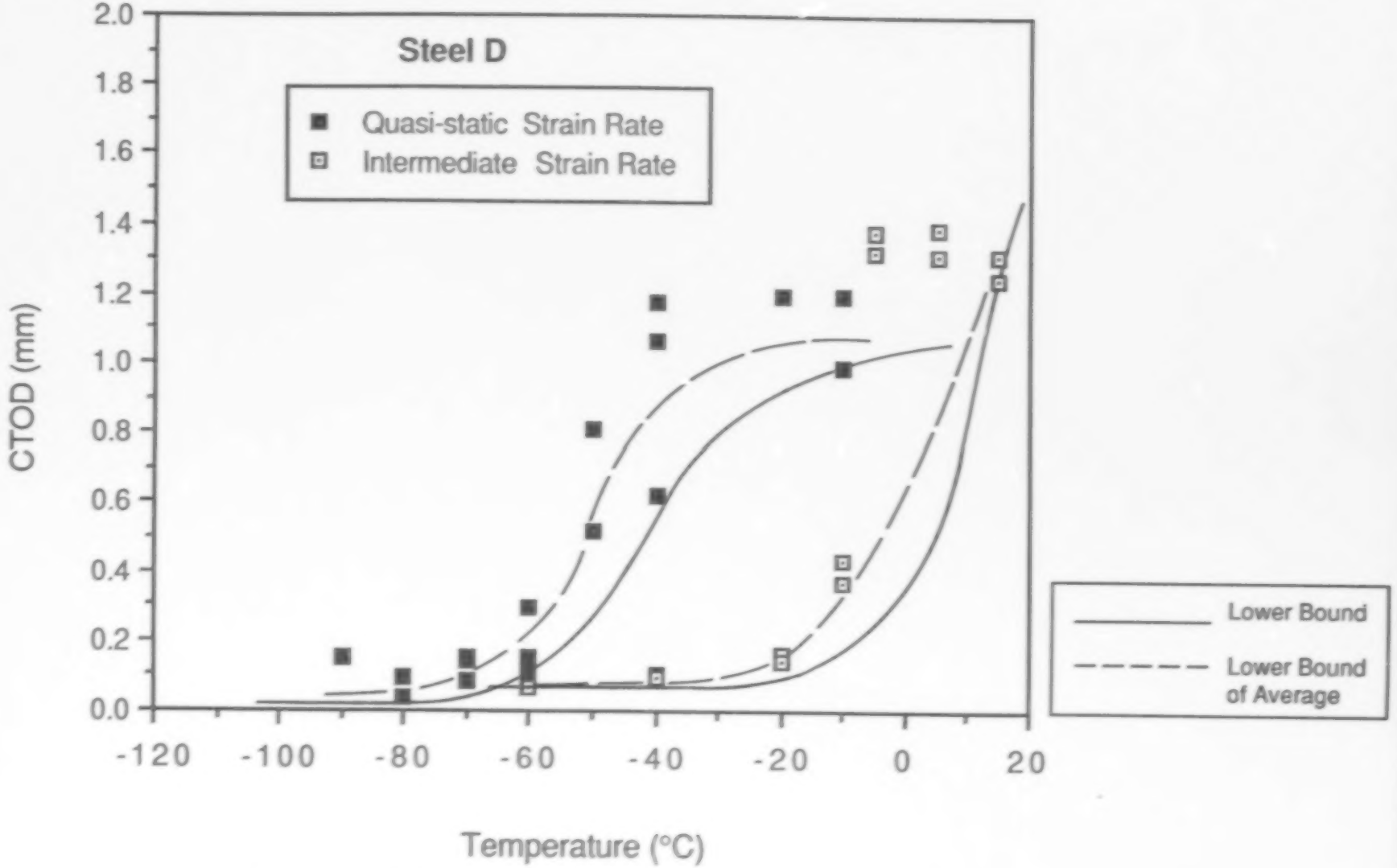

Figure 21: CTOD toughness of Steel D in the transverse orientation

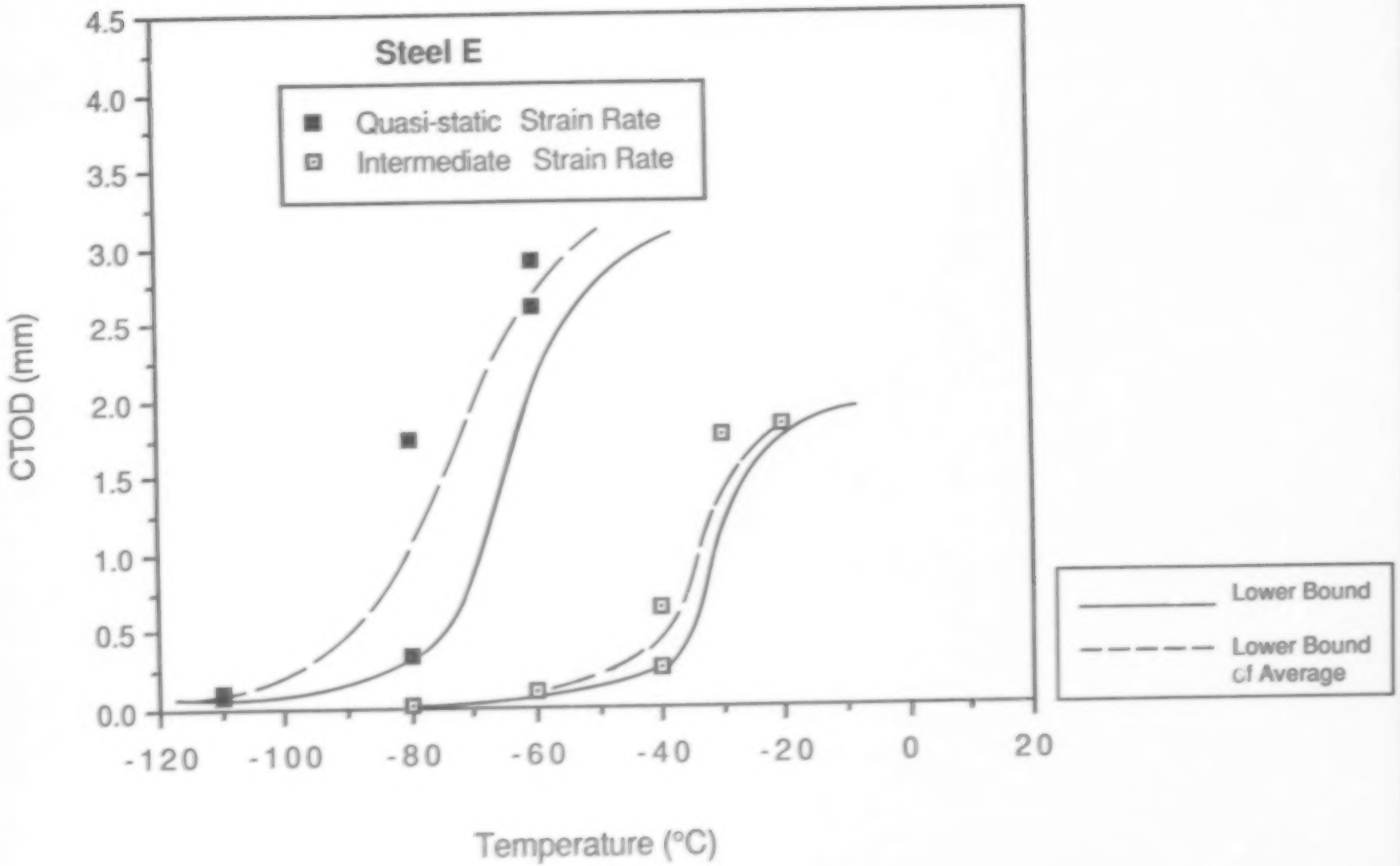

Figure 22 CTOD toughness of Steel E in the longitudinal orientation

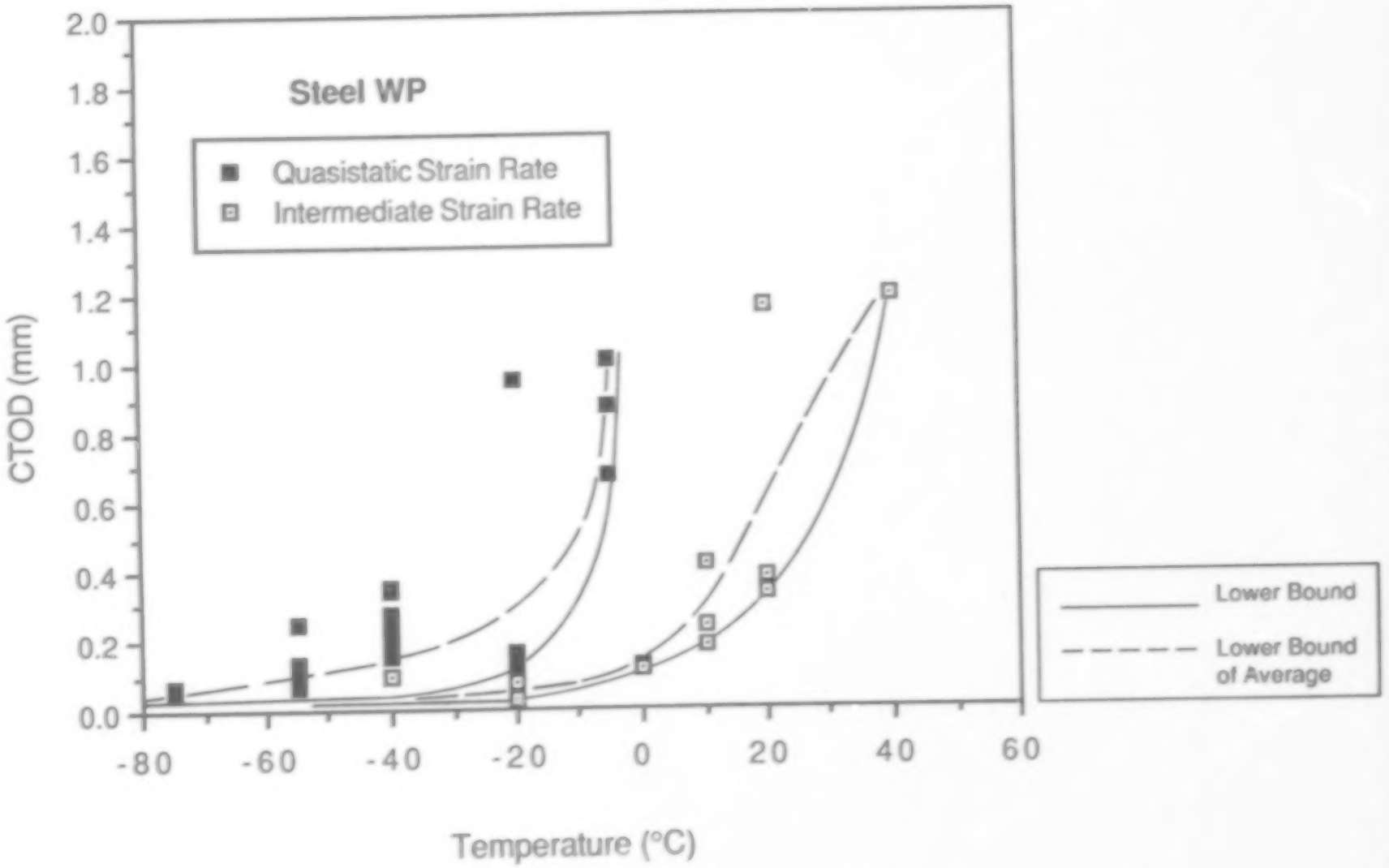

Figure 23: CTOD toughness of Steel WP in the longitudinal orientation

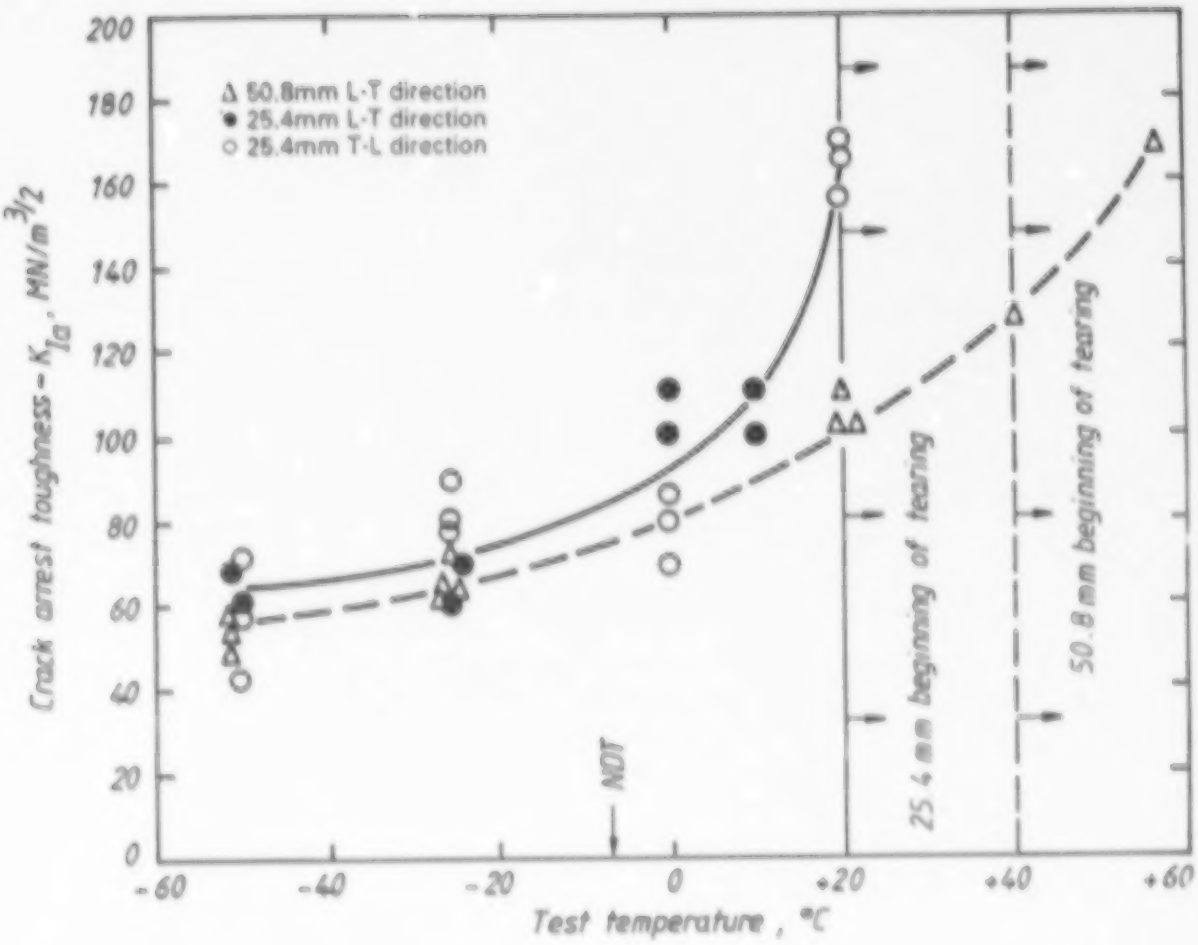

Figure 24: Effect of test temperature on the crack arrest toughness of A36 steel (Reproduced from Ref. 22)

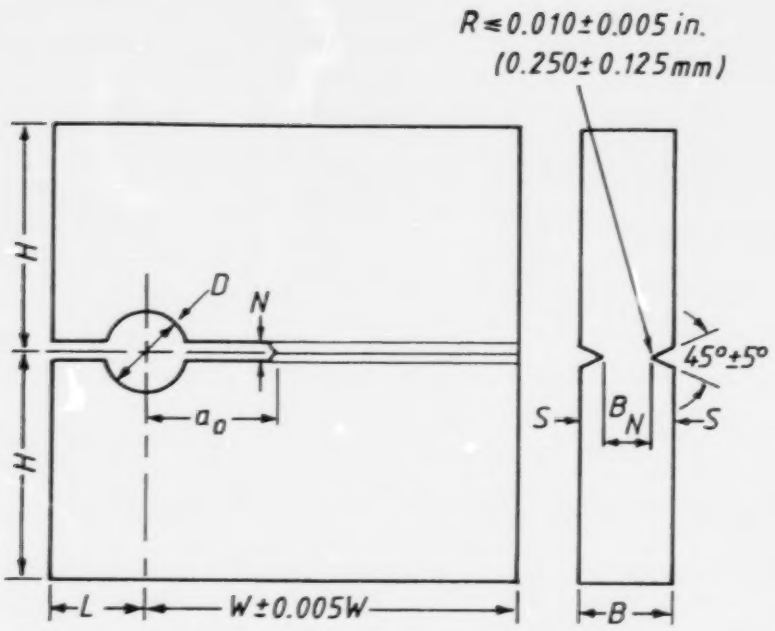

$H = 0.6W \pm 0.005W$

$S = (B - B_N)/2 \pm 0.01B$

$N \leq W/10$

$0.15W \leq L \leq 0.25W$

$0.30W \leq a_0 \leq 0.40W$

$0.125W \pm 0.005W \leq D \leq 0.250W \pm 0.005W$

B	W	H	N	L	D	S	a_o
25	165.0	99.0	12.7	33.0	31.5	3.175	57.9
50	178.0	106.7	12.7	35.6	31.5	6.350	62.2

Figure 25: Dimension of the crack arrest specimens used in the investigation (Reproduced from Ref. 22)

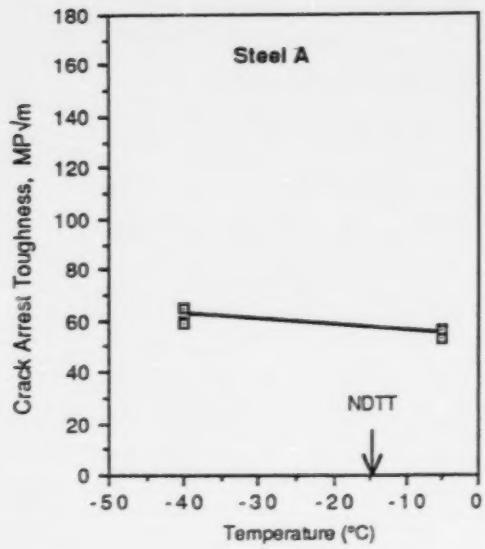

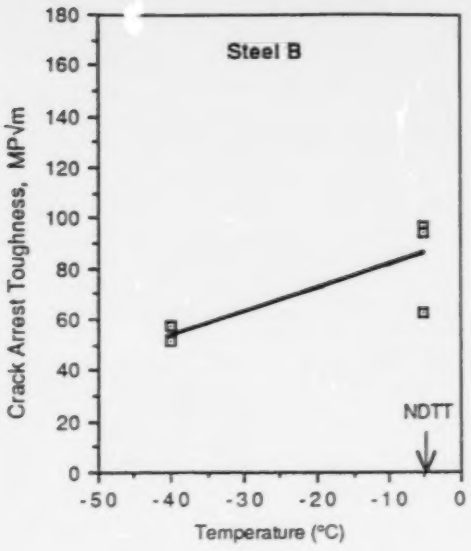

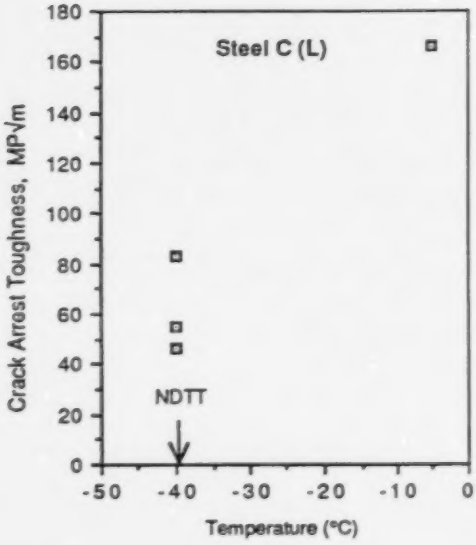

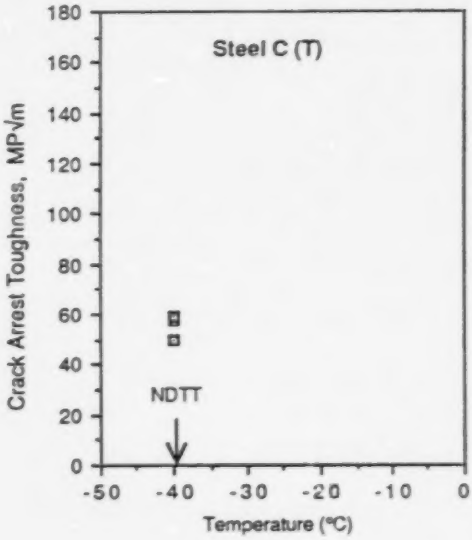

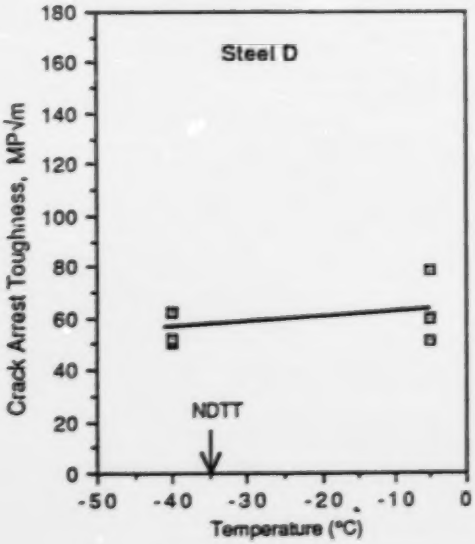

Figure 26: Crack arrest toughness of the steels at -5° and -40°C

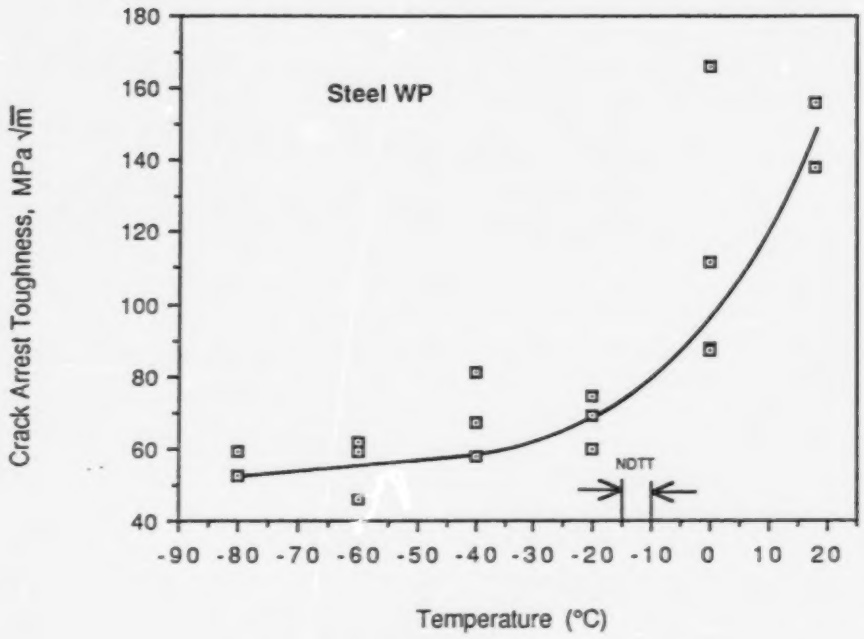

Figure 27: Crack arrest toughness of steel WP at various temperatures

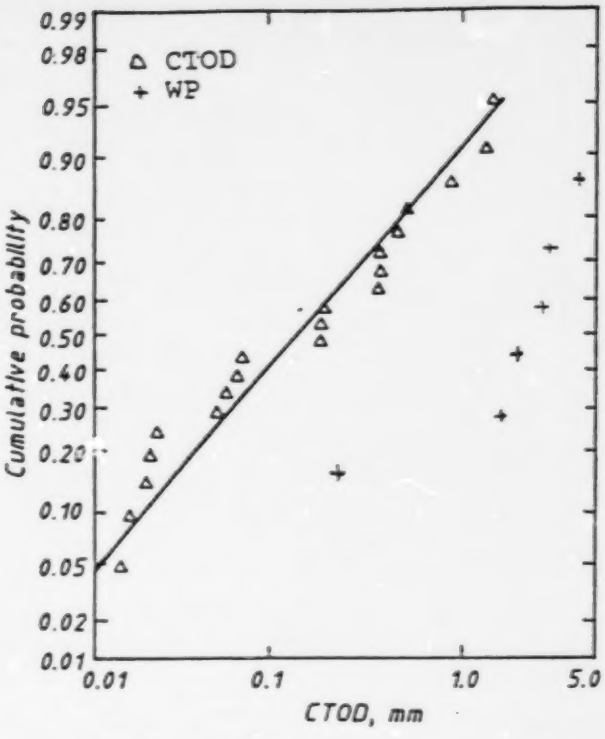

Set 1, 30% welding procedure, as-welded

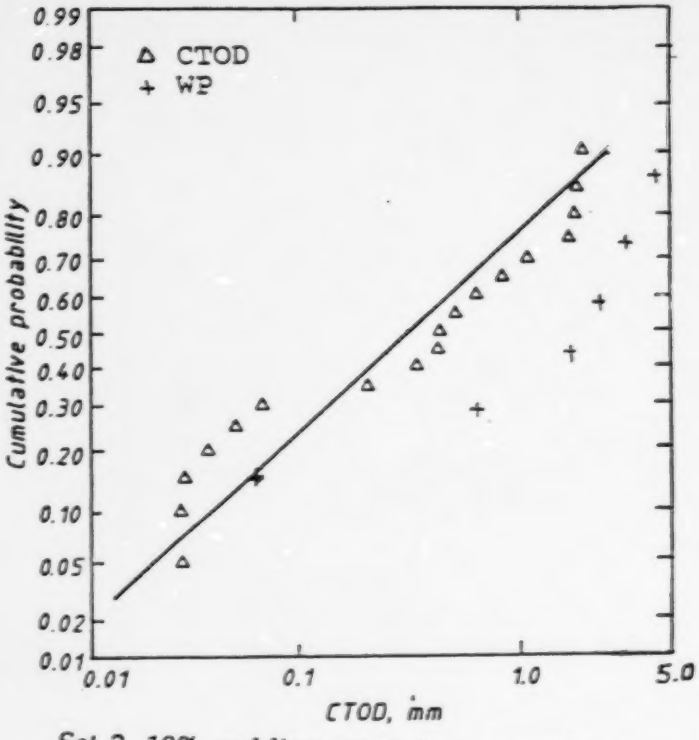

Set 2, 10% welding procedure, as welded

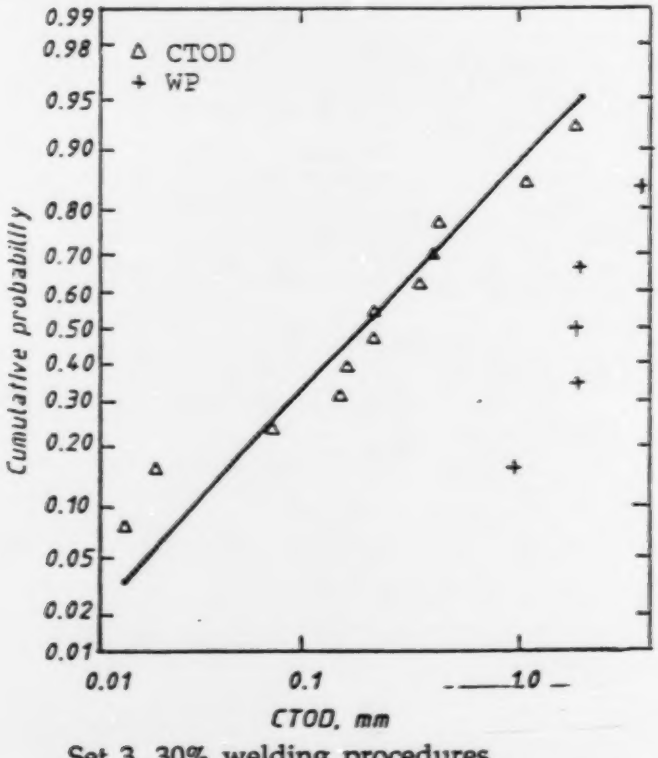

Set 3, 30% welding procedures, postweld heat treated

Figure 28: CTOD distributions for HAZ as found in standard BX2B specimens and in wide plate tests for various weld procedures/post weld heat treatment conditions (from Ref. 24)

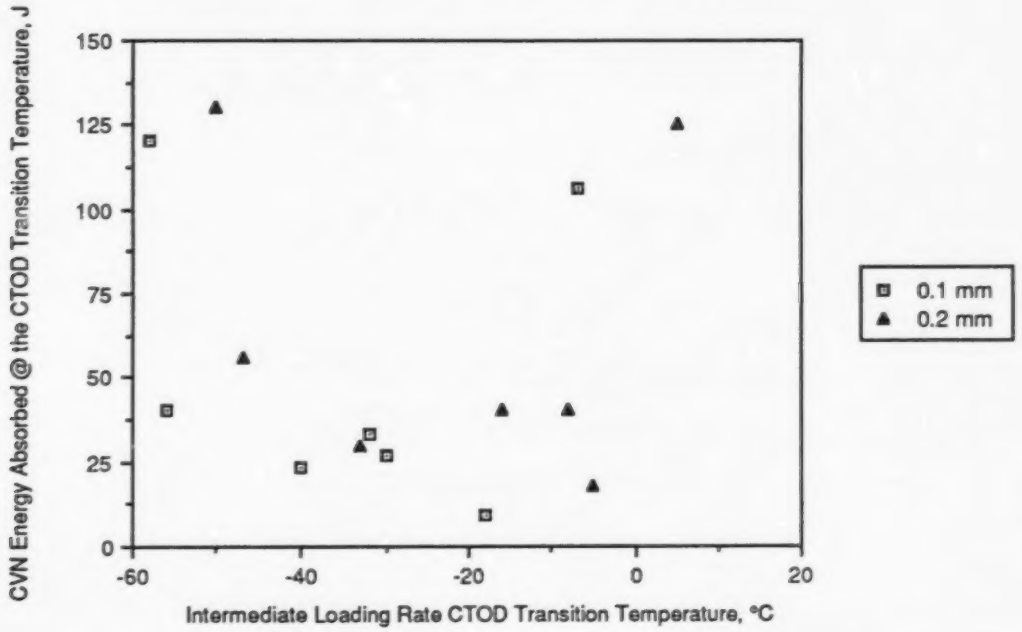

Figure 29: CVN energy absorbed at the 0.1 or 0.2mm CTOD (Int. Loading Rate) transition temperature for the steels tested

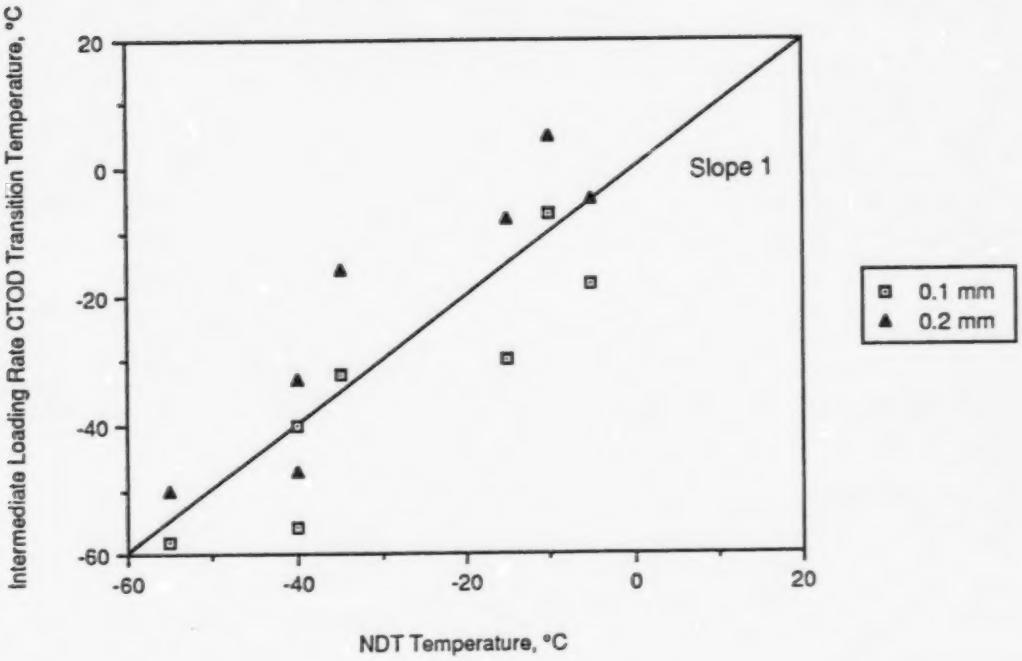

Figure 30: Correlation between the intermediate loading rate CTOD transition temperatures of the steels tested, and their NDT temperatures

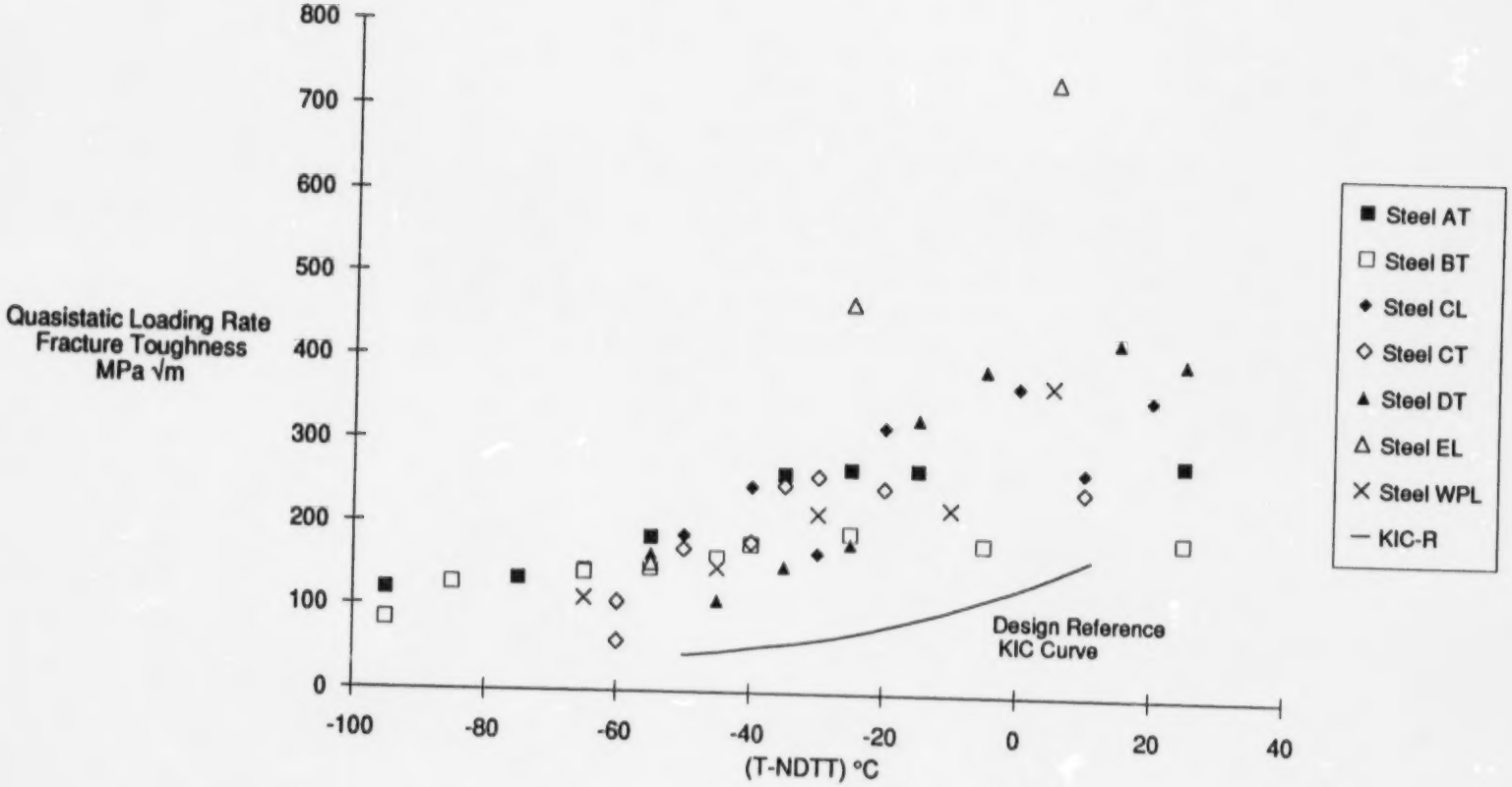

Figure 31(a): Quasistatic loading rate fracture toughness of the steels as a function of temperature referenced to their NDT temperature, along with Pellini's design-reference curve for K_{IC}

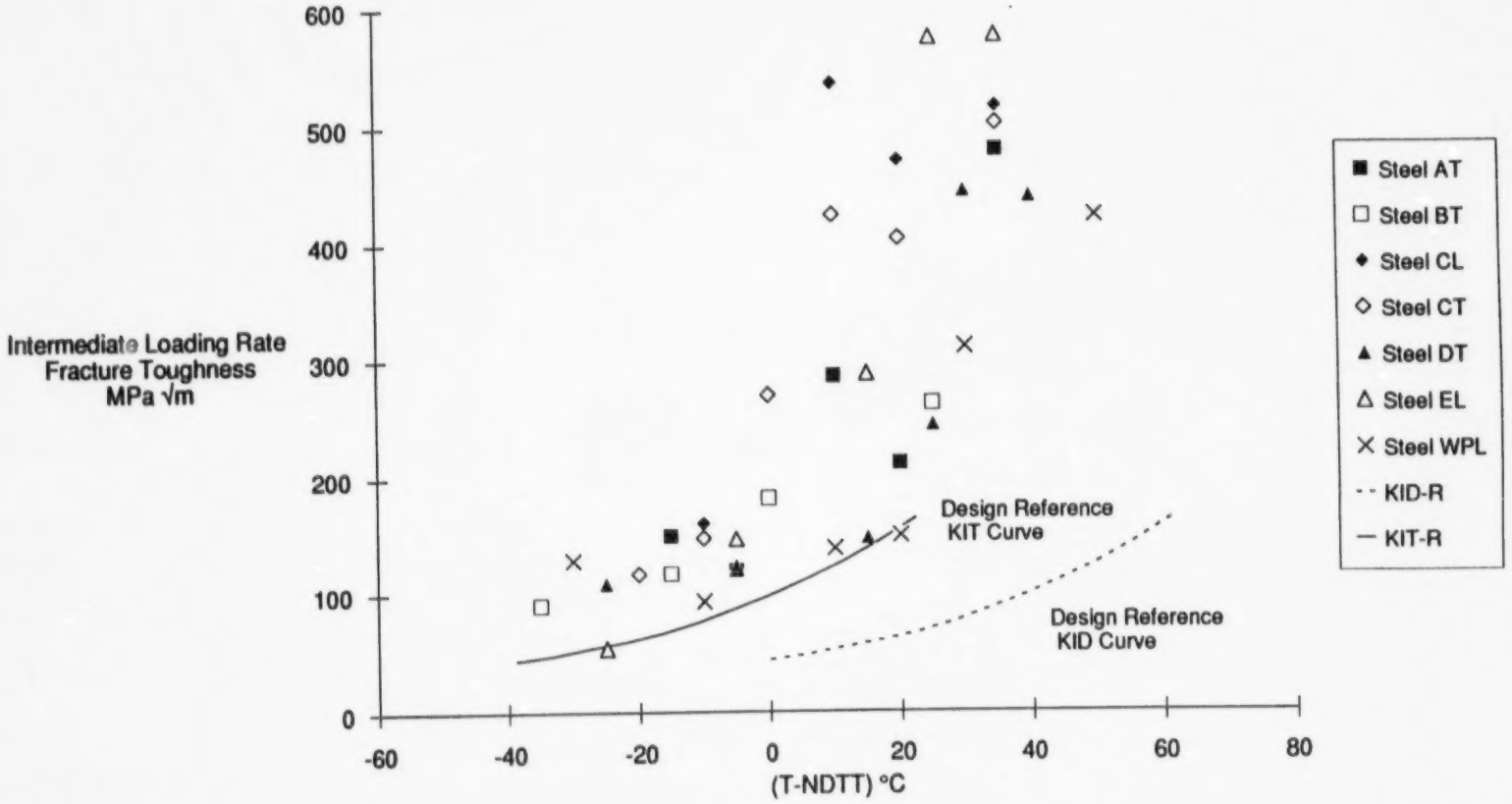

Figure 31(b): Intermediate loading rate fracture toughness of the steels as a function of temperature referenced to their NDT temperature, along with Pellini's design-reference curve for K_{ID} and $K_{I.Int}$

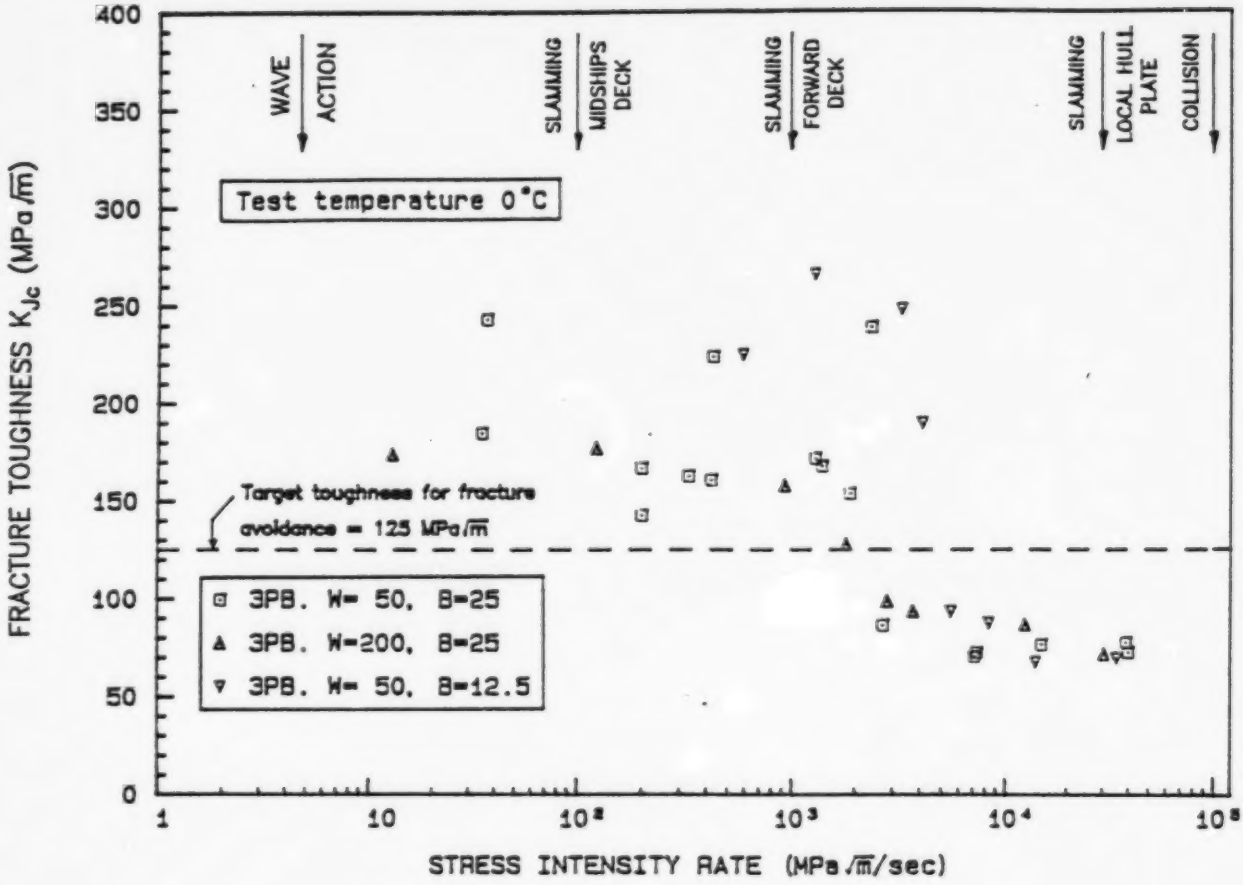

Figure 32: Effect of stress intensity rate on the fracture toughness of a ship steel at 0°C (Reproduced from Ref. 23)

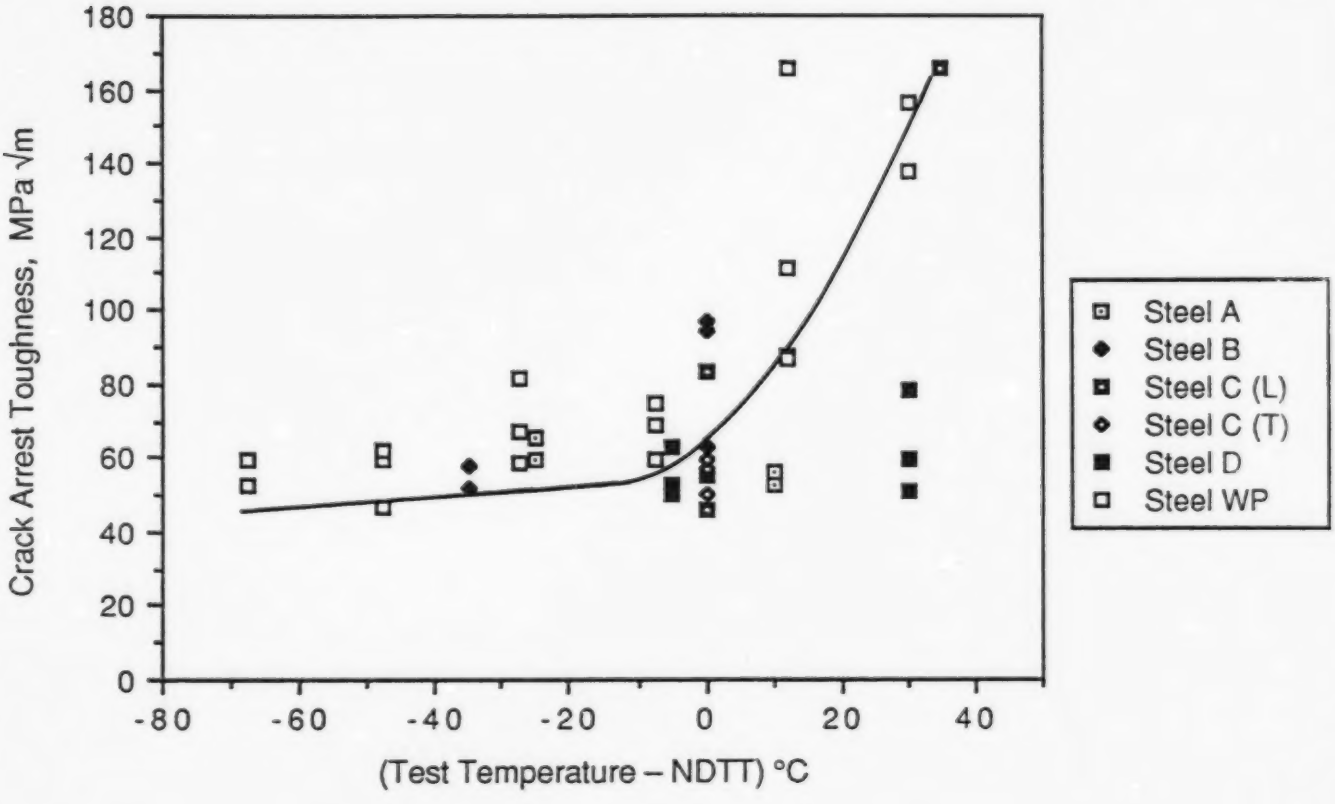

Figure 33: Crack arrest toughness of the steels as a function of the test temperature referenced to their NDT temperatures

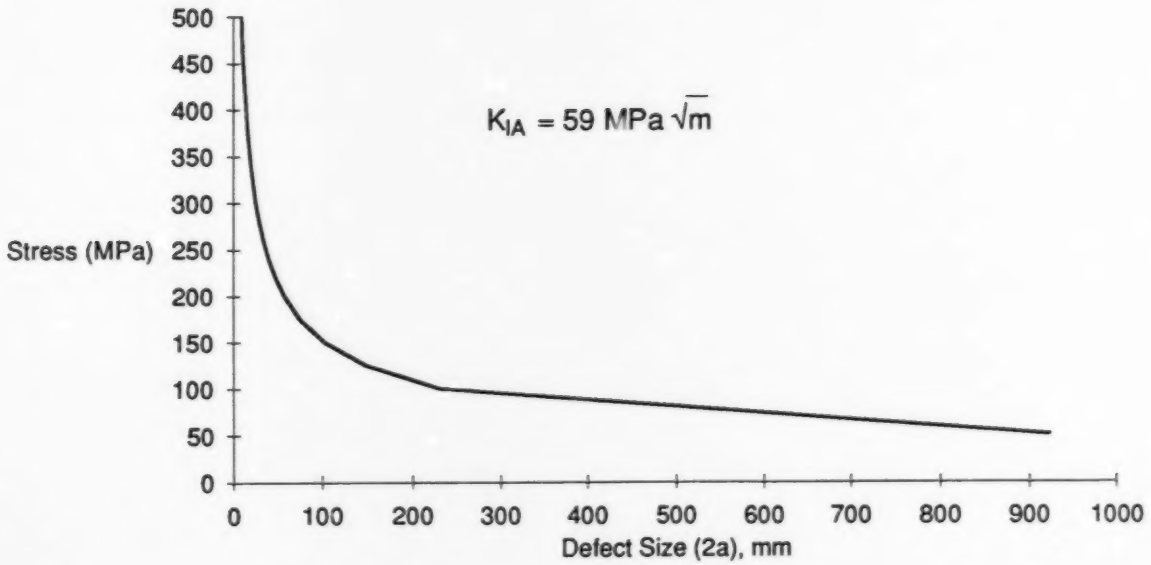

Figure 34: Stress-flaw size relationship for a through thickness crack in an infinite plate assuming K_{IA} = 59 MPa$\sqrt{m}$

APPENDIX A

Steel Selection Requirements Specified in CASPPR

STEEL SELECTION REQUIREMENTS SPECIFIED IN CASPPR

The proposed CASPPR steel distribution within the hull for ships navigating in the Arctic is schematically shown in Figure A1 and also in Table A1 (Proposed Revision to CASPPR, Schedule 3, 9/8/89).

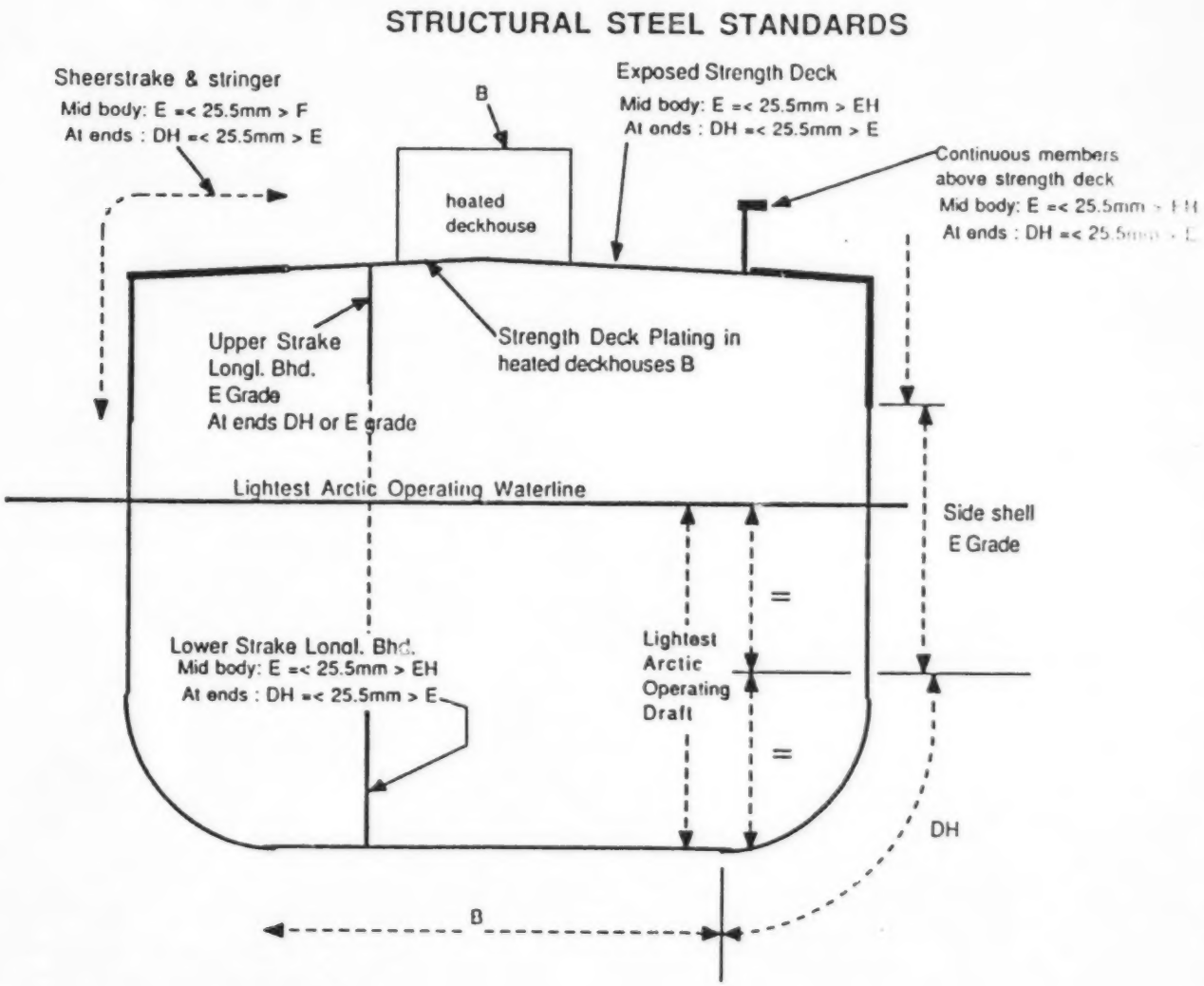

Figure A1: Distribution of Steels in a Ship Hull
(after Proposed Rev. CASPPR, Schedule 3)

TABLE A1

CASPPR REQUIREMENTS FOR STEEL SELECTION

ITEM	STRUCTURAL MEMBER INCLUDING ANY ATTACHED STRUCTURE FOR A DEPTH OF 740 mm	STEEL GRADES			
		FROM 0.2L AFT TO 0.3L FORWARD OF MIDSHIPS	FROM 0.2L AFT TO 0.3L FORWARD OF MIDSHIPS	OUTSIDE 0.2L AFT TO 0.3L FORWARD OF MIDSHIPS	OUTSIDE 0.2L AFT TO 0.3L FORWARD OF MIDSHIPS
	THICKNESS------->	<=25.5 mm	>25.5 mm	<=25.5 mm	>25.5 mm
1	Sheerstrake at strength deck	E	F	D H	E
2	Strength deck plating exposed or in unheated deckhouses	E	E H	D H	E
3	Strength deck plating in heated deckhouses	B	B	B	B
4	Side shell plating from lower edge sheerstrake to waterline at half the lightest operating draft.	E	E	E	E
5	Remainder of side shell to flat of bottom.	D H	D H	D H	D H
6	Flat of bottom and keel	B	B	B	B
7	Exposed non-strength deck plating	B	B	B	B
8	Continuous longitudinal members above strength deck	E	E H	D H	E
9	Upper strake of longitudinal bulkhead at strength deck	E	E	D H	E
10	Upper strake of top wing tank longitudinal bulkhead	E	E	D H	E
11	Lower strake of longitudinal bulkhead at bottom shell	D H	D H	D H	D H
12	Sternframes, rudder horns, rudders, ice horns, shaft brackets,bossings	-	-	D H	D H

APPENDIX B

Statistical Significance of the Results

By

Mark J. Tomin
Reltect Advisory Services Inc.

STATISTICAL SIGNIFICANCE OF THE RESULTS

B.1 Statistical Approach to Brittle Fracture

Fracture initiation is a function of random variables such as stress, crack size and fracture toughness. Fracture toughness itself depends on other random quantities, for example, temperature, microstructure of the material and strain rate. Fracture is a random event which depends on simultaneous incidence of the presence of a crack, low toughness (low temperature, high loading rate) and sufficient stress to propagate the crack.

This stochastic phenomenon can be taken into account only in a full probabilistic fracture analysis and Canadian Coast Guard and CANMET have sponsored several studies in this area (see References B1 and B2).

Only through probabilistic analysis can the weight of individual variables be assessed in view of contribution of other variables to fracture.

To show an example of such probabilistic analysis, some of the experimental data obtained for fracture toughness (CTOD) and reported in the main text, was used together with probability density functions (PDF) for crack size and assumed PDF for stress (applied, residual) in a simple crack initiation model. Monte Carlo simulation technique was used to obtain probability of failure.

In the following sections, the input data in the probabilistic model is briefly described.

B.2 Fracture Toughness

Fracture toughness is a random variable which exhibits a transition behaviour as a function of temperature. Bishop et al (Ref. B3) developed a technique, whereby at each temperature a Weibull two-parametric distribution can be obtained, which allows one to derive any confidence intervals (percentile) for a given set of data.

The method consists to fit the two-parameter Weibull distribution,

$$F(y) = Prob[Y \le y] = \begin{cases} 0, & y<0 \\ 1-e^{(-(y/\beta)^{\alpha})}, & y \ge 0 \end{cases}$$

where the parameters $\alpha(T)$ and $\beta(T)$ are functions of temperature. This equation represents the probability that an observed experimental value Y falls below an arbitrary value y.

To establish the functions $\alpha(T)$ and $ß(T)$, a simple iterative procedure combined with linear regression techniques are used. After some transformations, the above equation is recast in term of natural logarithms for α and ß. The iterative procedure is done in two stages. First, an estimate for ß is obtained by polynomial fitting assuming a value for α. This causes a bias in the estimation of ß, which is reduced by fitting α .

An important feature of this analysis is its use of the experimental scatter as an integral part of the iterative process. By this means, unrealistic predictions of the non-zero probabilities of negative energies can be prevented. Allowing the scatter to vary with temperature also can prevent the problem of assigning a lower bound to one region of the curve that is influenced by data from another region. For example, there is no reason to expect that the upper-shelf and lower shelf data will have the same variability.

To obtain a typical S-curve in the transition region, constraints are often necessary (zero derivative) to obtain the energy shelves in cases when not sufficient data exists in relevant regions.

The technique described above was used here to obtain lower (5%-tile) and upper (95%-tile) bound on CVN toughness (Figures B1 to B12) and CTOD fracture toughness (Figures B13 to B18). Only CTOD data for steels A, B and D was modelled for both quasi-static and intermediate strain rates using the Bishop technique to demonstrate the probabilistic approach.

B.3 Crack Size

Two crack distributions were used for the analysis. For small cracks, the Weibull distribution obtained by Wong and Rogerson (Ref. B4), Figure B19. This distribution is based on data obtained by Non-Destructive Testing of ship weldments. The three-parametric Weibull distribution has parameters $\alpha = 0.91$, $ß = 0.8$ and $\Theta = 0.1$mm.

The distribution for large cracks was obtained by Antoniu (Ref. B5) who collated data on 25,652 cracks detected over eight year period in 233 tankers. Lognormal distribution, Figure B20, fits well with the data. Lognormal distribution is commonly used for crack size because it does not allow for negative values. The parameters for the three-parametric lognormal distribution were: $\varepsilon = 0.55$, $\alpha = 5.44$ and $\Theta = 40.5$ mm.

B.4 Applied and Residual Stress

Applied stress was assumed to follow normal distribution with $\sigma_{mean} = 0.4\sigma_y$ and coefficient of variation 20%. For large cracks, it was assumed that the residual stress is small, $\sigma_{res} = 0.2\sigma_y$, and constant. For small cracks, residual stress was assumed to be equal to the yield stress σ_y.

B.5 Wide Plate Correlation (Safety) Factor

The correlation data between the crack size predicted from CTOD and the critical crack size obtained from Wide Plate Tests (Ref. B6), Figure B21, was used in the analysis. The safety factor, s, between the critical crack size (from WPT) and predicted crack size (from CTOD) was obtained form the data shown in Figure B21 (s = 2.5 at 51.2%-tile and s = 1 at 95.4%-tile). Normal distribution was used to fit the data with s_{mean} = 2.53 and standard deviation std = 0.85.

B.6 Fracture Criterion

Crack initiation criterion (limit state function) based on CTOD/WPT correlation was used to calculate probabilities of failure. The probability of failure was defined as follows

$$P_f = Prob[a - sa_c > 0] \qquad (10)$$

where 'a' is the crack depth for small cracks or half the through-thickness crack length for large cracks. a_c is the crack size obtained from the Burdekin and Dawes CTOD relationship, given by:

$$\delta = \frac{\sigma \pi a}{E} X \left(\frac{\sigma}{\sigma_y} - 0.25 \right) \qquad (B2)$$

B.7 Discussion of the Results

Table B1 contains probabilities of failure for all considered cases (small cracks, large cracks, temperatures -5°C and -40°C and steels AT, BT and DT).

TABLE B1: PROBABILITIES OF FAILURE

STEEL	LOADING RATE	SMALL CRACKS		LARGE CRACKS	
		-40°C	-5°C	-40°C	-5°C
AT	STATIC	3.134E-03	3.078E-03	5.795E-02	1.236E-02
	INTERM	2.439E-02	5.663E-03	3.482E-01	2.080E-01
BT	STATIC	3.879E-03	3.150E-03	4.274E-01	1.697E-01
	INTERM	7.633E-03	3.285E-03	9.694E-01	2.457E-01
DT	STATIC	1.382E-02	3.061E-03	1.055E-01	1.118E-02
	INTERM	1.932E-02	4.713E-03	7.530E-01	3.506E-02

It can be seen that the probability of failure for large cracks is one to two orders of magnitude higher than for small cracks.

For steel A (transverse orientation), there is almost one order of magnitude difference in probabilities of failure between the static and intermediate cases for both small and large cracks. This difference almost disappears at -5°C for small cracks but remains high (one order of magnitude) for large cracks.

It is interesting to note that for steels BT and DT, the difference between probabilities of failure corresponding to static and intermediate cases is not very pronounced (results are within the same order of magnitude). This is surprising in particular for steel DT, where at -40°C, the difference between quasi-static and intermediate CTOD was well defined. However, it is clear from Figures B15 and B16 that the CTOD Weibull distribution for the intermediate strain rate is much narrower than for that corresponding to the quasi-static case. Even though the average values would suggest (deterministically) that there would be greater difference between these two cases, only the probabilistic analysis can capture the significance of the scatter (or absence of data).

Probabilities of failure were calculated also for -20°C to obtain a third point so that the trend can be assessed. These three points were connected using straight line, Figures B22 to B27.

B.8 References

[B1] Tomin, M. and Lantos, S.L. (1986), "Evaluation of Fracture Toughness Data with Respect to Reliability of Subarctic and Arctic Structures", VERITAS Report No. 86-CGY-042.

[B2] Tomin, M., Nessim, M. and Cormeau, A. (1988), "Fracture Control for Arctic Structures: A Model for Analyzing Structural Details", VERITAS Report to CANMET.

[B3] Bishop, T.A., Markworth, A.J., and Rosenfield, A.R. (1983), "Analyzing Statistical Variability of Fracture Properties", Metallurgical Transaction A, Volume 14A, April 1983, pp. 687-693.

[B4] Wong, W.K. and Rogerson, J.H. (1983), "A Probabilistic Estimate of the Relative Value of Factors Which Control the Failure by Fracture of Offshore Structures", The Welding Institute Proc. Second Int. Conf. on Offshore Welded Structures, Paper No. 9.

[B5] Antoniou, A.C. (1977), "A Survey on Cracks in Tankers Under Repairs", PRADS - Int. Symp. on Practical Design in Shipbuilding, Tokyo, October.

Figure B1: Upper and Lower Bounds for CVN Energy - Steel A Longitudinal

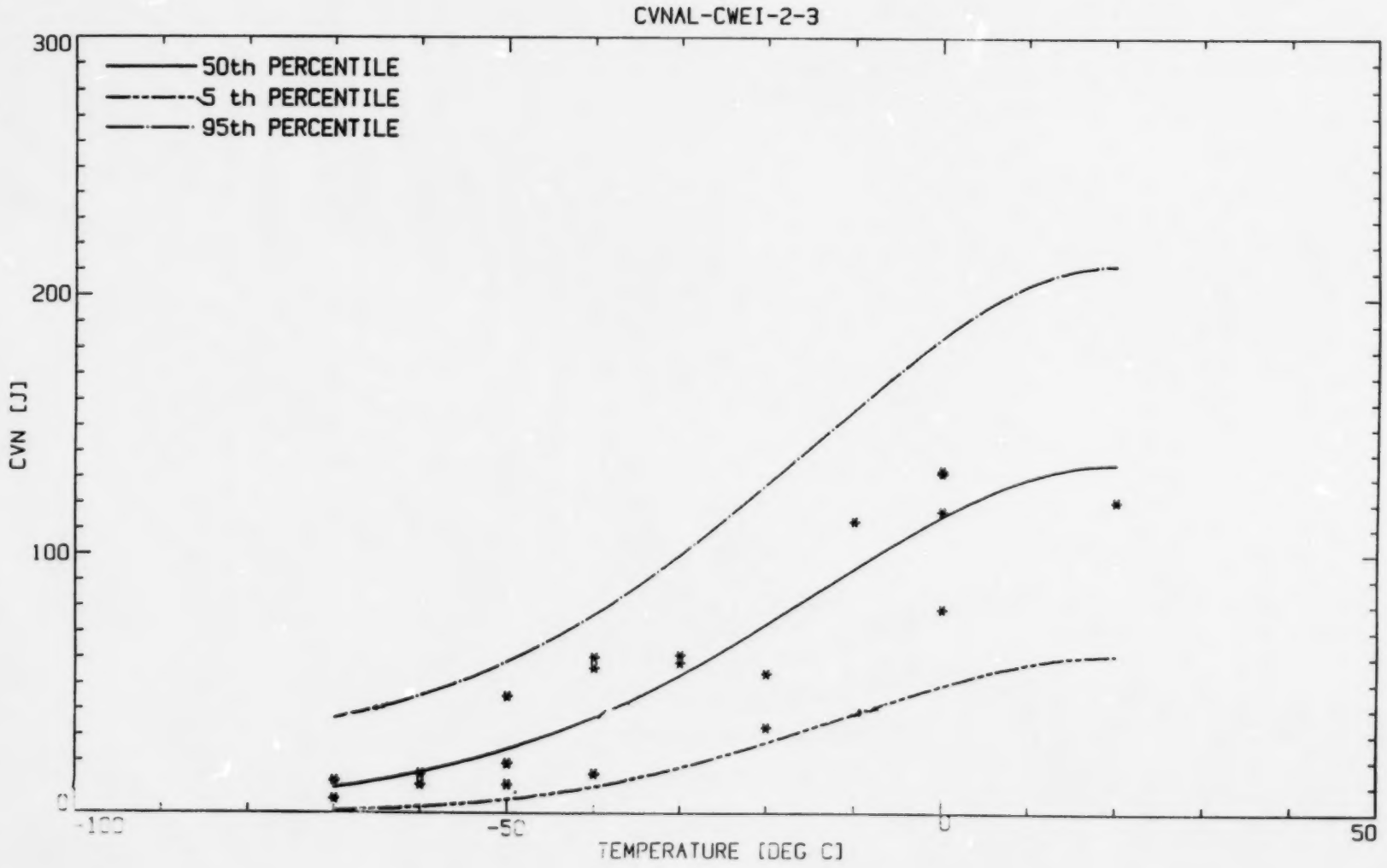

Figure B2 : **Upper and Lower Bounds for CVN Energy - Steel A Transverse**

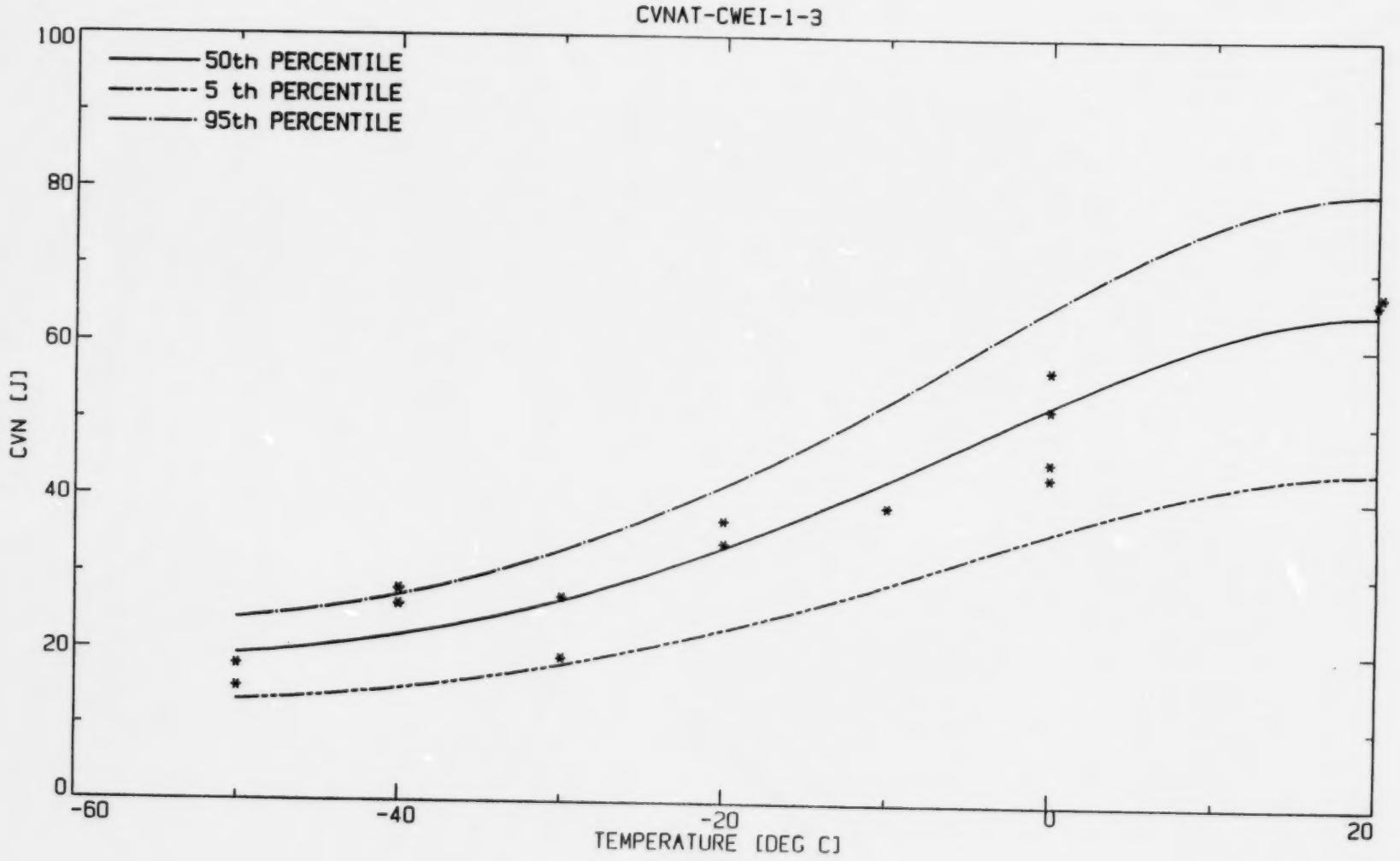

Figure B3 : **Upper and Lower Bounds for CVN Energy - Steel B Longitudinal**

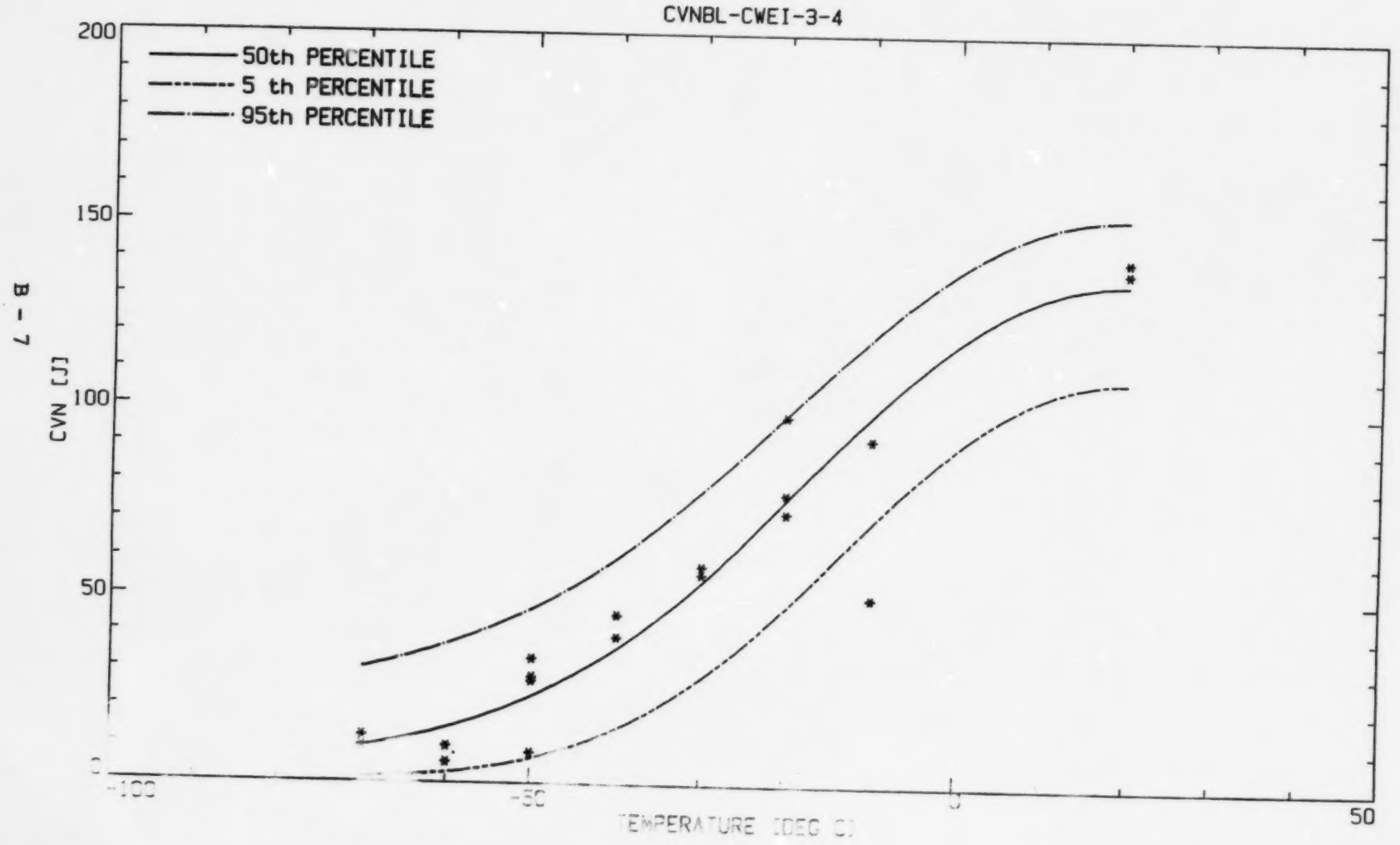

Figure B4 : **Upper and Lower Bounds for CVN Energy - Steel B Transverse**

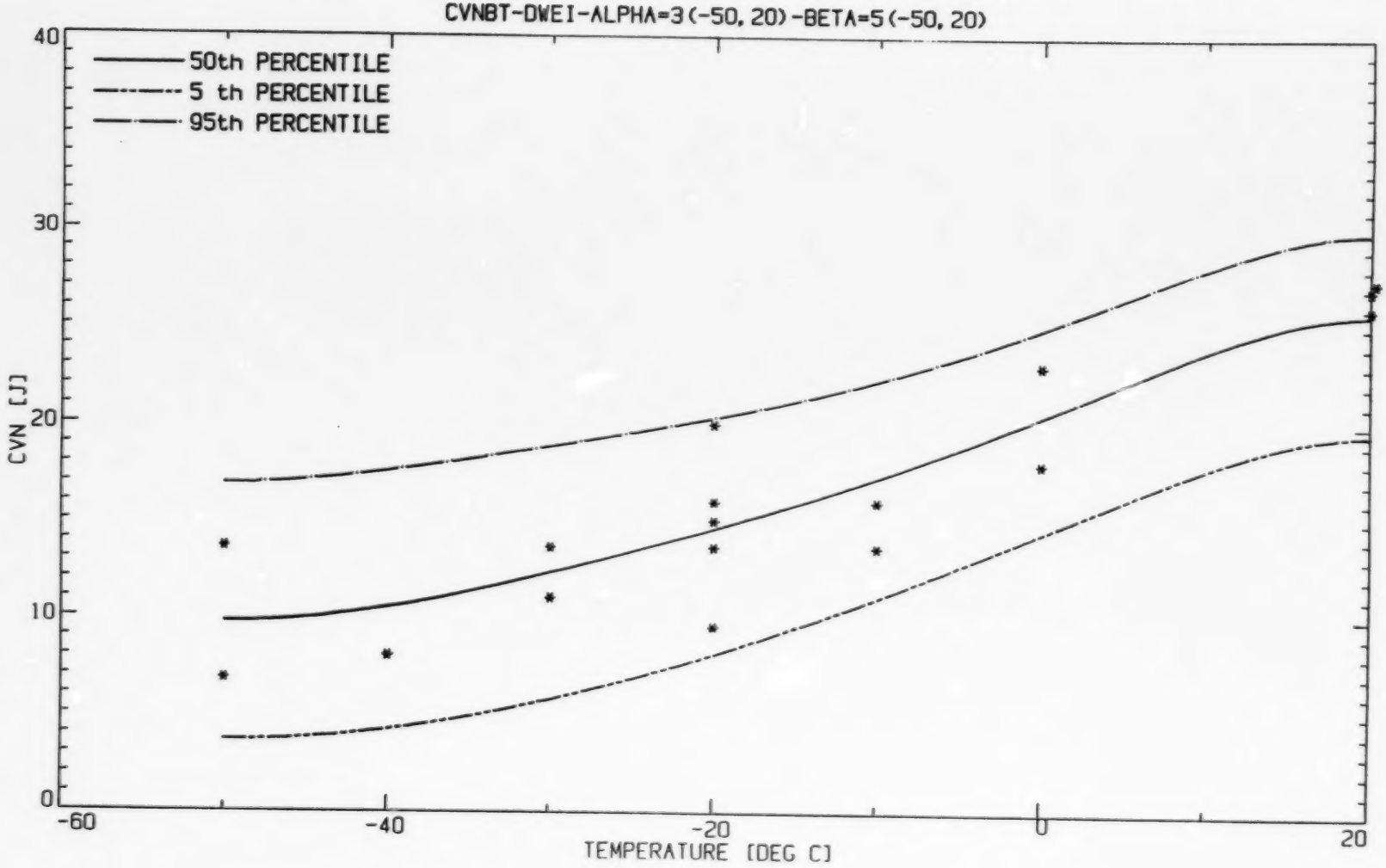

Figure B5: Upper and Lower Bounds for CVN Energy - Steel C Longitudinal

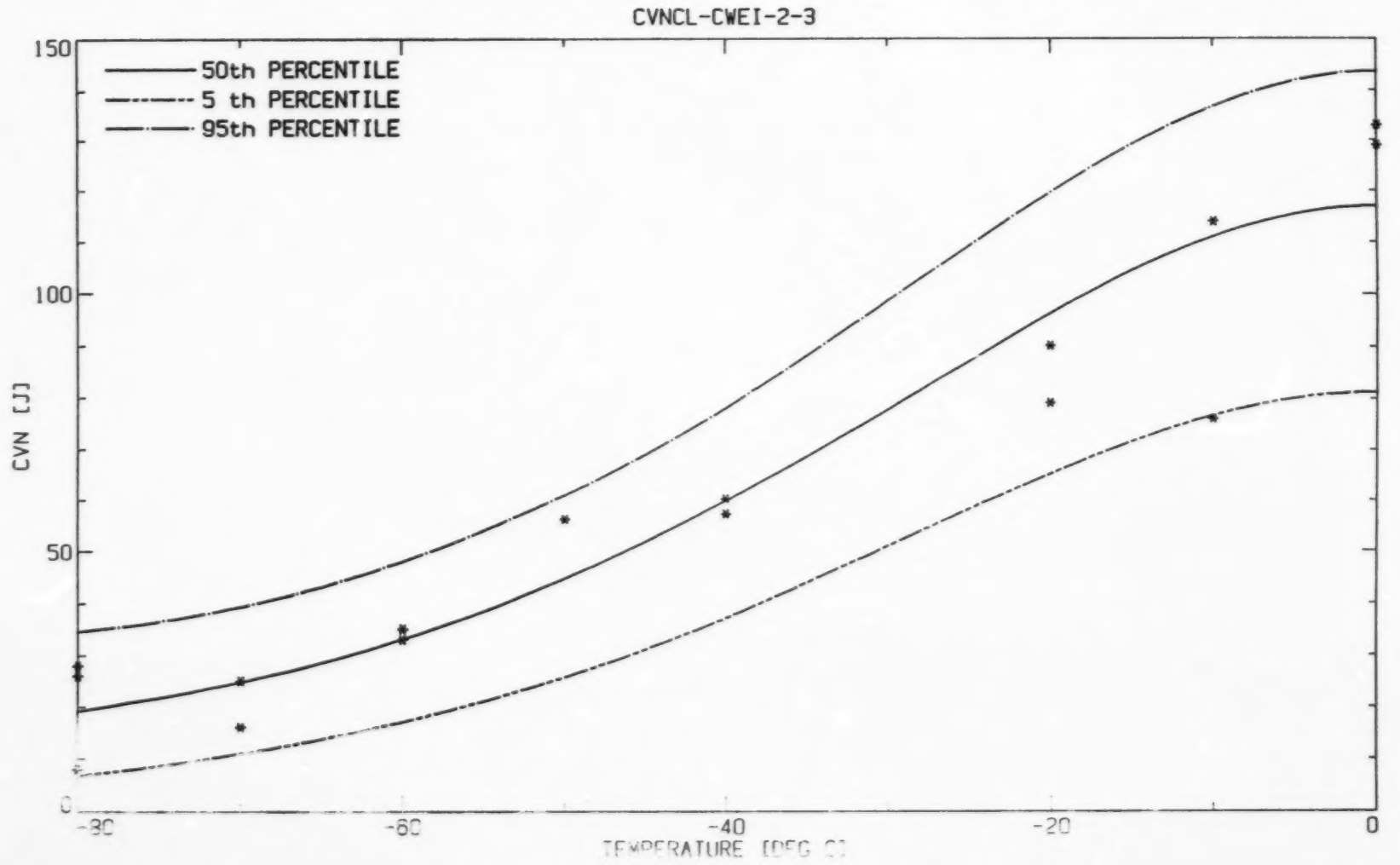

Figure B6 : Upper and Lower Bounds for CVN Energy - Steel C Transverse

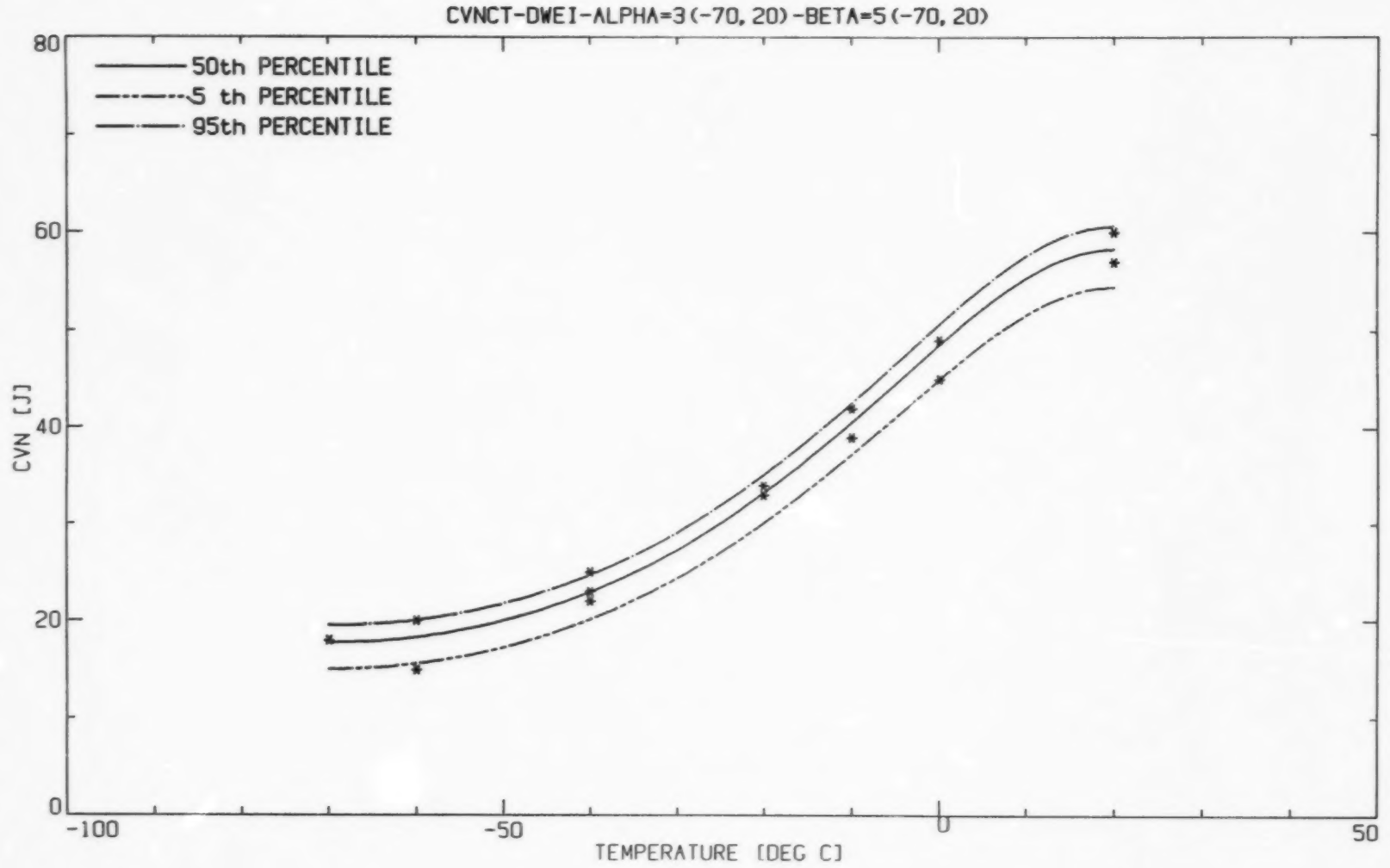

Figure B7 : **Upper and Lower Bounds for CVN Energy - SteelD Longitudinal**

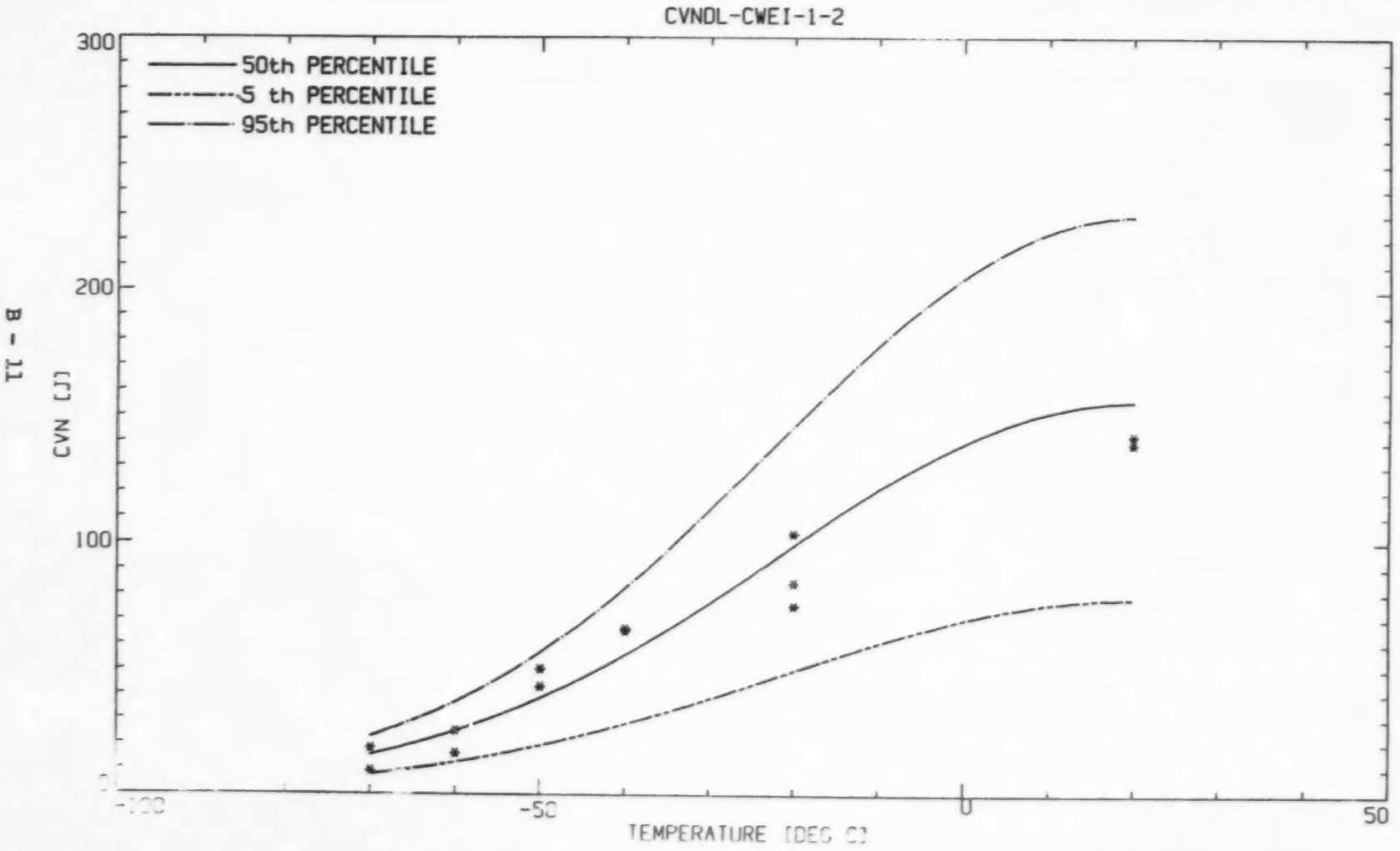

Figure B8: Upper and Lower Bounds for CVN Energy - Steel D Transverse

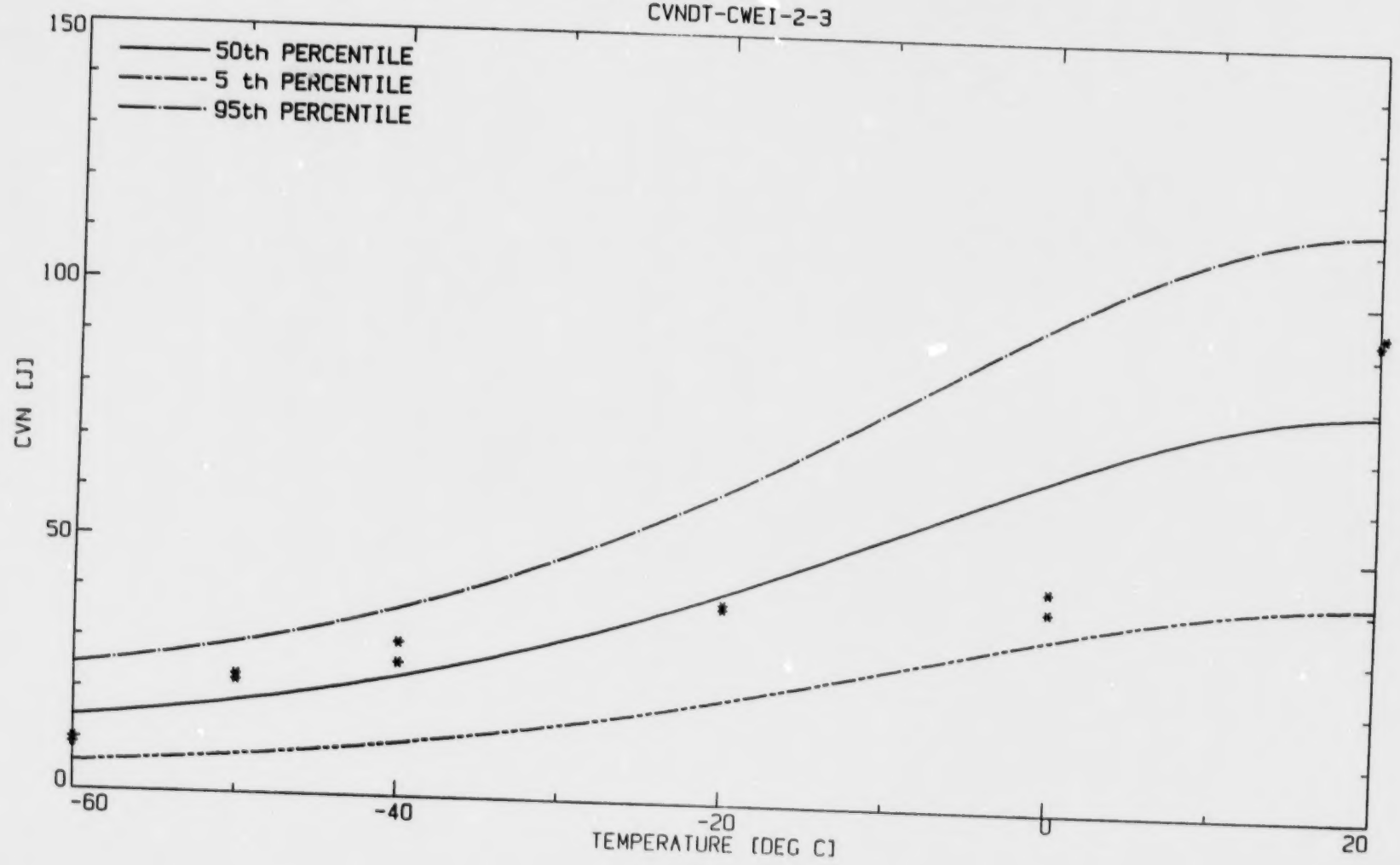

Figure B9 : Upper and Lower Bounds for CVN Energy - Steel E Longitudinal

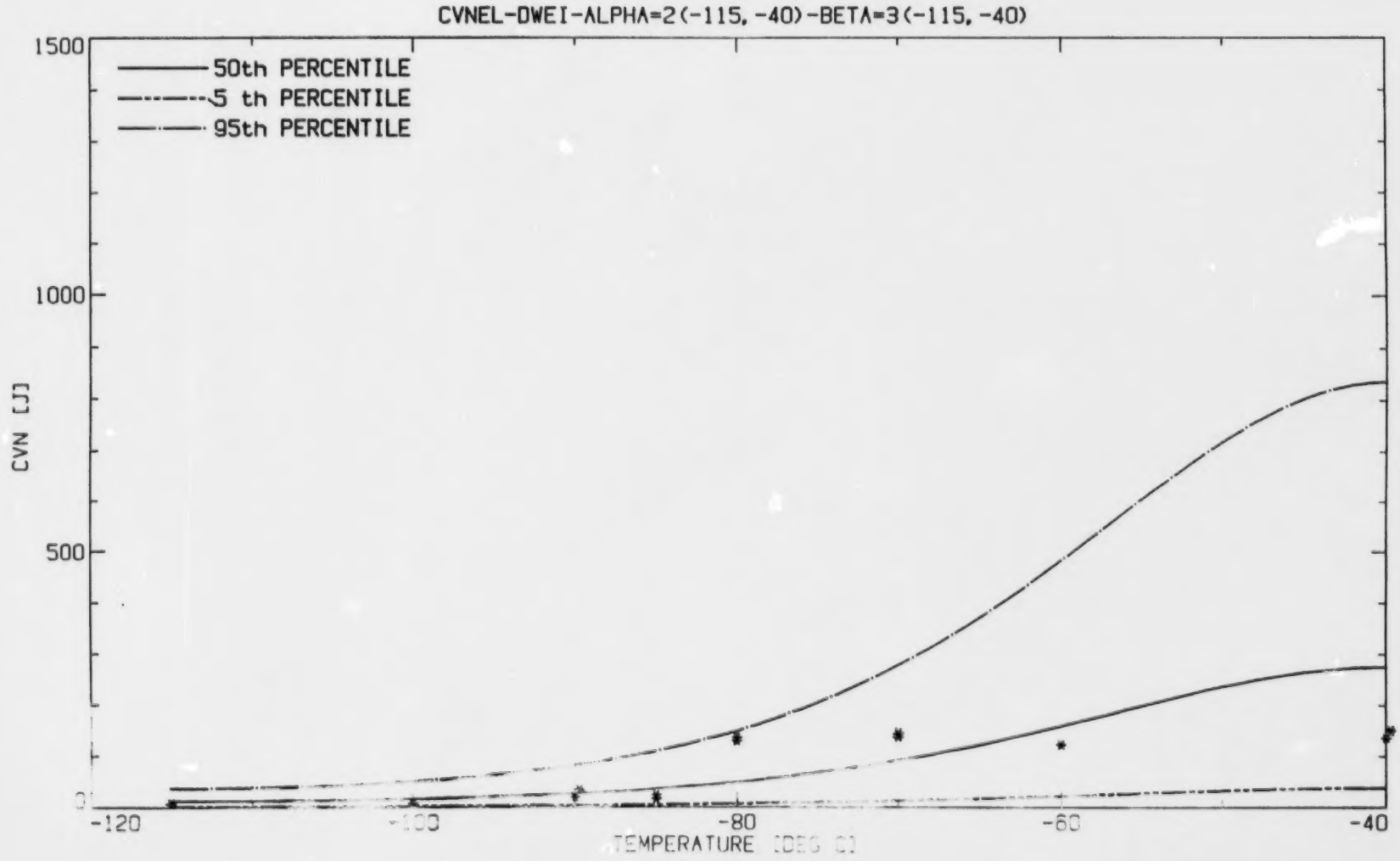

Figure B10 : Upper and Lower Bounds for CVN Energy - Steel E Transverse

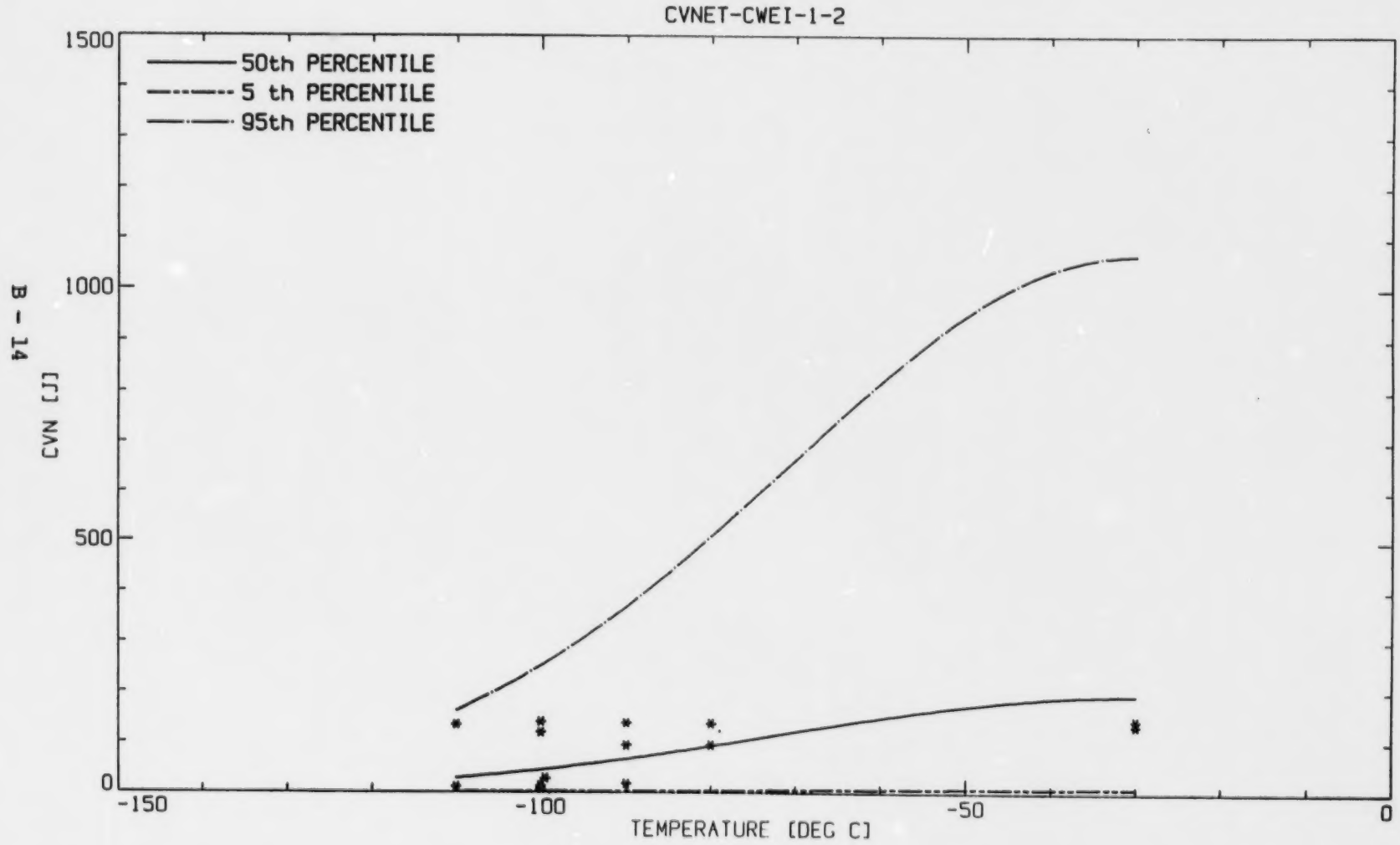

Figure B11: Upper and Lower Bounds for CVN Energy - Steel WP Longitudinal

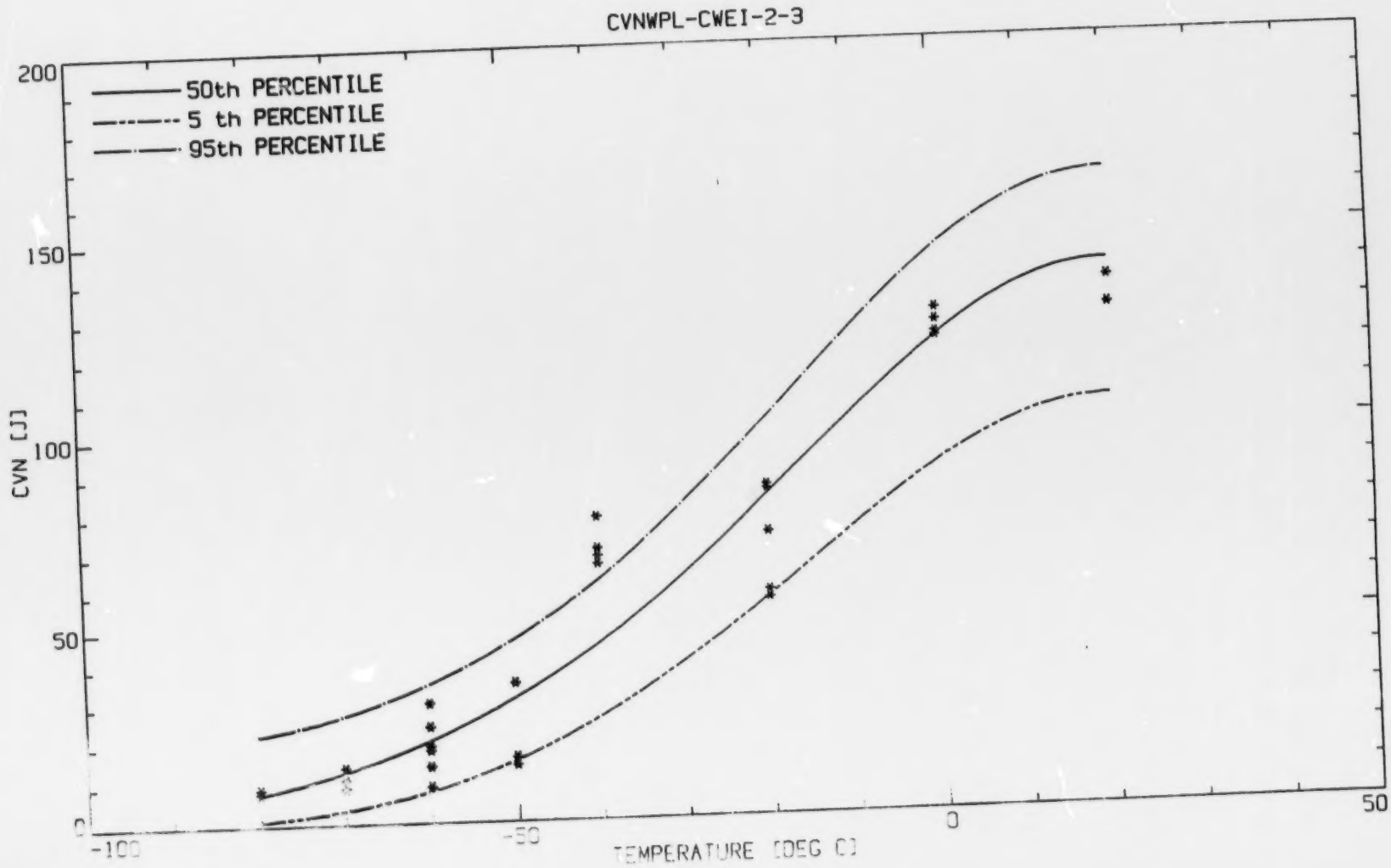

Figure B12 : Upper and Lower Bounds for CVN Energy - Steel WP Transverse

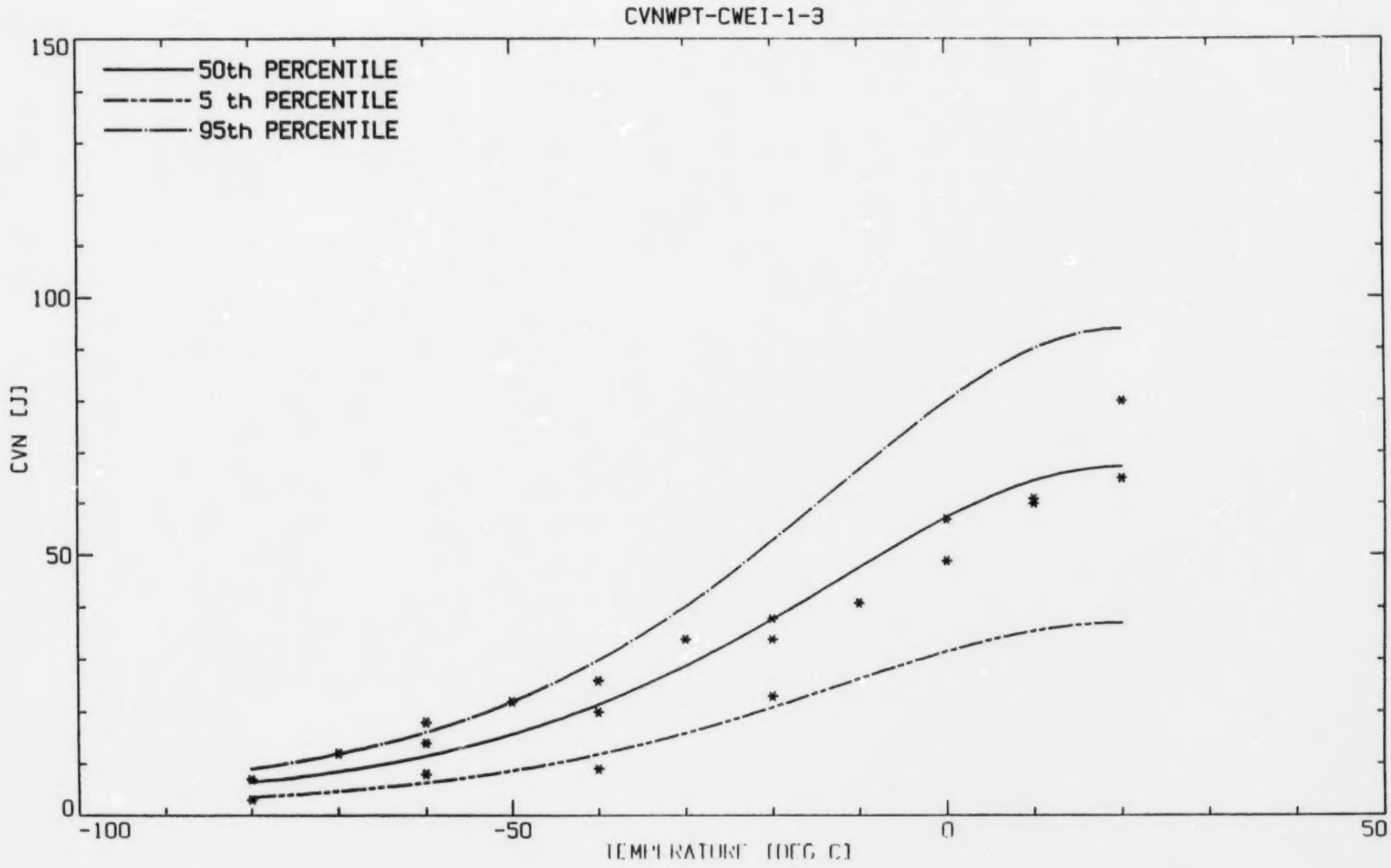

Figure B13 : Upper and Lower Bounds for CTOD Static - Steel A Transverse

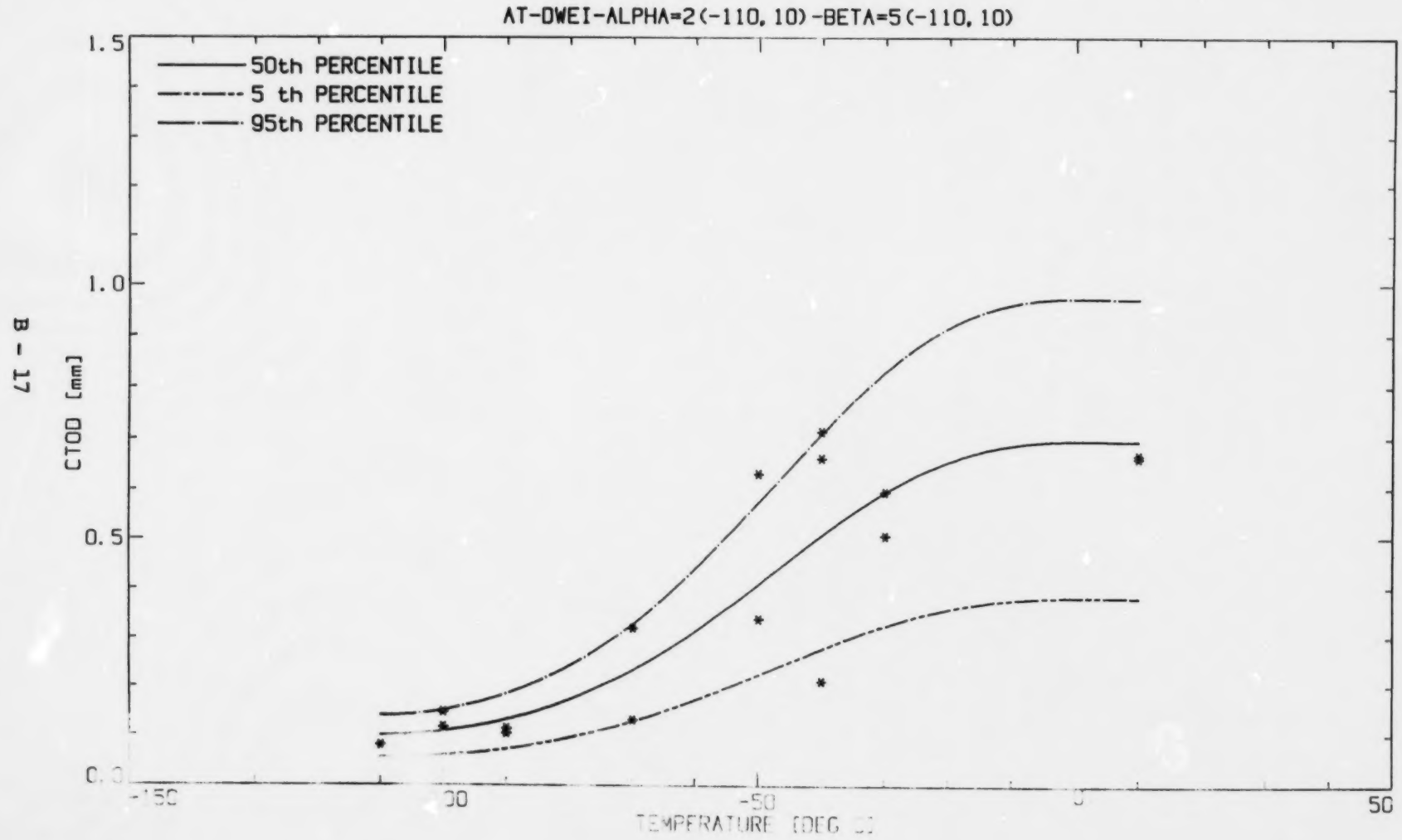

Figure B14 : Upper and Lower Bounds for CTOD Intermediate - Steel A Transverse

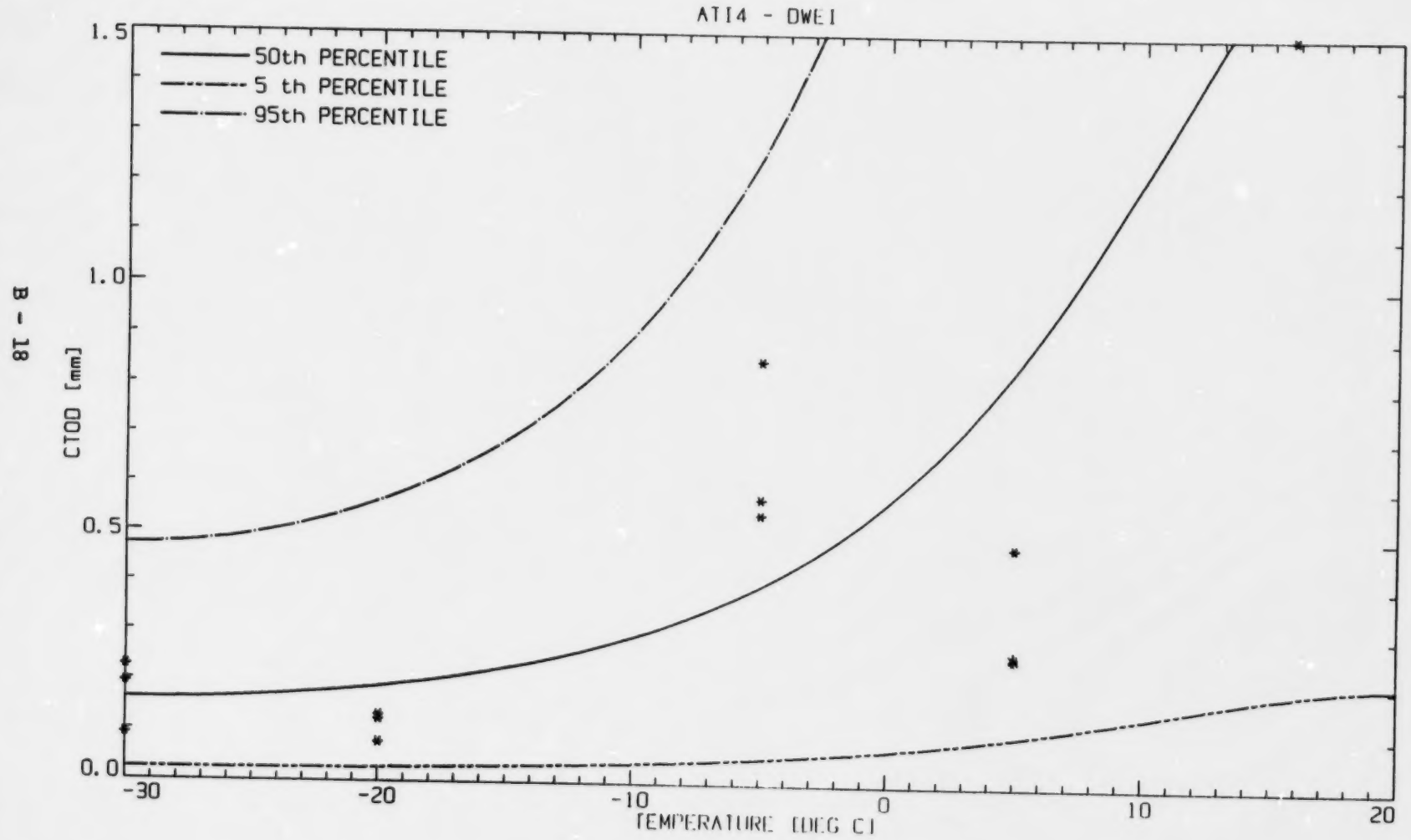

Figure B15 : Upper and Lower Bounds for CTOD Static - Steel B Transverse

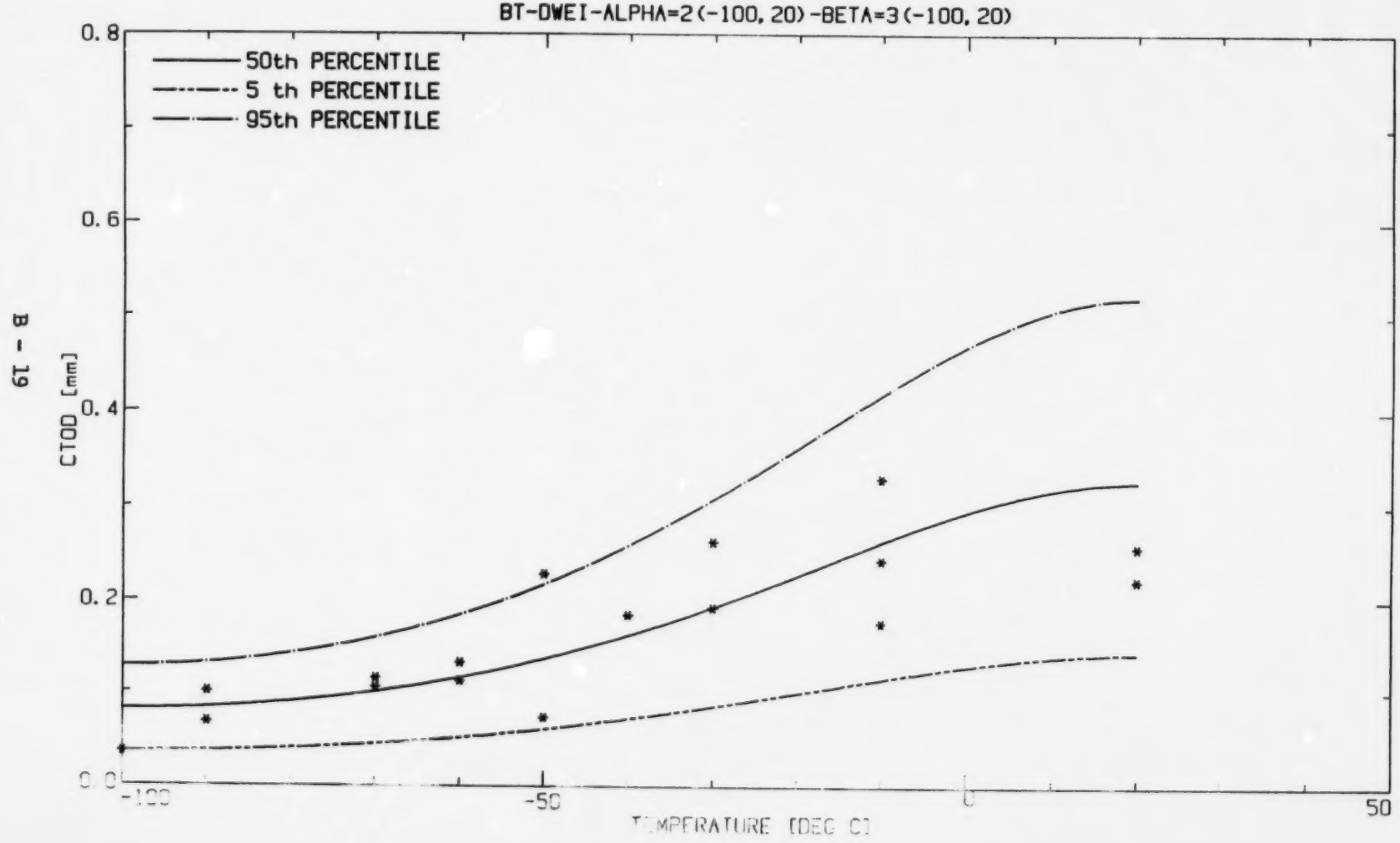

Figure B16: Upper and Lower Bounds for CTOD Intermediate - Steel B Transverse

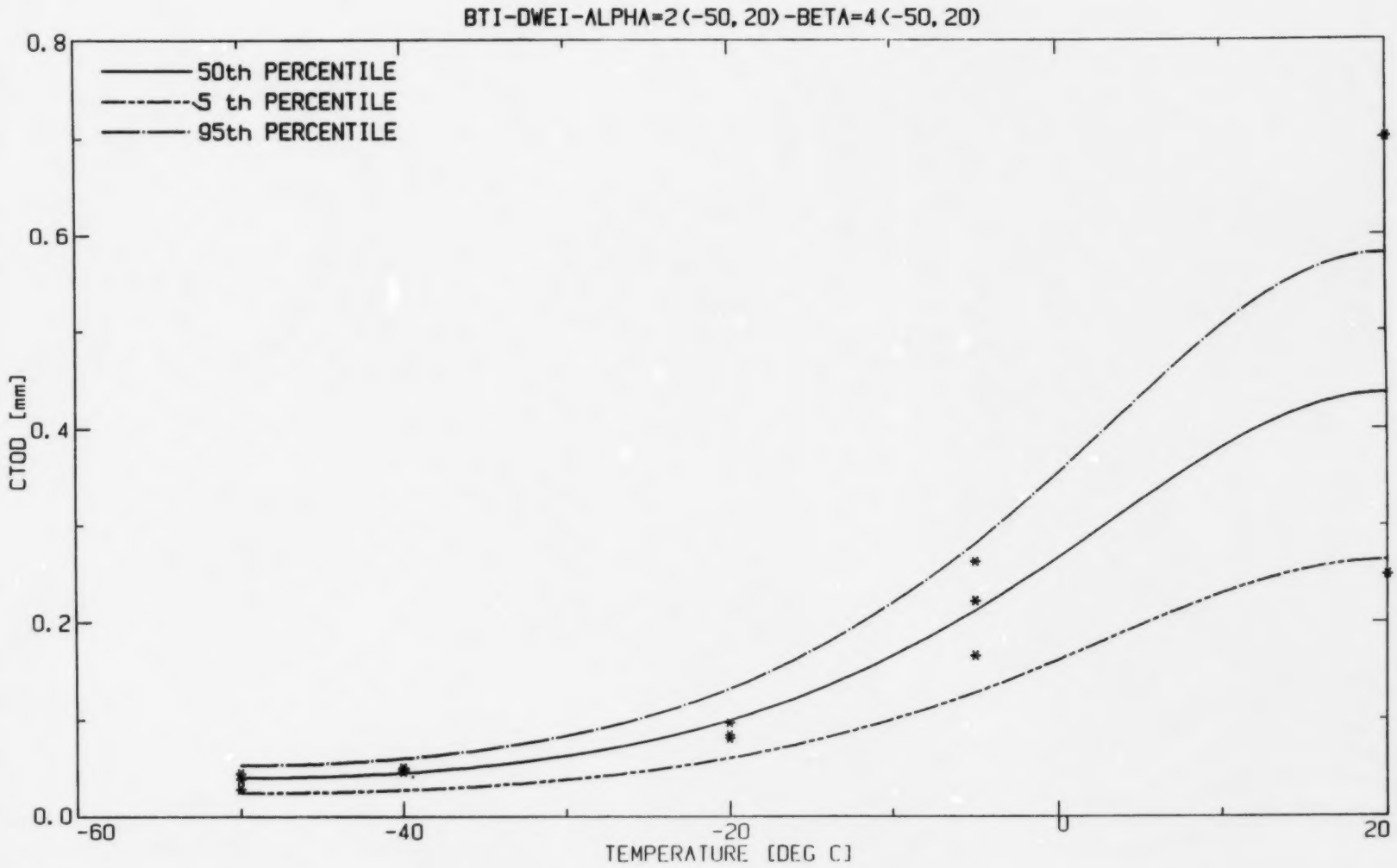

Figure B17: Upper and Lower Bounds for CTOD Static - Steel D Transverse

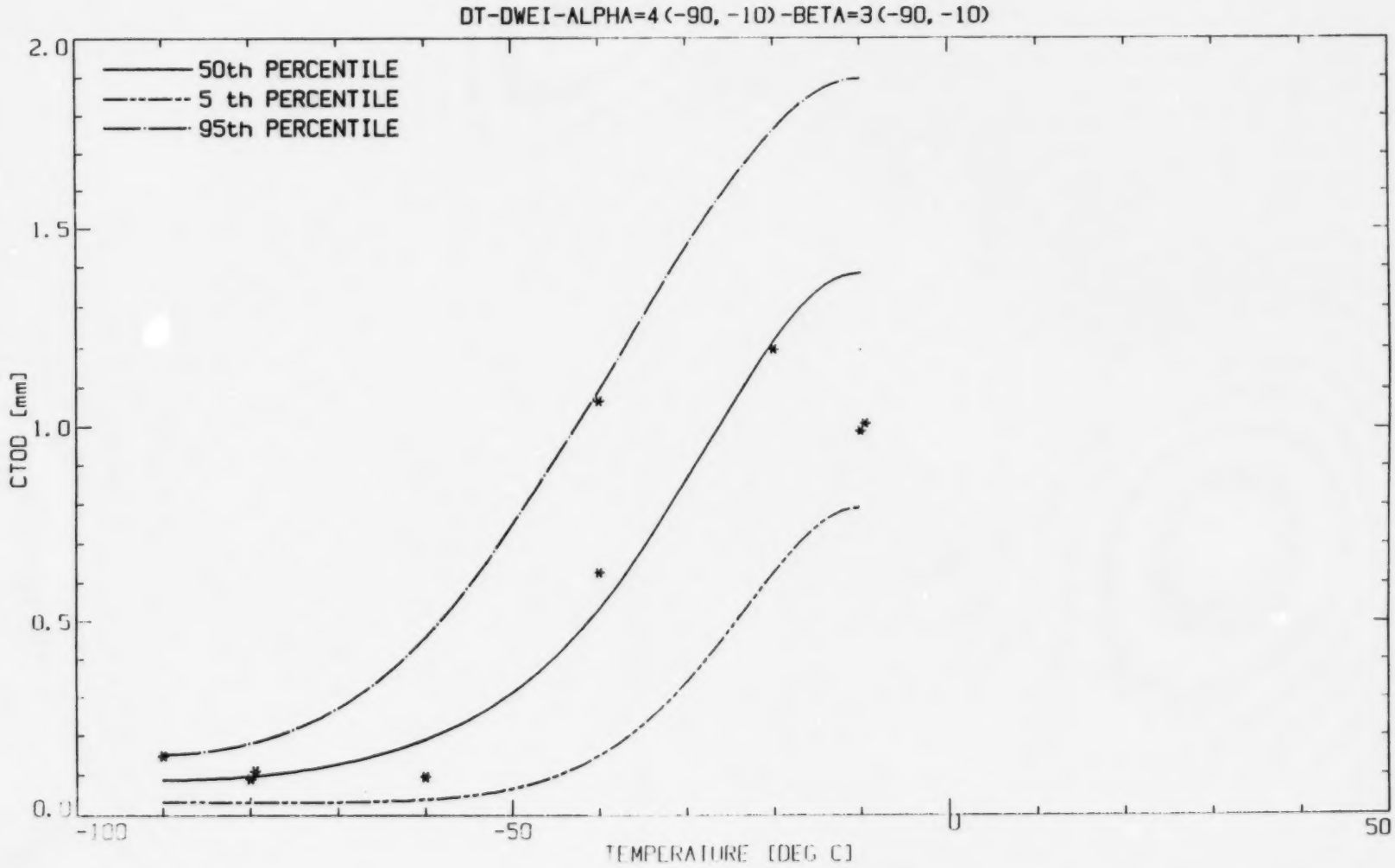

Figure B18 : Upper and Lower Bounds for CTOD Intermediate - Steel D Transverse

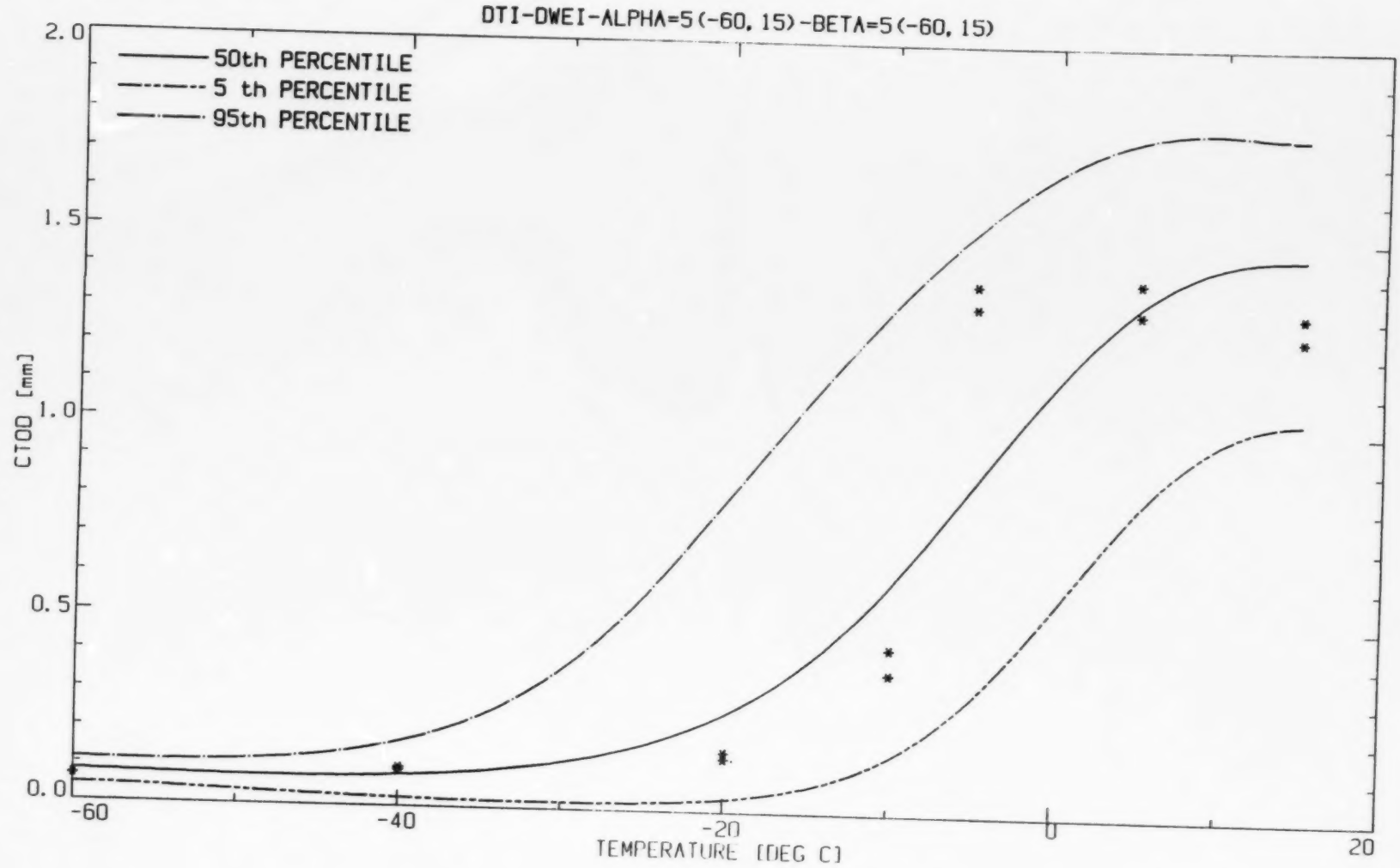

Tmin(Deg C)	Tmax(Deg C)
-7.00000E+01	2.00000E+01

COEFF.	ALPHA	BETA
C0	1.12989E+00	4.86320E+00
C1	5.36791E-03	1.53975E-02
C2	-1.34198E-04	-3.41789E-04
C3		-1.43833E-06

CVN REGRESSION COEFFICIENTS FOR TEMPERATURE DEPENDENT WEIBULL DISTRIBUTION [J] FOR STEEL A (Trans.)

Tmin(Deg C)	Tmax(Deg C)
-5.00000E+01	2.00000E+01

COEFF.	ALPHA	BETA
C0	1.91251E+00	4.01442E+00
C1		1.85909E-02
C2		-3.00388E-04
C3		-5.47945E-06

CVN REGRESSION COEFFICIENTS FOR TEMPERATURE DEPENDENT WEIBULL DISTRIBUTION [J] FOR STEEL A (Long.)

Tmin(Deg C)	Tmax(Deg C)
-5.00000E+01	2.00000E+01

COEFF.	ALPHA	BETA
C0	2.00854E+00	3.06766E+00
C1	2.26005E-02	1.55029E-02
C2	-3.39008E-04	-2.80308E-05
C3	-7.53351E-06	-5.07561E-06
C4		-1.96357E-07
C5		-2.50935E-09

CVN REGRESSION COEFFICIENTS FOR TEMPERATURE DEPENDENT WEIBULL DISTRIBUTION [J] FOR STEEL B (Trans.)

Tmin(Deg C)	Tmax(Deg C)
-7.00000E+01	2.00000E+01

COEFF.	ALPHA	BETA
C0	2.26252E+00	4.80993E+00
C1	2.08037E-02	1.32997E-02
C2	-3.99385E-04	-3.77975E-04
C3	-4.02359E-06	6.82136E-07
C4		3.12741E-08

CVN REGRESSION COEFFICIENTS FOR TEMPERATURE DEPENDENT WEIBULL DISTRIBUTION [J] FOR STEEL B (Long.)

Tmin(Deg C)	Tmax(Deg C)
-7.00000E+01	2.00000E+01

COEFF.	ALPHA	BETA
C0	3.53495E+00	3.89326E+00
C1	1.02050E-02	1.59073E-02
C2	-1.82233E-04	-2.33603E-04
C3	-2.42977E-06	-4.94691E-06
C4		-1.91420E-08
C5		-1.79494E-11

CVN REGRESSION COEFFICIENTS FOR TEMPERATURE DEPENDENT WEIBULL DISTRIBUTION [J] FOR STEEL C (Trans.)

Tmin(Deg C)	Tmax(Deg C)
-1.15000E+02	-4.00000E+01

COEFF.	ALPHA	BETA
C0	2.75925E-01	2.28300E+00
C1		-2.04378E-01
C2		-3.44333E-03
C3		-1.48100E-05

CVN REGRESSION COEFFICIENTS FOR TEMPERATURE DEPENDENT WEIBULL DISTRIBUTION [J] FOR STEEL E (Long.)

Tmin(Deg C)	Tmax(Deg C)
-8.00000E+01	0.00000E-01

COEFF.	ALPHA	BETA
C0	1.96634E+00	4.81405E+00
C1	0.00000E-01	0.00000E-01
C2	-1.64534E-04	-5.56526E-04
C3		-3.62090E-06

CVN REGRESSION COEFFICIENTS FOR TEMPERATURE DEPENDENT WEIBULL DISTRIBUTION [J] FOR STEEL C (Long.)

Tmin(Deg C)	Tmax(Deg C)
-6.00000E+01	2.00000E+01

COEFF.	ALPHA	BETA
C0	1.36579E+00	4.27163E+00
C1	2.43628E-03	1.77215E-02
C2	-6.09069E-05	-3.33167E-04
C3		-3.66233E-06

CVN REGRESSION COEFFICIENTS FOR TEMPERATURE DEPENDENT WEIBULL DISTRIBUTION [J] FOR STEEL D (Trans.)

Tmin(Deg C)	Tmax(Deg C)
-7.00000E+01	2.00000E+01

COEFF.	ALPHA	BETA
C0	1.32665E+00	5.03064E+00
C1		1.14188E-02
C2		-2.85470E-04

CVN REGRESSION COEFFICIENTS FOR TEMPERATURE DEPENDENT WEIBULL DISTRIBUTION [J] FOR STEEL D (Long.)

Tmin(Deg C)	Tmax(Deg C)
-1.10000E+02	-3.00000E+01

COEFF.	ALPHA	BETA
C0	-1.53797E-01	5.42894E+00
C1		-1.76364E-02
C2		-2.93940E-04

CVN REGRESSION COEFFICIENTS FOR TEMPERATURE DEPENDENT WEIBULL DISTRIBUTION [J] FOR STEEL E (Trans.)

	AT QUASI-STATIC		AT INTERMEDIATE STRAIN RATE	
	ALPHA	BETA	ALPHA	BETA
C0	1.4658251E+00	-2.7920941E-01	2.1758097E-01	-2.6876566E-01
C1		8.7307839E-05	-4.0978310E-03	7.6806866E-02
C2		-7.4917480E-05	3.4148590E-05	5.8175466E-04
C3		4.2983847E-06	2.2765728E-06	-4.0913787E-05
C4		3.0551394E-08		-1.2098313E-06
C5		-1.3585000E-11		-1.5332382E-08

CTOD REGRESSION COEFFICIENTS FOR TEMPERATURE DEPENDENT WEIBULL DISTRIBUTION [mm] FOR STEEL A (Trans.)

	BT QUASI-STATIC		BT INTERMEDIATE STRAIN RATE	
	ALPHA	BETA	ALPHA	BETA
C0	1.1464937E+00	-1.1079421E+00	1.6422962E+00	-1.2494138E+00
C1		9.7049819E-03		4.3007966E-02
C2		-1.9409964E-04		-6.0935854E-04
C3		-1.6174970E-06		-1.5051207E-05
C4				-1.7880451E-08

CTOD REGRESSION COEFFICIENTS FOR TEMPERATURE DEPENDENT WEIBULL DISTRIBUTION [mm] FOR STEEL B (Trans.)

	DT QUASI-STATIC		DT INTERMEDIATE STRAIN RATE	
	ALPHA	BETA	ALPHA	BETA
C0	1.2726544E+00	2.6598325E-01	1.2986081E+00	2.1487516E-01
C1	-5.7770353E-02	-2.8462948E-02	7.2038934E-02	3.6536936E-02
C2	-3.7293187E-03	-1.5812749E-03	-1.9481633E-04	-1.7535731E-03
C3	-5.9904196E-05	-1.0541832E-05	-7.7354714E-05	-1.5101291E-06
C4	-2.8880828E-07		-9.9974477E-07	1.0661093E-06
C5			-1.9099609E-09	1.0655280E-08

CTOD REGRESSION COEFFICIENTS FOR TEMPERATURE DEPENDENT WEIBULL DISTRIBUTION [mm] FOR STEEL D (Trans.)

Tmin(Deg C)	Tmax(Deg C)
-8.00000E+01	2.00000E+01

COEFF.	ALPHA	BETA
C0	2.14912E+00	4.84771E+00
C1	7.64779E-03	1.32749E-02
C2	-1.91195E-04	-3.04428E-04
C3		-9.14866E-07

CVN REGRESSION COEFFICIENTS FOR TEMPERATURE DEPENDENT WEIBULL DISTRIBUTION [J] FOR WP PLATE (LONGITUDINAL)

Tmin(Deg C)	Tmax(Deg C)
-8.00000E+01	2.00000E+01

COEFF.	ALPHA	BETA
C0	1.47771E+00	4.13192E+00
C1		1.51748E-02
C2		-3.16974E-04
C3		-2.07983E-06

CVN REGRESSION COEFFICIENTS FOR TEMPERATURE DEPENDENT WEIBULL DISTRIBUTION [J] FOR WP PLATE (TRANSVERSE)

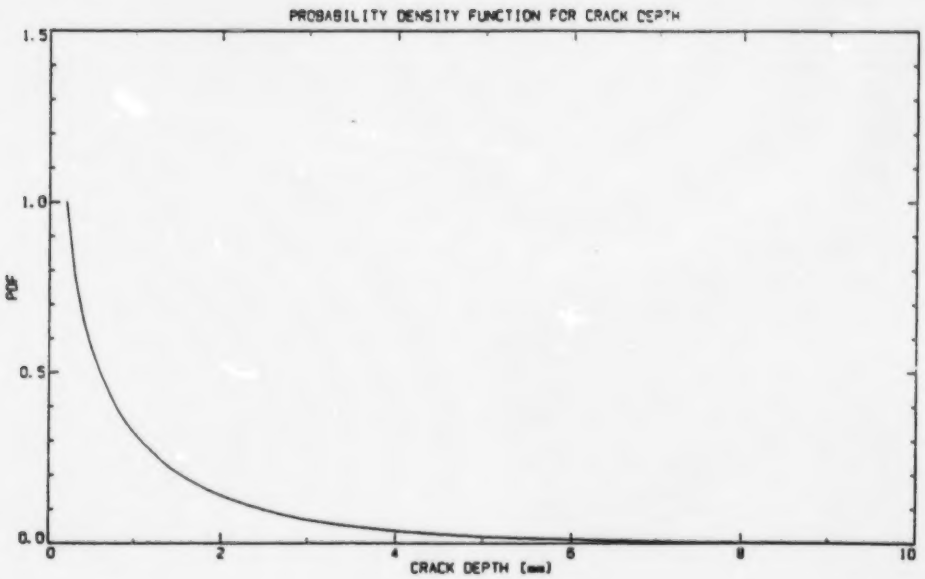

Figure B19: Weibull Probability Distribution for Crack Size (Small Cracks)

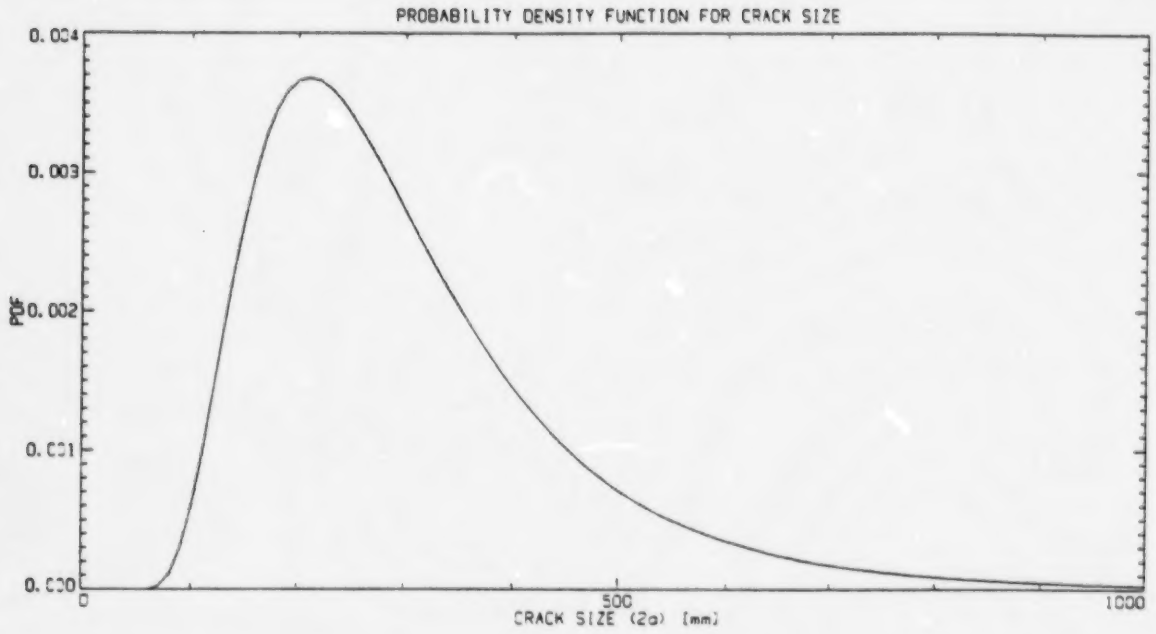

Figure B20: Lognormal Probability Distribution for Defect Size (Large Cracks)

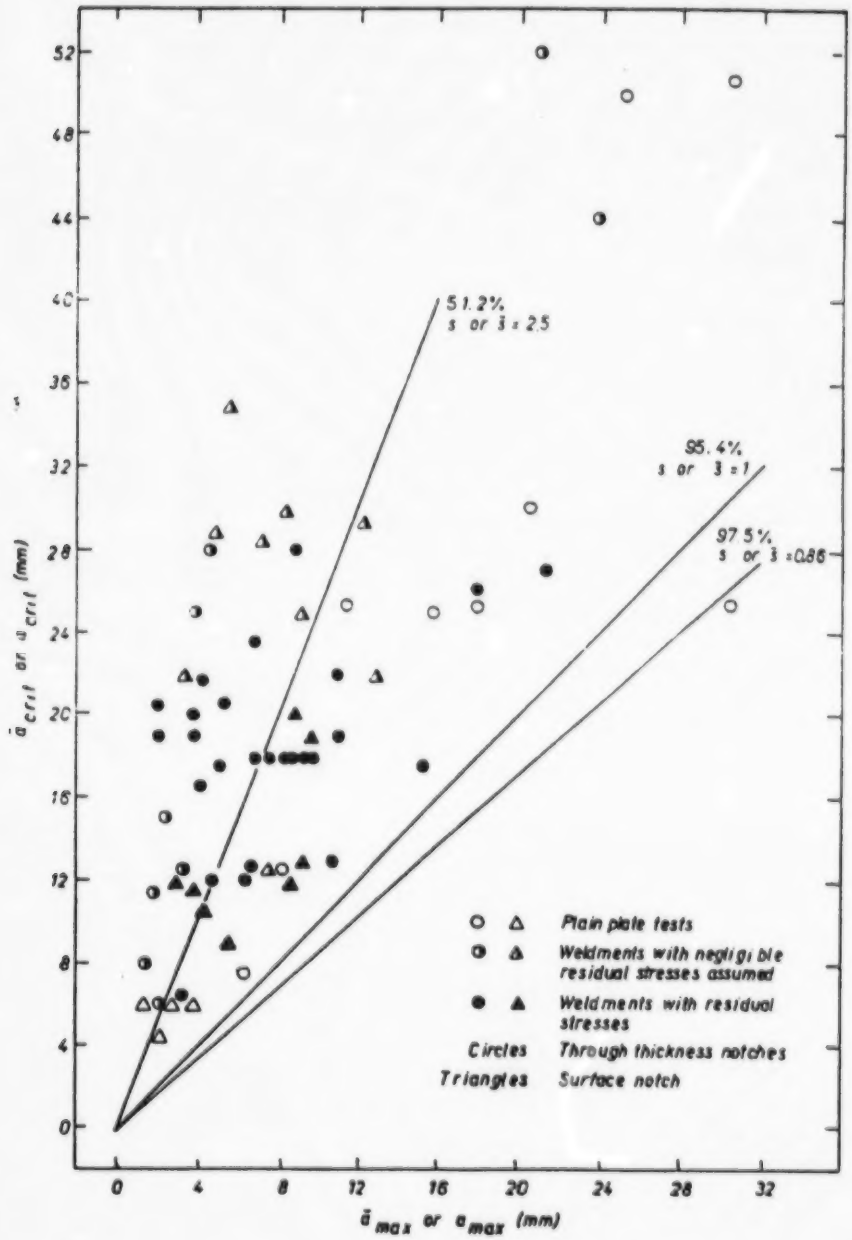

Figure B21: Correlation between predicted crack size and critical crack size from WPT (Ref. B6)

Figure B22: Probability of Failure as a function of Temperature - Steel AT Small Cracks

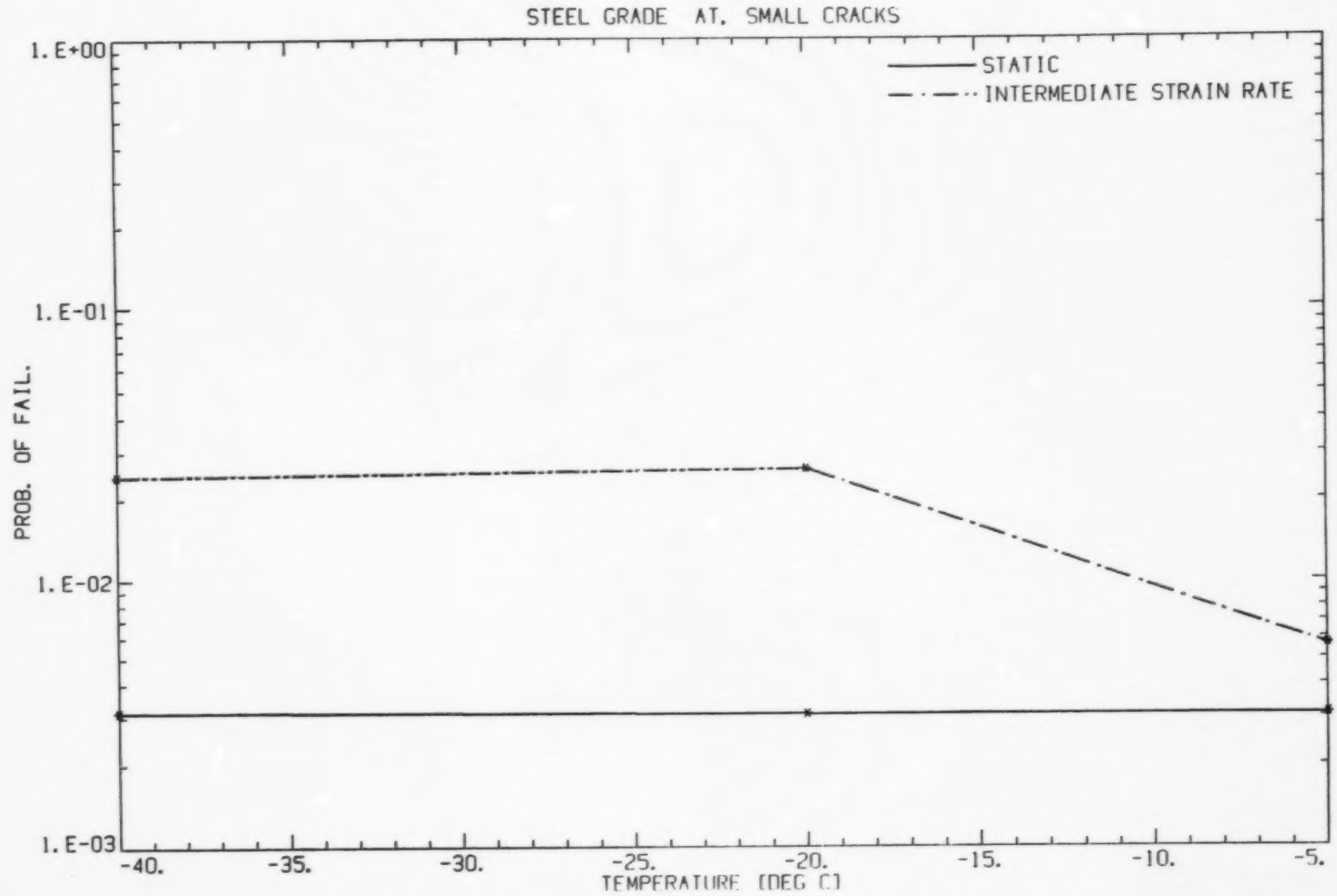

Figure B23: Probability of Failure as a function of Temperature - Steel AT Large Cracks

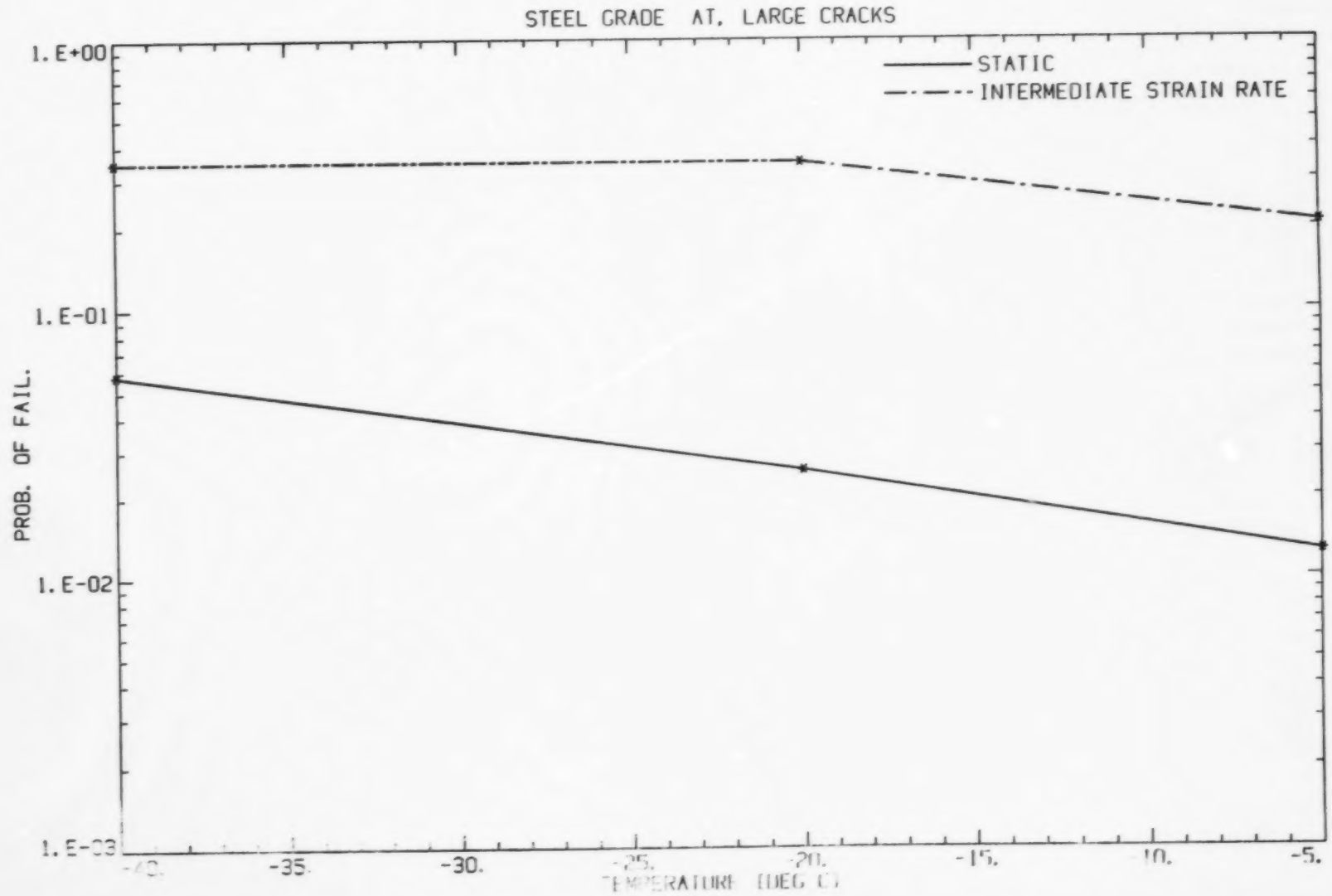

Figure B24: Probability of Failure as a function of Temperature - Steel BT Small Cracks

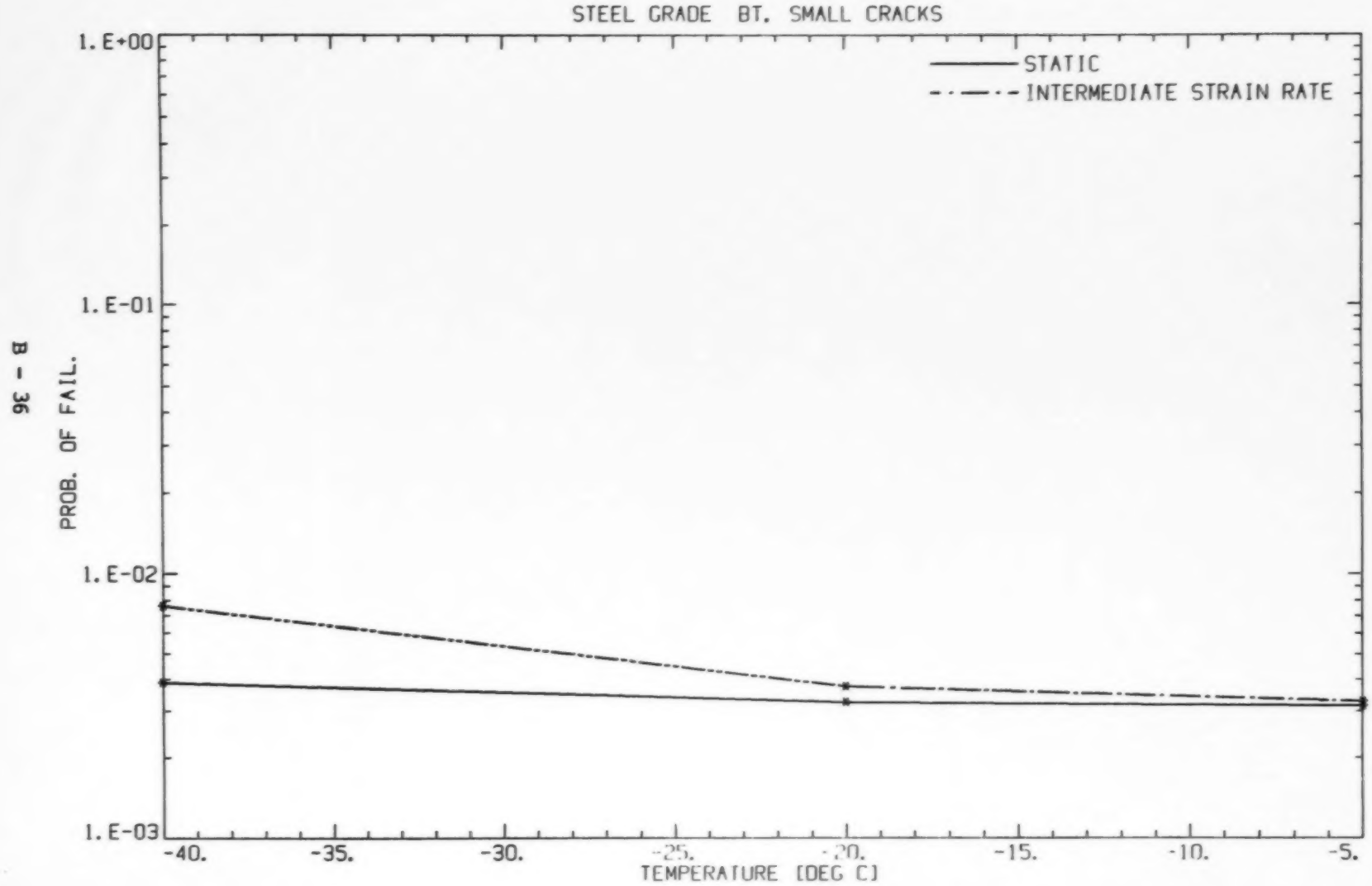

Figure B25: Probability of Failure as a function of Temperature - Steel BT Large Cracks

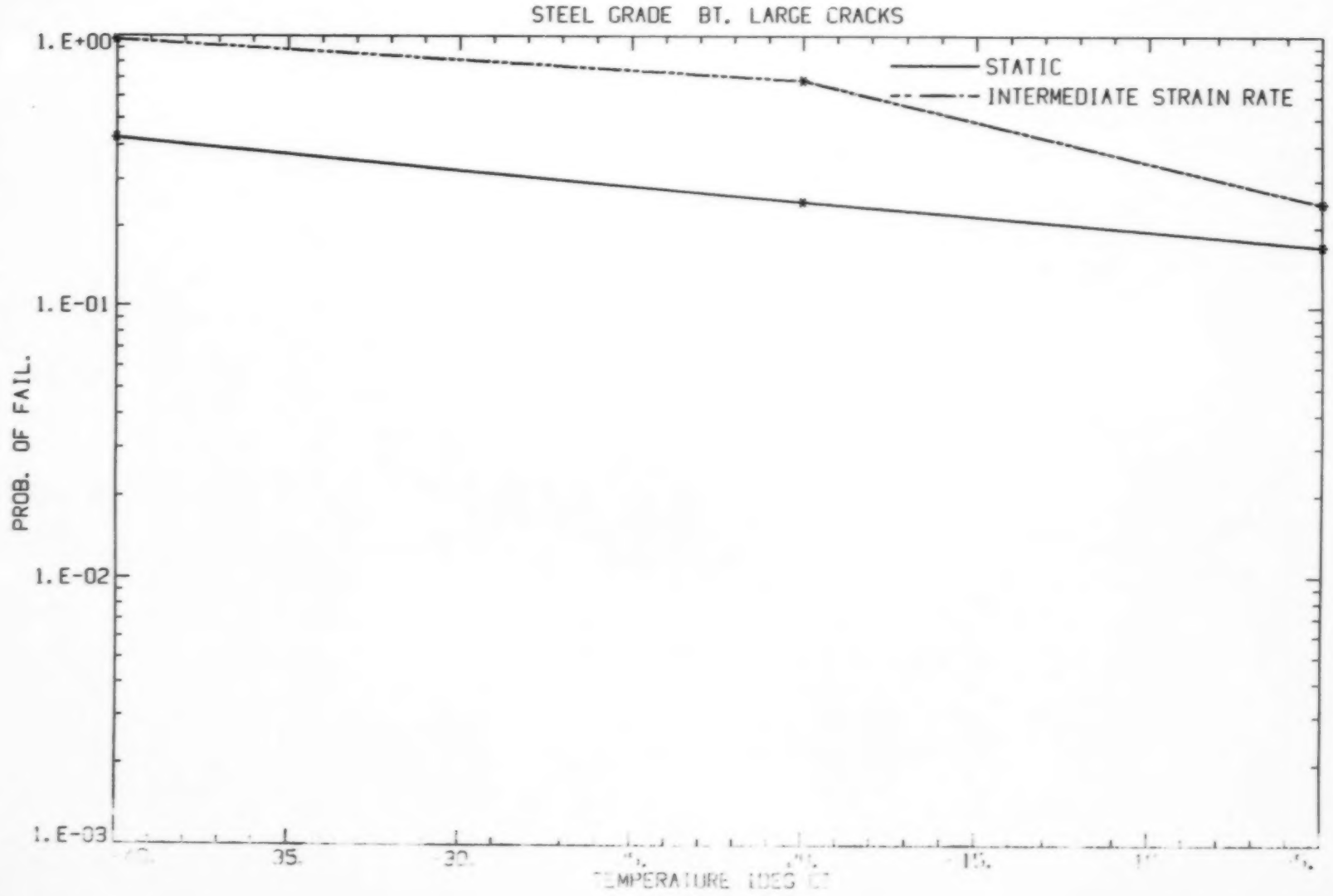

Figure B26: Probability of Failure as a function of Temperature - Steel DT Small Cracks

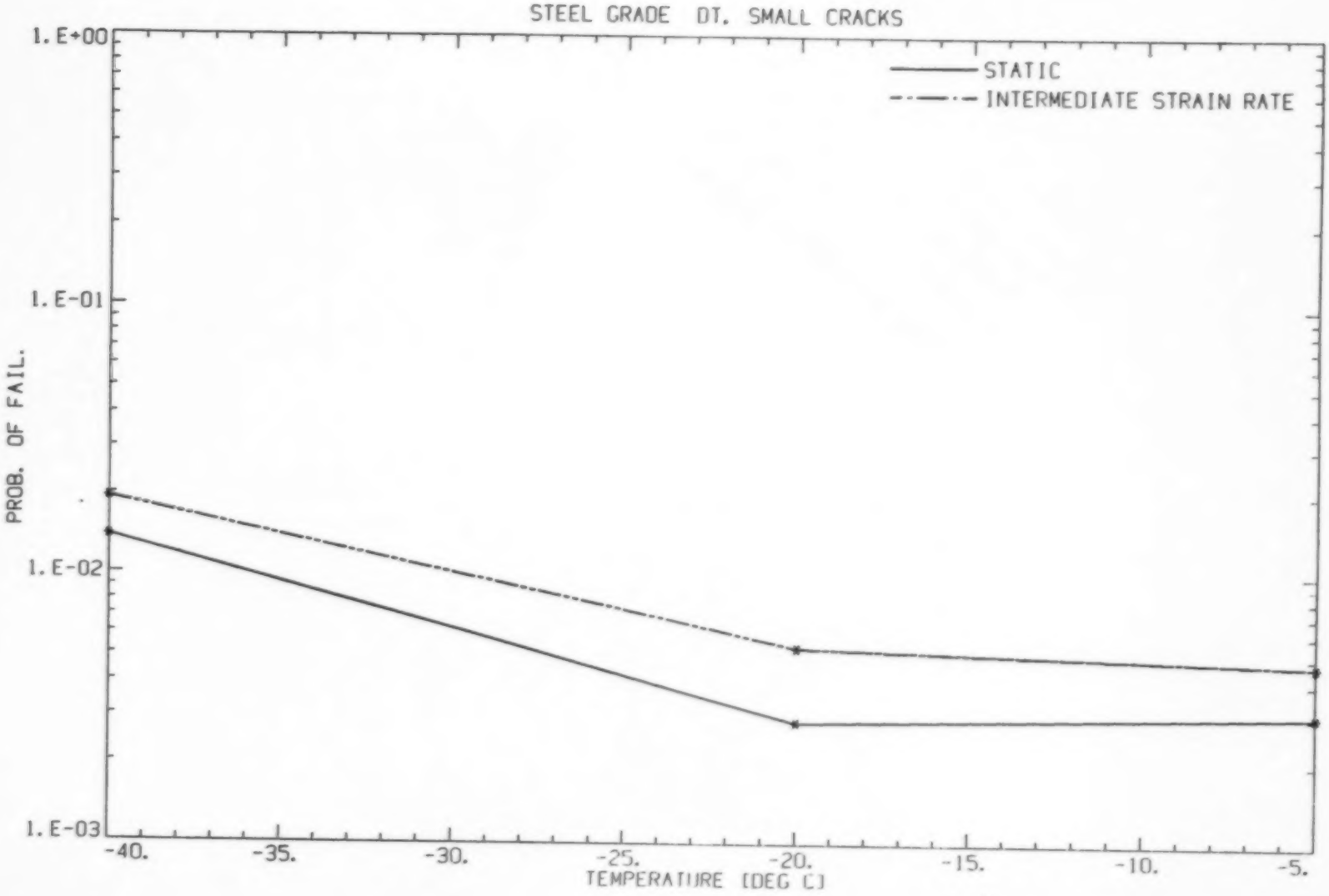

Figure B27: **Probability of Failure as a function of Temperature - Steel DT Large Cracks**

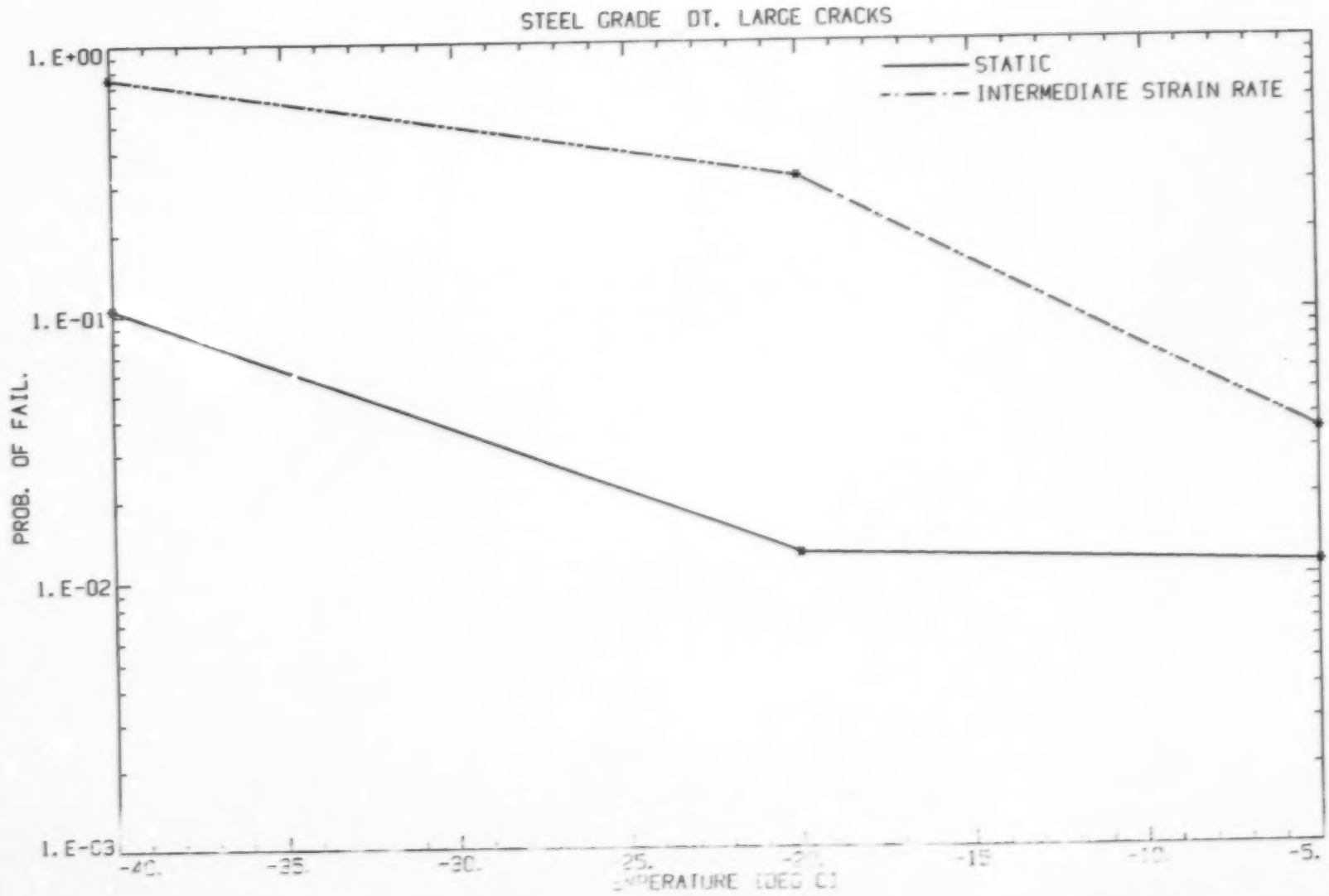

APPENDIX C

Significance of the Results With Respect to CASPPR

By

Mark J. Tomin
Reltec Advisory Services Inc.

SIGNIFICANCE OF THE RESULTS WITH RESPECT TO CASPPR

In this section, the results reported in the main text are discussed with respect to the CASPPR steel selection requirements (these are presented for reference in Appendix A). These requirements were previously assessed on the basis of the NK WPT approach (Refs. C1 and C2). The discussion here aims also on making a cautious judgement with respect to the NK WPT approach as used for verification of the CASPPR requirements.

C.1 Verification of CASPPR Requirements using NK WPT Approach

The NK WPT approach to defining fracture plan for ships was described in Section 1.2 of the main text. It was used for preliminary screening of CASPPR steel selection requirements with respect to prevention of unstable fracture from long (fatigue) cracks in the field of low residual (reaction) stresses and from short cracks in the field of high residual stresses.

In the approach taken to verify CASPPR requirements, it was assumed that residual stresses for long cracks (far-field residual and reaction stresses) are equal to 20% of the yield strength (ß=0.2) and the residual stresses for short cracks in the weld or HAZ are equal to the yield strength (ß=1.0).

To assess the CASPPR requirements, the maximum allowable defect size was calculated for two design temperatures: -5°C for submerged parts of the hull and -40°C for the exposed areas. It was further assumed that the allowable defect length is 250 mm in the parent plate (long cracks) and 15% of the plate thickness for short cracks for t≤50mm and 7.5 mm for t>50mm (Ref. C3).

Using the NK WPT approach, the following was concluded:

Bottom Plating and Side Shell below LAOD

The proposed CASPPR steel selection requirements are satisfied for both thickness ranges t≤25 mm and t>25 mm (t<70 mm) for long cracks and applied stresses exceeding 90% of yield strength (α=0.9).

Similarly, it was shown that the CASPPR requirements are satisfied for short cracks in the weld metal or HAZ.

Strength Deck

The CASPPR steel selection requirements are satisfied for Grade E and applied stresses up to 90% of the yield strength for t≤25 mm from 0.2L aft to 0.3L forward of midships and outside 0.2L aft to 0.3L forward of midships for both t≤25 mm as well as for t>25 mm (long and short cracks).

The requirement for t>25 mm (t≤50 mm)is satisfied for long cracks up to 70% of the yield strength for both EH32 and EH36.

Discussion of the Results

Small Cracks

Table C1 compares the maximum small crack size obtained using the NK WPT approach to the maximum small crack sizes calculated from the CTOD values using the following equation:

$$\delta = \frac{\sigma \pi a}{E} X \left(\frac{\sigma}{\sigma_y} - 0.25 \right) \qquad \text{(C1)}$$

In both cases, it was assumed that α=0.4 (primary member) and ß=1 (residual stresses equal σ_y for small cracks). The maximum tolerable (critical) crack sizes, calculated using NK WPT approach, are for 25 mm thick plate, the value in bracket for EH36 steel is for 50 mm thickness.

For the minimum temperature -5°C, it can be seen that for the intermediate loading rate case, the crack size obtained from CTOD for grade DH32 (nearest equivalent grade for steel B) in the transverse orientation is smaller than that obtained from the NK WPT assessment. This is not supprising since this steel does not strictly meet the transverse minimum requirements to qualify it as grade DH32. There are no CTOD values measured for steel WP at -5°C.

At -40°C for the quasi-static case, the actual maximum crack sizes predicted from the CTOD criterion are higher than those from the NK WPT assessment, making the NK WPT approach conservative.

The situation is different in the case of intermediate strain rates at -40°C. The crack sizes, oriented parallel to the rolling direction, obtained from the CTOD criterion are smaller for steels DH32 and EH36, (nearest equivalent grades for steels B, and C and D respectively), than those obtained from NK WPT. The opposite is true for grades B (nearest equivalent grade for steel A, transverse orientation) and grade EH36 in longitudinal direction (steel C). It should be noted that for steel A (transverse direction), the CTOD value measured for -30°C was used for the maximum crack size calculation. It can be seen from Figure 17 in the main text, that the value used would make a plausible extrapolation to -40°C. It should be noted that the maximum crack obtained for steel WP at -40°C at the intermediate strain rate is based only on one value.

However, even in those cases where the NK WPT seems to give unconservative results in comparison with CTOD approach, the crack sizes obtained from the CTOD analysis still meet the postulated requirements for crack initiation from small cracks.

TABLE C1

COMPARISON BETWEEN MAXIMUM SMALL CRACK LENGTHS FROM CTOD AND THOSE OBTAINED FROM NK WPT

PLATE	σ_y -5°C (MPa)	$CTOD_1$ AT -5°C (mm)	MAX. CRACK (mm)	MAX. NK CRACK (mm)	σ_y -40°C (MPa)	$CTOD_5$ AT -40°C (mm)	MAX. CRACK (mm)	$CTOD_1$ AT -40 C (mm)	MAX. CRACK (mm)	MAX. NK CRACK (mm)
AT (GR B)	305	0.66	629	162	340	0.53	453	0.17**	145**	86
BT (DH32)	378	0.22	169	192	413	0.18	127	0.05	35	102
WP (DH36)	390	N/A	N/A	158	420	0.26	180	0.10	69***	84
CL (EH36)	398	1.80	1,314	281	433	N/A	N/A	0.45	302	150
CT (EH36)	390	1.63	1,215	(201)*	426	N/A	N/A	0.10	68	(107)*
DT (EH36)	376	1.35	1,044	(201)*	411	0.85	601	0.10	71	(107)*
ET (MACS)	459	N/A	N/A	N/A	494	N/A	N/A	0.44	259	N/A

NOTE: N/A = NOT AVAILABLE
* CRACK SIZE FOR t=50 mm
** BASED ON -30°C, VALUE AT -40°C NOT AVAILABLE
***ONLY ONE VALUE AT -40°C

TABLE C2

COMPARISON BETWEEN MAXIMUM LARGE CRACK LENGTHS FROM CTOD AND THOSE OBTAINED FROM NK WPT

PLATE	σ_y -5°C (MPa)	$CTOD_1$ AT -5°C (mm)	MAX. CRACK (mm)	MAX. NK CRACK (mm)	σ_y -40°C (MPa)	$CTOD_3$ AT -40°C (mm)	MAX. CRACK (mm)	$CTOD_1$ AT -40°C (mm)	MAX. CRACK (mm)	MAX. NK CRACK (mm)
AT (GR B)	305	0.66	1,205	883	340	0.53	868	0.17**	279**	471
BT (DH32)	378	0.22	324	1,044	413	0.18	243	0.05	67	557
WP (DH36)	390	N/A	N/A	861	420	0.26	345	0.10	133***	459
CL (EH36)	398	1.80	2,519	1,529	433	N/A	N/A	0.45	579	815
CT (EH36)	390	1.63	2,328	(1,096)	426	N/A	N/A	0.10	131	(584)*
DT (EH36)	376	1.35	2,000	N/A	411	0.85	1,152	0.10	136	(584)*
ET (MACS)	459	N/A	N/A	N/A	494	N/A	N/A	0.44	496	N/A

NOTE: N/A = NOT AVAILABLE
* CRACK SIZE FOR t=50 mm
** BASED ON -30°C, VALUE AT -40°C NOT AVAILABLE
***ONLY ONE CTOD VALUE AT -40°C

Large Cracks

Table C2 compares the maximum large crack size obtained using the NK WPT approach to the maximum large crack sizes calculated from the CTOD values using Equation C1 above. In both cases, it was assumed that α=0.4 (primary member) and ß=0.2 (residual stresses equal to $0.2\sigma_y$ for large cracks). The maximum tolerable (critical) crack sizes, calculated using NK WPT approach, are for 25 mm thick plate, the value in bracket for EH36 steel is for 50 mm thickness.

Again, the crack sizes obtained from CTOD criterion at -5 C and intermediate strain rates excede those obtained from NK WPT assessment except in the case of grade DH32 (nearest equivalent grade for steel B). See the reason for small cracks above. There is no CTOD data available at -5°C.

The same is true for the quasi-static case at -40°C. At the intermediate strain rate and -40°C, the NK WPT results are unconservative in all cases compared to CTOD assessment and the crack sizes do not meet the postulated 250 mm requirement except for EH36 in longitudinal direction (steel C) and for MACS steel.

C.2 Significance of the Results

Orientation of the Specimens

The CTOD values were measured mostly in the transverse orientation. All plates showed high anisotropy of fracture toughness in the transition area, the transverse orientation being the weaker, except MACS steel for which the CVN toughness was at the upper shelf at -40°C in both orientations. As was already noted, it must be stressed that steel B did not meet the CVN requirements in transverse direction for grade DH32, and steel C met this requirement only marginally.

The steel performance in terms of crack initiation can still be regarded as good in the transverse orientation, even though some of these steels do not meet the basic CVN qualification requirements. It should be noted that one important requirement introduced in CASPPR is that plates are to be oriented in the fore-aft direction during construction so that the principal bending stresses would act along the rolling direction of the plates. The recognition of the weaker transverse orientation in terms of resistance against crack initiation and propagation, is fully respected in CASPPR.

Effect of Strain Rate

The NK WPT approach seems conservative except for -40°C at the intermediate strain rates in the transverse direction, except for steel WP for which the CTOD values were measured in the longitudinal direction. Furthermore, it should be remembered that the 'high' intermediate strain rates ($2x10^{-1}$ s^{-1}) take place at the bow plate where the service temperature is -5°C. At this temperature, the resistance against crack initiation of the studied steels is high even at the intermediate strain rates (NK WPT assessment is conservative). The strain rates decrease fast with the distance from the region of impact. The strain rates in the deck caused by ice ramming, are one to two orders of magnitude lower than the 'high' intermediate strain rates in the bow plate or bow frame.

It should be also noted that the downward ice ramming produces prevailing compressive stresses in the 'cold' (exposed) deck area midship.

Extent of Obtained Data

One should be cautious in making conclusions based on the experimental data obtained in this program, giving proper weight to the results, depending on the number of results and their statistical spread. As was shown in Appendix B, even though the average values of CTOD for the quasi-static and intermediate strain rates show clearly distinct shift in the transition curve, it is impossible to determine the statistical significance of this difference since only two values were obtained at each strain rate. The statistically unacceptable small number of data then penalizes the Weibull distribution at the relevant temperature (-40°C in this case) leading to similar probabilities of failure for both quasi-static and intermediate strain rates.

Even though caution is needed when interpreting the data, it is very valuable to know that this data supports the CASPPR steel selection requirements despite the fact that the data represents the worst possible case of ship steels in particular grades and orientation (transverse direction and two steels not meeting the CVN requirements).

Use of F Grade

The MACS steel tested is grade F steel CVN tested at -60°C. This steel was included in CASPPR steel selection requirements to ensure superior toughness properties for sheerstrakes and stringers midships for thicknesses greater than 25.5 mm. The studied steel confirmed that it would operate at -40°C at its upper CVN energy shelf, with 100% shear. Considerable crack arresting properties are ensured by having NDTT 15°C below the minimum design temperature of -40°C. The CTOD values at -40°C and intermediate strain rates correspond to the transition region and provide good protection against crack initiation from both small and large defects.

C.3 Conservatism of the Proposed Requirements

It should be pointed out that the conditions conducive to brittle fracture require simultaneous occurrence of low fracture toughness, sufficient defect size as well as high stress. The WPT results are based on the assumption that the principal tensile stresses act normal to the crack plane. Also, wide plate tests use a uniform far-field fracture stress. Both these assumptions are very conservative when compared to real ship structural situations where cracks could be oriented at an angle to the principal stresses different from 90° and would propagate in a stress field characterized by a gradient.

Furthermore, the 'infinite' plate assumption is extremely conservative. In real, the plates are stiffened, thus reducing considerably the propensity of defects to fracture (crack initiation). It has been shown (Ref. C4) that the stiffening effect reduces the probability of fracture by one to two orders of magnitude and that ships can operate at probabilities of failure $\approx 10^{-1}$ due to their inherent structural redundancy.

It is obvious that probability of fracture will be highly dependent on the time of exposure to low temperatures (temperature distribution). From the limited probabilistic analysis presented in Appendix B, it is obvious that this approach allows to draw some important conclusions.

Significant improvement of the probabilistic model would follow from inclusion of the temperature distributiuon of the operating temperatures. The probabilities of failure would be lowered if shown that the mean operating temperature is above those minimum design temperatures assumed by CASPPR (-5°C for submerged parts of the hull and -40°C for exposed areas). The recent projects, funded by the Coast Guard (Refs. C5 and C6) aim at obtaining more information on temperature distribution in the Canadian Arctic relevant to arctic shipping.

The Weibull fracture toughness distributions presented in Appendix B provide the necessary input into full probabilistic treatment of fracture in various areas of the hull.

C.4 CONCLUSIONS

The experimental program provided extremely valuable results. Despite the fact that at some temperatures, more results are needed to provide an acceptable statistical basis, the data obtained provides the 'lower bound' for toughness of common ship (hull) steels. This data supports the soundness of the CASPPR philosophy to steel selection for ships navigating in ice.

The following are measures adopted in CASPPR which aim at preventing brittle (catastrophic) fractures in ships navigating in the Arctic waters:

- Ship steel Grade A, which had no guaranteed toughness properties, was eliminated from use;

- Extra high strength Grade F, with the requirement of 40 J (L) at -60°C, was introduced at sheerstrakes midships for thicknesses greater than 25 mm;

- Higher grades in bottom areas were used to account for high strain rates and high tensile loads from downward ice breaking;

- The plate orientation during ship building is controlled so that the rolling direction is fore-aft.

Appropriateness of these measures was confirmed by the results of this Program.

C.5 RECOMMENDATIONS FOR FUTURE WORK

The current Program aimed at obtaining a fracture toughness database for current ship steels and at the same time at providing a basis for CASPPR steel selection requirements. These results will be combined with the results of other research programs currently in progress (e.g. the Canadian Wide Plate Test Program).

In the author's opinion, the following are areas which need further work:

- additional results at temperatures where insufficient data leads to high spread in the Weibull distribution of fracture toughness, are needed;

- it is anticipated that the proposed large scale program for temperature measurement (Ref. C6) will provide a typical temperature distribution profile for arctic shipping; this will provide the necessary input for full probabilistic treatment of fracture initiation in ships for arctic navigation;

- fracture analysis should be applied to more realistic details used in the hull structure;

- data obtained through all relevant projects (mainly funded by Canadian Coast Guard and CANMET) should be compiled into one database (model) to update the basis for CASPPR requirements generated in the current Program.

C.6 REFERENCES

[C1] Tomin, M., (1989), "CASPPR Subcommittee Report Chapter 7: Steel Selection", RELTEC Report to Canadian Coast Guard, January 1989.

[C2] Tomin, M. (1990), "Implementation of ASPPR Materials Requirements", RELTEC Report to Canadian Coast Guard Northern, Transport Canada Report No. TP10434.

[C3] Tomin, M., and Rengaard, O. (1988), "Development of Steel Plate Requirements for Fixed Offshore Structures", Veritas Report No. 84-CGY-023.

[C4] Tomin, M., Nessim, M., and Cormeau, A. (1988), "Fracture Control for Arctic Structures: A Model for Analyzing Structural Details", Veritas Report to CANMET.

[C5] Tomin, M., and Edgecombe, M. (1989), "Experimental Design Temperature Database for Arctic Shipping", RELTEC Report REL-03-89 to Transport Canada.

[C6] Tomin, M., Edgecombe, M., and Cormeau, A. (1990), "Analysis of a Design Temperature Database for Arctic Shipping", RELTEC Report to Canadian Coast Guard Northern, Transport Canada Report No. TP 10408E.